

# TROPICAL FOCK-GONCHAROV COORDINATES FOR $SL_3$ -WEBS ON SURFACES I: CONSTRUCTION

DANIEL C. DOUGLAS AND ZHE SUN

**ABSTRACT.** For a finite-type surface  $\mathfrak{S}$ , we study a preferred basis for the commutative algebra  $\mathbb{C}[\mathcal{X}_{SL_3(\mathbb{C})}(\mathfrak{S})]$  of regular functions on the  $SL_3(\mathbb{C})$ -character variety, introduced by Sikora and Westbury. These basis elements come from the trace functions associated to certain tri-valent graphs embedded in the surface  $\mathfrak{S}$ . We show that this basis can be naturally indexed by positive integer coordinates, defined by Knutson-Tao rhombus inequalities. These coordinates are related, by the geometric theory of Fock and Goncharov, to the tropical points at infinity of the dual version of the character variety.

For a finitely generated group  $\Gamma$  and a suitable Lie group  $G$ , a primary object of study in low-dimensional geometry and topology is the character variety

$$\mathcal{X}_G(\Gamma) = \{\rho : \Gamma \longrightarrow G\} // G$$

consisting of group homomorphisms  $\rho$  from  $\Gamma$  to  $G$ , considered up to conjugation. Here, the quotient is taken in the algebraic geometric sense of Geometric Invariant Theory [MFK94]. Character varieties can be explored using a wide variety of mathematical skill sets. Some examples include the Higgs bundle approach of Hitchin [Hit92], the dynamics approach of Labourie [Lab06], and the representation theory approach of Fock and Goncharov [FG06].

We are interested in the case where the group  $G$  is the special linear group  $SL_n(\mathbb{C})$ . Adopting the viewpoint of algebraic geometry, one can study the  $SL_n(\mathbb{C})$ -character variety  $\mathcal{X}_{SL_n(\mathbb{C})}(\Gamma)$  by means of its commutative algebra of regular functions  $\mathbb{C}[\mathcal{X}_{SL_n(\mathbb{C})}(\Gamma)]$ . An example of a regular function is the trace function  $\text{Tr}_\gamma : \mathcal{X}_{SL_n(\mathbb{C})}(\Gamma) \rightarrow \mathbb{C}$  associated to an element  $\gamma \in \Gamma$ , sending a representation  $\rho$  to the trace  $\text{Tr}(\rho(\gamma)) \in \mathbb{C}$  of the matrix  $\rho(\gamma) \in SL_n(\mathbb{C})$ . A theorem of Procesi [Pro76] says that the trace functions  $\text{Tr}_\gamma$  generate the algebra of functions  $\mathbb{C}[\mathcal{X}_{SL_n(\mathbb{C})}(\Gamma)]$  as an algebra, and also identifies all of the relations.

Sikora [Sik01] provided a geometric description of Procesi's result in the case where  $\Gamma$  is the fundamental group  $\pi_1(\mathfrak{S})$  of a topological space  $\mathfrak{S}$ ; see also the earlier work of Bullock [Bul97] for the case of  $SL_2(\mathbb{C})$ . Sikora extended the notion of a trace function to include functions  $\text{Tr}_W \in \mathbb{C}[\mathcal{X}_{SL_n(\mathbb{C})}(\mathfrak{S})]$  on the character variety  $\mathcal{X}_{SL_n(\mathbb{C})}(\mathfrak{S}) = \mathcal{X}_{SL_n(\mathbb{C})}(\pi_1(\mathfrak{S}))$  that are associated to homotopy classes of certain  $n$ -valent graphs  $W$ , called webs, in the space  $\mathfrak{S}$ . He proved that the trace functions  $\text{Tr}_W$  span the algebra of functions  $\mathbb{C}[\mathcal{X}_{SL_n(\mathbb{C})}(\mathfrak{S})]$  as a vector space, and he also represented the relations pictorially in terms of the associated graphs.

In the current work, we restrict our attention to the case where the Lie group is  $SL_3(\mathbb{C})$  and where the space  $\mathfrak{S}$  is a punctured finite-type surface, namely the space obtained by removing finitely many points from a closed surface  $\bar{\mathfrak{S}}$ . In particular, the surface  $\mathfrak{S}$  has

---

*Date:* November 4, 2020.

This work was partially supported by the U.S. National Science Foundation grants DMS-1107452, 1107263, 1107367 “RNMS: GEometric structures And Representation varieties” (the GEAR Network). The first author was also partially supported by the U.S. National Science Foundation grants DMS-1406559 and 1711297, and the second author by the China Postdoctoral Science Foundation grant 2018T110084, the FNR AFR Bilateral grant COALAS 11802479-2, and the Huawei Young Talents Programme at IHES.

empty boundary. Sikora and Westbury [SW07] proved that the collection of trace functions  $\text{Tr}_W$  associated to non-elliptic webs  $W$ , which are certain planar webs embedded in the surface  $\mathfrak{S}$ , forms a linear basis for the algebra of functions  $\mathbb{C}[\mathcal{X}_{\text{SL}_3(\mathbb{C})}(\mathfrak{S})]$ .

An analogous result [HP93, Prz91] in the case of  $\text{SL}_2(\mathbb{C})$  says that the collection of trace functions  $\text{Tr}_\gamma$  associated to planar multi-curves  $\gamma$  embedded in the surface  $\mathfrak{S}$  forms a linear basis for the algebra of functions  $\mathbb{C}[\mathcal{X}_{\text{SL}_2(\mathbb{C})}(\mathfrak{S})]$ . Now, a classical combinatorial fact is that if the punctured surface  $\mathfrak{S}$  is equipped with an ideal triangulation  $\lambda$ , then the geometric intersection numbers  $\iota(\gamma, E)$  of a curve  $\gamma$  with the edges  $E$  of  $\lambda$  furnish an explicit system of positive integer coordinates on the collection of planar multi-curves  $\gamma$ . These coordinates can be characterized completely by finitely many triangle inequalities and parity conditions.

Our main result generalizes these  $\text{SL}_2$ -properties to the case  $n = 3$ .

**Theorem 1.** *For a punctured surface  $\mathfrak{S}$  with empty boundary, equipped with an ideal triangulation  $\lambda$ , the Sikora–Westbury  $\text{SL}_3$ -web basis for the algebra of functions  $\mathbb{C}[\mathcal{X}_{\text{SL}_3(\mathbb{C})}(\mathfrak{S})]$  admits an explicit system of positive integer coordinates, which can be characterized completely by finitely many Knutson–Tao rhombus inequalities [KT99] and modulo 3 congruence conditions.*

In a companion paper [DSa] (see also [DSb]), we address the dependence on triangulations.

**Theorem 2.** *The coordinates of Theorem 1 are natural with respect to the action of the mapping class group of the surface  $\mathfrak{S}$ . More precisely, if a different ideal triangulation  $\lambda'$  is chosen, then the induced coordinate transformation takes the form of a tropicalized  $\mathcal{A}$ -coordinate cluster transformation, in the language of Fock and Goncharov [FG06, FG07].*

This research was inspired by papers of Xie [Xie13], Kuperberg [Kup96], and Goncharov and Shen [GS15].

At its heart, Theorem 1 is purely topological, merely describing how to assign coordinates to pictures. We have motivated these web pictures  $W$  by their association with trace functions  $\text{Tr}_W$ . So, it is desirable to tie directly the coordinates to the trace functions. Such a relationship is well-known for  $\text{SL}_2(\mathbb{C})$  (see, for instance, [Foc97]). In that case, the trace functions  $\text{Tr}_\gamma$  for curves  $\gamma$  can be expressed as Laurent polynomials  $\text{Tr}_\gamma = \text{Tr}_\gamma(X_i^{1/2})$  in  $N_2$ -many variables  $X_i^{1/2}$ , where  $N_2$  is the number of coordinates. Moreover, the coordinates of a curve  $\gamma$  can be read off as the exponents of the highest term of the trace polynomial  $\text{Tr}_\gamma(X_i^{1/2})$ . This is a manifestation of the tropical geometric nature of these coordinates.

There should be a similar story for  $\text{SL}_3(\mathbb{C})$ . Using Fock and Goncharov’s theory, one can express the trace functions  $\text{Tr}_W$  for webs  $W$  as Laurent polynomials  $\text{Tr}_W = \text{Tr}_W(X_i^{1/3})$  in  $N_3$ -many variables  $X_i^{1/3}$ , where  $N_3$  is the number of coordinates appearing in Theorem 1. Conjecturally, these coordinates are precisely the exponents of the highest term of the trace polynomial  $\text{Tr}_W(X_i^{1/3})$ . This idea was Xie’s [Xie13] point of departure, and our coordinates are constructed following his lead.

Kuperberg’s landmark paper [Kup96] motivated Sikora and Westbury’s work, and laid the topological foundation for ours as well. He proved that a basis for the vector space of  $\text{SL}_3(\mathbb{C})$ -invariant tensors, which lies inside a tensor product of finite-dimensional irreducible representations of  $\text{SL}_3(\mathbb{C})$ , can be indexed by a collection of pictures drawn on an ideal polygon  $\mathfrak{D}_k$  (equivalently, one can consider  $\mathfrak{sl}_3(\mathbb{C})$ -invariant tensors for the Lie algebra  $\mathfrak{sl}_3(\mathbb{C})$ ). Along the way, he showed how the pictures for the ideal polygon  $\mathfrak{D}_k$  can be obtained by gluing together the more basic pictures for an ideal triangle  $\mathfrak{D}_3$ . We apply Kuperberg’s “local” pictorial ideas in order to analyze “global” pictures that are drawn on a triangulated surface

$(\mathfrak{S}, \lambda)$ . We are also interested in how our work relates to other methods for studying webs, such as the affine building approach of [FKK13] and the cluster algebra approach of [FP16].

Motivated in part by the Fock-Goncharov Duality Conjecture [FG06], Goncharov and Shen [GS15] developed a general method by which bases of algebras of functions on moduli spaces can be indexed by “positive integral tropical points”, namely the preimage points mapping to  $\mathbb{Z}_{\geq 0}$  under a “tropicalized potential function” (for another approach to the Fock-Goncharov Duality Conjecture, see [GHKK18, GS18]; and for a quantum  $SL_2$ -version, see [AK17]). These bases are defined abstractly, employing the geometric Satake correspondence. Goncharov and Shen showed that, for an ideal triangle  $\mathfrak{D}_3$  equipped with a general linear symmetry group, the positive integral tropical points correspond to solutions of the Knutson-Tao rhombus inequalities. In Theorem 1, we also make use of these inequalities in order to assign positive integer coordinates to pictures, in the rank 2 setting. We do not know the extent to which our construction agrees with that of [GS15]. Preliminary computations mentioned in [GHKK18] suggest that such a connection is likely, however highly non-trivial. For another geometric application of the Goncharov-Shen potential function, see [HS19].

Frohman and Sikora [FS20] also recently constructed integer coordinates for a slightly more general version of the  $SL_3$ -web basis appearing in Theorem 1. They implement the same topological strategy as we do, however their coordinates are different from ours. They do not characterize the values taken by their coordinates, and they do not address the question of naturality under changing the triangulation. Their proof is algebraic in nature, as it uses the Sikora-Westbury theorem saying that the non-elliptic webs are linearly independent, which ultimately relies on the Diamond Lemma from non-commutative algebra. On the other hand, we give a purely topological-combinatorial proof of Theorem 1, which does not require using this linear independence. A potential application of our work is to give an alternative geometric proof of this Sikora-Westbury theorem, by using Theorem 1 together with the  $SL_3$ -quantum trace map [Dou, Dou20]; compare [BW11, §8] for the  $SL_2$ -case.

## ACKNOWLEDGEMENTS

This research would not have been possible without the help and support of many people, whose time and patience often seemed limitless. In particular, we are profoundly grateful to Dylan Allegretti for his involvement during the early stages of the project, Charlie Frohman for his guidance from the very beginning, Francis Bonahon and Viktor Kleen for helping us sort through our ideas and for technical assistance, and Tommaso Cremaschi for his invaluable feedback after reading too many drafts. Much of this work was completed during very enjoyable visits to Tsinghua University in Beijing (supported by a GEAR graduate internship grant) and the University of Southern California in Los Angeles. We would like to take this opportunity to extend our enormous gratitude to these institutions for their warm hospitality and many tasty dinners (the first author was especially fond of the sōngshǔ guìyú).

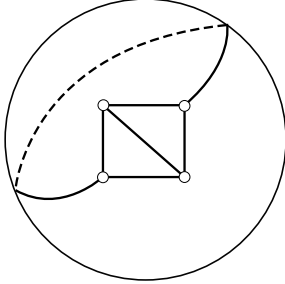
## 1. GLOBAL WEBS

We introduce the primary topological objects of study.

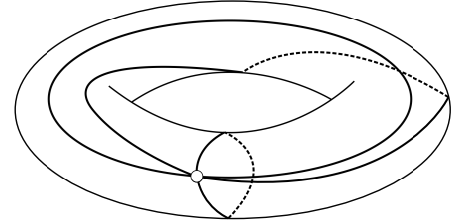
**1.1. Topological setting.** Let  $\mathfrak{S}$  be an oriented *punctured surface* with empty boundary  $\partial\mathfrak{S} = \emptyset$ , obtained by removing finitely many points  $P$ , called *punctures*, from a closed surface  $\bar{\mathfrak{S}}$ . We require that there is at least one puncture, and that the Euler characteristic  $\chi(\mathfrak{S})$  of the punctured surface  $\mathfrak{S}$  is strictly less than zero,  $\chi(\mathfrak{S}) < 0$ . These topological

conditions guarantee the existence of an *ideal triangulation*  $\lambda$  of the punctured surface  $\mathfrak{S}$ , namely a triangulation  $\bar{\lambda}$  of the closed surface  $\bar{\mathfrak{S}}$  whose vertex set is equal to the set of punctures  $P$ . See Figure 1 for some examples of ideal triangulations.

We always assume that our ideal triangulations  $\lambda$  do not contain any *self-folded triangles*. This means that all of the triangles in  $\lambda$  have three distinct edges. Such a  $\lambda$  always exists.



(A) Four times punctured sphere



(B) Once punctured torus

FIGURE 1. Ideal triangulations

## 1.2. Webs.

**Definition 3.** A *simple global web*, or just *global web* or *web*,  $W = \{w_i\}$  on the surface  $\mathfrak{S}$  is a finite collection of connected closed oriented tri-valent graphs or curves  $w_i$  embedded in  $\mathfrak{S}$ , such that the images of the components  $w_i$  are mutually disjoint, and such that each vertex of  $w_i$  is either a *source* or a *sink*, namely the orientations either go all in or all out, respectively. Here, closed means that the components  $w_i$  have empty boundary.

For an example, in Figure 2 we show a web on the once punctured torus, which has four components consisting of two tri-valent graphs and two curves.

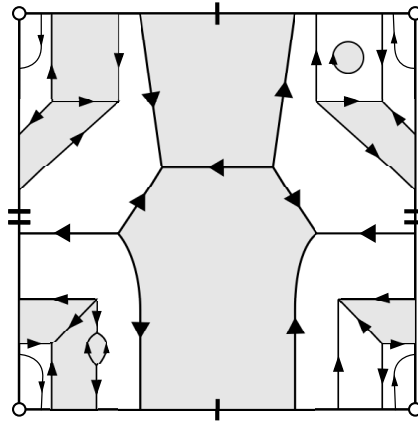


FIGURE 2. Web

**Definition 4.** Two webs  $W$  and  $W'$  on the surface  $\mathfrak{S}$  are *parallel-equivalent* if  $W$  can be taken to  $W'$ , preserving orientation, by a sequence of moves of the following two types:

- (1) an *isotopy* of the web, namely a smoothly varying family of webs;

- (2) a *global parallel-move*, exchanging two closed curves that together form the boundary of an embedded annulus  $A$  in the surface  $\mathfrak{S}$ ; see Figure 3.

In this case, we say that the webs  $W$  and  $W'$  belong to the same *parallel-equivalence class*.

Intuitively, we think of parallel-equivalent as meaning homotopic on the surface.

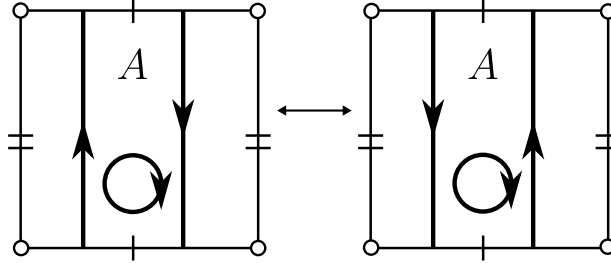


FIGURE 3. Global parallel-move

### 1.3. Faces.

**Definition 5.** A *face*  $D$  of a web  $W$  on the surface  $\mathfrak{S}$  is a contractible component of the complement  $W^c \subseteq \mathfrak{S}$  of the web. A  $n$ -*face*  $D_n$  is a face with  $n$ -sides, counted with multiplicity. An alternative name for a 0-face  $D_0$ , 2-face  $D_2$ , 4-face  $D_4$ , and 6-face  $D_6$  is a *disk*-, *bigon*-, *square*-, and *hexagon*-, respectively.

For an example, the web shown in Figure 2 above has one disk-face, one bigon-face, two square-faces, and two hexagon-faces; these faces are shaded in the figure. Notice that one of the hexagon-faces consists of five edges of the web, one edge being counted twice.

By orientation considerations, faces must have an even number of sides.

Bigon- and square-faces always consist of exactly two and four edges, respectively, of  $W$ .

In figures, we often omit the web orientations, as in Figure 4.

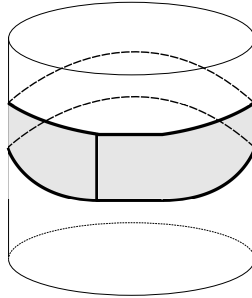


FIGURE 4. Prohibited square-face

### 1.4. Non-elliptic webs.

**Definition 6.** A web  $W$  on the surface  $\mathfrak{S}$  is called *non-elliptic* if it has no disk-, bigon-, or square-faces. Otherwise,  $W$  is called *elliptic*.

Notice that if  $W$  is a non-elliptic web, and if  $W'$  is another web that is parallel-equivalent to  $W$ , then  $W'$  is also non-elliptic. We denote the set of parallel-equivalence classes of non-elliptic webs by  $\mathcal{W}_{\mathfrak{S}}$ .

## 2. LOCAL WEBS

As a technical device, we study webs-with-boundary in the disk.

**2.1. Ideal polygons.** For a non-negative integer  $k \geq 0$ , an *ideal  $k$ -polygon*  $\mathfrak{D}_k$  is the surface  $\mathfrak{D}_0 - P$  obtained by removing  $k$  punctures  $P \subseteq \partial\mathfrak{D}_0$  from the boundary of the closed disk  $\mathfrak{D}_0$ .

Observe that, when  $k > 0$ , the boundary  $\partial\mathfrak{D}_k$  of the ideal polygon consists of  $k$  ideal arcs.

### 2.2. Local webs.

**Definition 7.** A *simple local web*, or just *local web*,  $W = \{w_i\}$  in an ideal polygon  $\mathfrak{D}_k$  ( $k \geq 0$ ) is a finite collection of connected compact oriented tri-valent graphs or curves  $w_i$  embedded in  $\mathfrak{D}_k$ , such that the images of the components  $w_i$  are mutually disjoint, and such that each vertex of  $w_i$  is either a source or sink. We require that  $\partial W = W \cap \partial\mathfrak{D}_k$  and that each point  $v \in \partial W$  is considered as a mono-valent vertex.

For some examples of local webs, see Figure 5. There,  $k = 4$ .

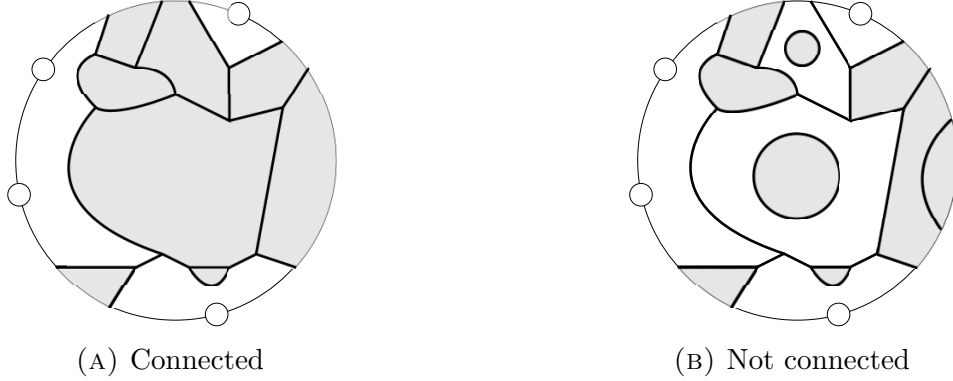


FIGURE 5. Local webs

### 2.3. External faces.

**Definition 8.** A *face*  $D$  of a local web  $W$  in an ideal polygon  $\mathfrak{D}_k$  ( $k \geq 0$ ) is a contractible component of the complement  $W^c \subseteq \mathfrak{D}_k$  of  $W$  that is *puncture-free*, meaning that  $D$  does not limit to any punctures  $p \in P$ . A  $n$ -*face*  $D_n$  is a face with  $n$ -sides. Here, a maximal segment  $\alpha \subseteq (\partial\mathfrak{D}_k) \cap D_n$  of the boundary  $\partial\mathfrak{D}_k$  contained in the face  $D_n$  is counted as a side, called a *boundary side*. An *external face*  $D^{\text{ext}}$  (resp. *internal face*  $D^{\text{int}}$ ) of the local web  $W$  is a face having at least one (resp. no) boundary side.

In contrast to internal faces, external faces can have an odd number of sides. An alternative name for an external 2-face  $D_2^{\text{ext}}$ , 3-face  $D_3^{\text{ext}}$ , 4-face  $D_4^{\text{ext}}$  with one boundary side, and 5-face  $D_5^{\text{ext}}$  with one boundary side is a *cap*-, *fork*-, *H*-, and *half-hexagon*-face, respectively; see Figure 6. Also, as for global webs (see Definition 5), an alternative name for an internal 0-face  $D_0^{\text{int}}$ , 2-face  $D_2^{\text{int}}$ , 4-face  $D_4^{\text{int}}$ , and 6-face  $D_6^{\text{int}}$  is a *disk*-, *bigon*-, *square*-, and *hexagon*-face.

For example, the connected local web in Figure 5a has one fork-face, two H-faces, one half-hexagon-face, one external 6-face, one bigon-face, one square-face, and one internal 8-face. Also, the disconnected local web in Figure 5b has one cap-face, one fork-face, one H-face, one half-hexagon-face, one external 6-face, two disk-faces, one bigon-face, and one square-face.

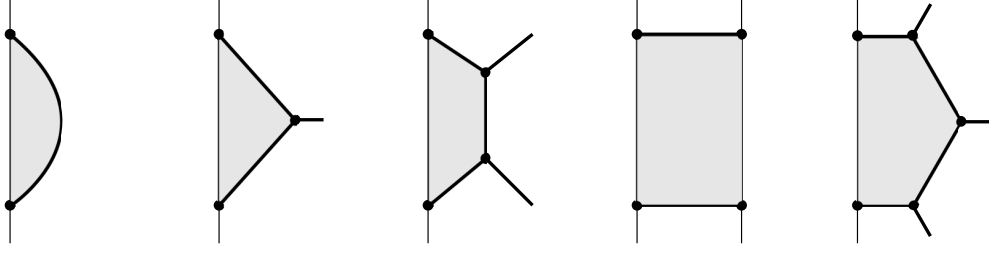


FIGURE 6. Cap-, fork-, H-, external 4-, and half-hexagon-face

#### 2.4. Combinatorial identity.

**Proposition 9** (compare [Kup96, §6.1]). *Let  $W$  be a connected local web in the closed disk  $\mathfrak{D}_0$  with non-empty boundary  $\partial W \neq \emptyset$ . Then,*

$$2\pi = \sum_{\text{internal faces } D_n^{\text{int}}} \left(2\pi - \frac{\pi}{3}n\right) + \sum_{\text{external faces } D_n^{\text{ext}}} \left(\pi - \frac{\pi}{3}(n-2)\right).$$

*Proof.* Since  $W$  is connected, its complement  $W^c \subseteq \mathfrak{D}_0$  contains at most one annulus, which necessarily contains the boundary  $\partial \mathfrak{D}_0$ . Such an annulus does not exist, since  $W$  has non-empty boundary  $\partial W \neq \emptyset$ . Thus, every component  $D$  of  $W^c$  is contractible, and of course puncture-free, so  $D$  is a face.

It follows that the closed disk  $\mathfrak{D}_0$  can be “tiling” by the dual graph of the local web  $W$ . More precisely, the vertices of the dual graph are the faces of  $W$ , and the complement of the dual graph consists of triangles. In Figure 7, we demonstrate this tiling procedure for the connected local web with non-empty boundary  $W$  that we saw in Figure 5a above (after forgetting the punctures).

This tiling gives rise to a flat Riemannian metric with conical singularities and piecewise-geodesic boundary on the closed disk  $\mathfrak{D}_0$ , by requiring that each triangle in the tiling is Euclidean equilateral. The result follows by applying the Gauss-Bonnet theorem to this singular flat surface.  $\square$

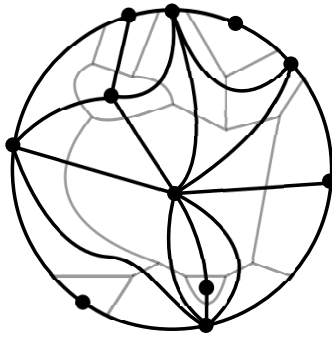


FIGURE 7. Tiling the closed disk with the dual graph of a local web

#### 2.5. Non-ellipticity.

**Definition 10.** As for global webs, a local web  $W$  in an ideal polygon  $\mathfrak{D}_k$  is *non-elliptic* if  $W$  has no disk-, bigon-, or square-faces. Otherwise,  $W$  is called *elliptic*; see Figure 8.

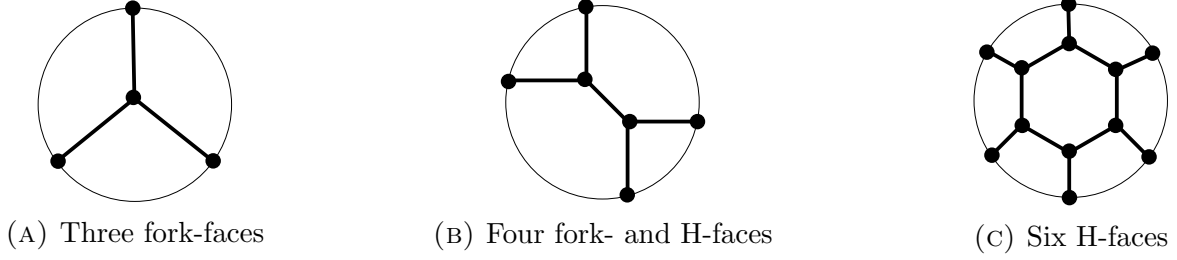


FIGURE 8. Non-elliptic local webs in the closed disk

**Lemma 11.** *Let  $W$  be a non-elliptic local web in the closed disk  $\mathfrak{D}_0$  such that  $W$  is connected, has non-empty boundary  $\partial W \neq \emptyset$ , and has at least one tri-valent vertex. Then  $W$  has at least three fork- and/or  $H$ -faces.*

*Proof.* We apply the formula of Proposition 9. For each internal face  $D_n^{\text{int}}$  of  $W$ , the internal angle  $2\pi - (\pi/3)n \leq 0$  is non-positive, since  $n \geq 6$  by non-ellipticity. For each external face  $D_n^{\text{ext}}$ , necessarily  $n \geq 2$ , and the external angle  $\pi - (\pi/3)(n-2) \leq 0$  is non-positive if and only if  $n \geq 5$ . By hypothesis,  $W$  has no cap-faces (else  $W$  would be an arc). So, those external faces  $D_n^{\text{ext}}$  with a positive contribution satisfy  $n = 3, 4$ . The result follows since fork- and  $H$ -faces contribute  $2\pi/3$  and  $\pi/3$ , respectively, in the formula.  $\square$

**Lemma 12.** *Non-elliptic local webs  $W$  in an ideal polygon  $\mathfrak{D}_k$  ( $k \geq 0$ ) having empty boundary  $\partial W = \emptyset$  do not exist.*

*Proof.* Suppose otherwise. We may assume  $W$  is connected. Since  $W$  is non-elliptic,  $W$  is not a loop (this uses that  $\mathfrak{D}_k$  is contractible). Then, the “rim” of  $W$  forms the boundary of a smaller closed disk  $\mathfrak{D}'_0 \subseteq \mathfrak{D}_k$  containing a sub-web  $W' \subseteq W$  that has non-empty boundary  $\partial W' \neq \emptyset$ . By non-ellipticity,  $W'$  does not have a cap-face, so  $W'$  has a tri-valent vertex. Applying Lemma 11 to connected components of  $W'$ , an analysis of inner-most components leads to the fact that  $W'$  has at least one fork- or  $H$ -face. By non-ellipticity,  $W'$  does not have an  $H$ -face, and it does not have a fork-face by orientation considerations applied to  $W$ .  $\square$

Lemma 12 plus a small argument allows us to relax the hypotheses of Lemma 11 as follows.

**Proposition 13.** *Let  $W$  be a non-elliptic local web in the closed disk  $\mathfrak{D}_0$  such that  $W$  is connected and has at least one tri-valent vertex. Then  $W$  has at least three fork- and/or  $H$ -faces. If, in addition,  $W$  is assumed not to have any cap-faces, then the connectedness hypothesis above is superfluous.*  $\square$

## 2.6. Essential and rung-less local webs.

**Definition 14.** A local web  $W$  in an ideal polygon  $\mathfrak{D}_k$  ( $k \geq 0$ ) is *essential* if the following two conditions are satisfied:

- (1) the local web  $W$  is non-elliptic;
- (2) the local web  $W$  is *taut*, namely, for any compact arc  $\alpha$  embedded in  $\mathfrak{D}_k$  whose boundary  $\partial\alpha$  lies in a single component  $E$  of the boundary  $\partial\mathfrak{D}_k$ , the number of intersection points  $\iota(W, E)$  of  $W$  with  $E$  does not exceed the number of intersection points  $\iota(W, \alpha)$  of  $W$  with  $\alpha$ , that is  $\iota(W, E) \leq \iota(W, \alpha)$ ; see Figures 9 and 10.

Note that essential local webs cannot have any cap- or fork-faces, but can have  $H$ -faces. Later, we will need the operation of adding or removing an  $H$ -face, depicted in Figure 11.



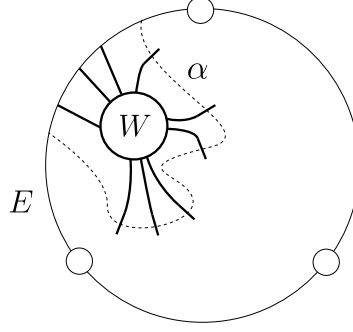
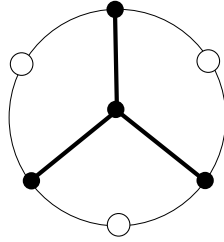
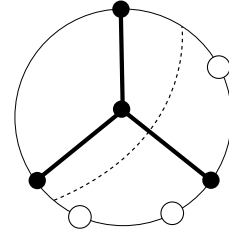


FIGURE 9. Tautness condition for an essential local web



(A) Essential



(B) Non-elliptic, but not essential

FIGURE 10. More non-elliptic webs

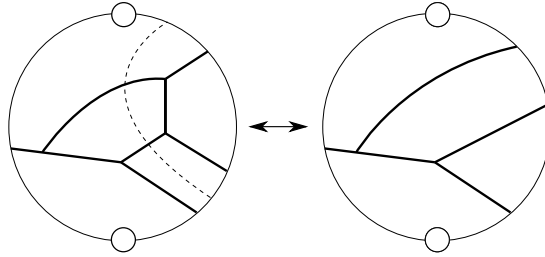


FIGURE 11. Adding or removing an H-face

**Definition 15.** A local web  $W$  in an ideal polygon  $\mathfrak{D}_k$  ( $k \geq 0$ ) is *rung-less* if it does not have any H-faces; see Figure 12.

**Remark 16.**

- (1) A consequence of Proposition 13, which we will not use, is that essential local webs in the closed disk  $\mathfrak{D}_0$  or ideal monoangle  $\mathfrak{D}_1$  do not exist.
- (2) Kuperberg [Kup96, §4, 6.1] uses the terminology “(core of a) non-convex non-elliptic web in the  $k$ -clapsed web space” for what we call a “(rung-less) essential local web in the ideal  $k$ -polygon”.

**2.7. Ladder-webs in ideal biangles.** Another name for an ideal 2-polygon  $\mathfrak{D}_2$  is an *ideal biangle*, or just *biangle*, denoted by  $\mathfrak{B}$ . The boundary  $\partial\mathfrak{B}$  consists of two ideal arcs  $E'$  and  $E''$ , called the *boundary edges* of the biangle. We want to characterize essential local webs  $W$  in the biangle  $\mathfrak{B}$ ; compare (1) in Remark 16.



FIGURE 12. More essential webs

**Definition 17.** For any surface  $\mathfrak{S}'$ , possibly with boundary, an *immersed multi-curve*, or just *multi-curve*,  $\Gamma = \{\gamma_i\}$  on  $\mathfrak{S}'$  is a finite collection of connected compact oriented curves  $\gamma_i$  embedded in  $\mathfrak{S}'$ , such that  $\partial\gamma_i = \gamma_i \cap \partial\mathfrak{S}'$ . Note that different  $\gamma_i$  and  $\gamma_j$  might intersect in  $\mathfrak{S}'$ . The component  $\gamma_i$  is a *loop* (resp. *arc*) if it has empty (resp. non-empty) boundary.

**Definition 18.** A *symmetric strand-set pair*  $S = (S', S'')$  for the biangle  $\mathfrak{B}$  is a pair of finite sequences  $S = (S', S'') = \{(s'_i), (s''_j)\}_{i,j=1,\dots,n}$  of disjoint oriented *strands* located on the boundary  $\partial\mathfrak{B} = E' \cup E''$ , such that the strands  $s'_i$  (resp.  $s''_j$ ) lie on the boundary edge  $E'$  (resp.  $E''$ ), and such that the number of *in-strands* (resp. *out-strands*) on  $E'$  is equal to the number of out-strands (resp. in-strands) on  $E''$ ; see the left-most picture in Figure 13.

The *local picture*  $\langle W(S) \rangle$  in the biangle  $\mathfrak{B}$  associated to a symmetric strand-set pair  $S = (S', S'')$  is the unique (up to ambient isotopy of  $\mathfrak{B}$ ) multi-curve obtained by connecting the strands on  $E'$  to the strands on  $E''$  in an “order preserving” and “minimally intersecting” way, as illustrated in the middle picture in Figure 13. Notice that the multi-curve  $\langle W(S) \rangle$  possesses only arc components.

A pair of arcs  $\gamma_1$  and  $\gamma_2$  in the local picture  $\langle W(S) \rangle$  are *oppositely-oriented with respect to the biangle  $\mathfrak{B}$*  if  $\gamma_1$  and  $\gamma_2$  go into (resp. out of) and out of (resp. into)  $E'$ , respectively. Observe that  $\gamma_1$  and  $\gamma_2$  intersect if and only if (1) they are oppositely-oriented, and (2) they intersect exactly once. Let  $\mathcal{P}(S) \subseteq \mathfrak{B}$  denote the set of intersection points  $p$  of pairs of oppositely-oriented arcs in the local picture  $\langle W(S) \rangle$ .

The *ladder-web*  $W(S)$  in the biangle  $\mathfrak{B}$  obtained from a symmetric strand-set pair  $S = (S', S'')$  is the unique (up to ambient isotopy of  $\mathfrak{B}$ ) local web obtained by resolving each intersection point  $p \in \mathcal{P}(S)$  into two vertices connected by a “horizontal” edge, called a *rung*; see Figures 13 and 14.

The following statement is implicit in [Kup96, Lemma 6.7] and also appears in [FS20, §9].

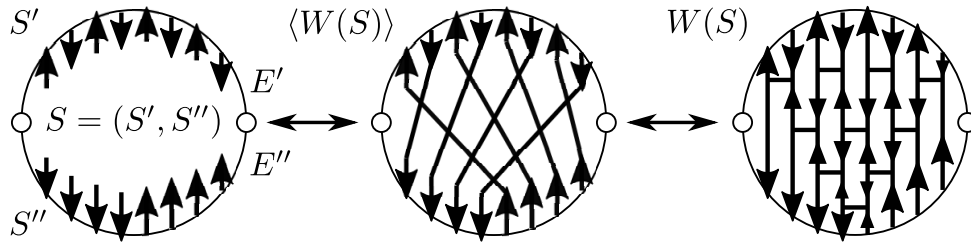


FIGURE 13. Construction of a ladder-web

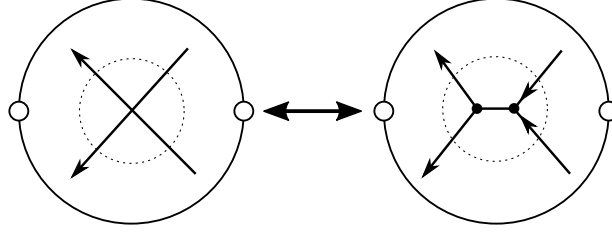


FIGURE 14. Replacing a local crossing with an H

**Proposition 19.** *The ladder-web  $W(S)$  is essential. Conversely, given an essential local web  $W$  in the biangle  $\mathfrak{B}$ , there exists a unique symmetric strand-set pair  $S = (S', S'')$  such that  $W = W(S)$ . Thus,  $W$  is a ladder-web.*

*Proof.* For the first statement, the non-ellipticity of  $W(S)$  follows because two oppositely-oriented curves in the local picture  $\langle W(S) \rangle$  do not cross more than once (if there were a square-face, a pair of curves would cross twice), and the tautness of  $W(S)$  is immediate.

Conversely, let  $W$  be an essential local web in  $\mathfrak{B}$ . The collection of ends of  $W$  located on the boundary edges  $E' \cup E''$  determines a strand-set pair  $S = (S', S'')$ . We show that  $S$  is symmetric and  $W = W(S)$ . In particular,  $S$  is uniquely determined.

If  $W$  has a tri-valent vertex, let  $\overline{W}$  denote the induced local web in the closed disk  $\mathfrak{D}_0$  underlying  $\mathfrak{B}$ , obtained by filling in the two punctures of  $\mathfrak{B}$ . Applying Proposition 13 to  $\overline{W}$  guarantees that  $\overline{W}$  (possibly minus some arc components) has at least three fork- and/or H-faces. At most two of these faces can “straddle” the two punctures of  $\mathfrak{B}$ , so we gather  $W$  has one fork- or H-face  $D^{\text{ext}}$  lying on  $E'$  or  $E''$ . Since  $W$  is taut,  $D^{\text{ext}}$  is an H-face.

We can then remove this H-face from  $\mathfrak{B}$  (recall Figure 11), obtaining a local web  $W_1$  that is essential and has strictly fewer tri-valent vertices than  $W$ . Repeating this process, we obtain a sequence of essential local webs  $W = W_0, W_1, \dots, W_n$  such that  $W_n$  has no tri-valent vertices and is obtained from  $W$  by removing finitely many H-faces. By non-ellipticity,  $W_n$  consists of a collection of arcs  $\gamma_i^{(n)}$  (as opposed to loops), and since  $W_n$  is taut, each arc  $\gamma_i^{(n)}$  connects to both boundary edges  $E'$  and  $E''$  of the biangle  $\mathfrak{B}$ .

By replacing each removed H-face with a local crossing (Figure 14), we obtain a multi-curve  $\Gamma$  in  $\mathfrak{B}$  consisting of arcs  $\gamma_i^{(0)}$ , each of which intersects both edges  $E'$  and  $E''$ , and such that only oppositely-oriented arcs  $\gamma_i^{(0)}$  intersect; see Figure 15. In particular, the strand-set pair  $S = (S', S'')$  is symmetric.

We claim  $\Gamma$  is the local picture  $\langle W(S) \rangle$ . Since only oppositely-oriented arcs intersect,  $\Gamma$  is “order preserving”. It remains to show  $\Gamma$  is “minimally intersecting”, namely that no arcs intersect more than once. Suppose they did. Then, because only oppositely-oriented arcs intersect, there would be an embedded bigon  $B$  in the complement  $\Gamma^c \subseteq \mathfrak{B}$ ; see the right side of Figure 16. Such an embedded bigon  $B$  corresponds in the local web  $W$  to a square-face, violating the non-ellipticity of  $W$ . We gather  $\Gamma = \langle W(S) \rangle$ , as claimed.

By definition of the multi-curve  $\Gamma$  and the local web  $W(S)$ , it follows that  $W = W(S)$ .  $\square$

For technical reasons, in §7 we will need the following concept.

**Definition 20.** The *local picture*  $\langle W_{\mathfrak{B}} \rangle$  associated to an essential local web  $W_{\mathfrak{B}}$  in the biangle  $\mathfrak{B}$  is the local picture  $\langle W(S) \rangle$  (see Definition 18) corresponding to the unique symmetric strand-set pair  $S = (S', S'')$  such that  $W_{\mathfrak{B}} = W(S)$ ; see Figure 15.

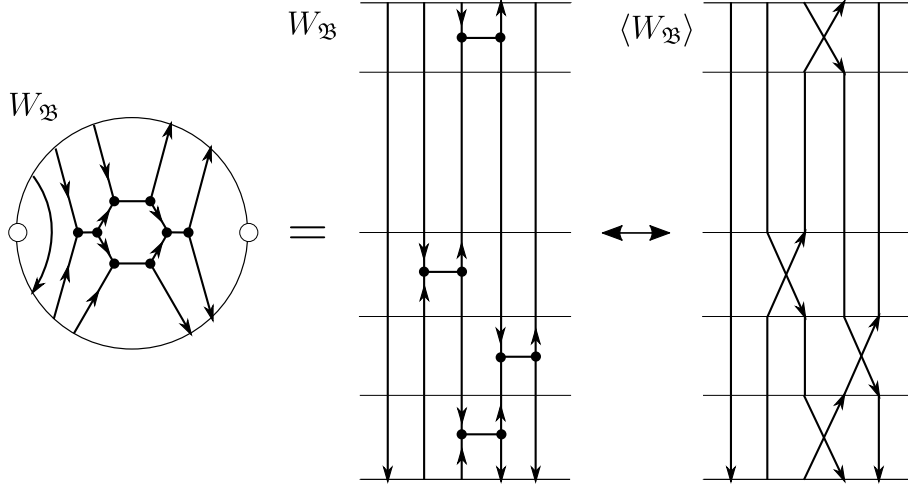


FIGURE 15. Essential local web  $W_{\mathfrak{B}}$  in the biangle, and its corresponding local picture  $\langle W_{\mathfrak{B}} \rangle$

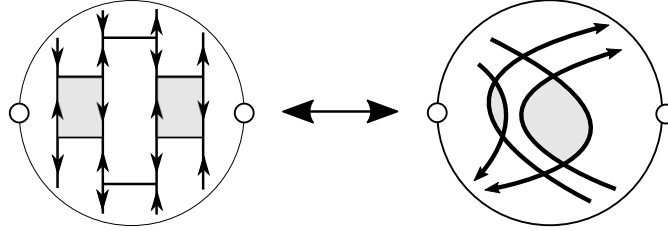


FIGURE 16. Prohibited ladder-webs and local pictures

**2.8. Honeycomb-webs in ideal triangles.** Another name for an ideal 3-polygon  $\mathfrak{D}_3$  is an *ideal triangle*, or just *triangle*, denoted by  $\mathfrak{T}$ . We want to characterize rung-less essential local webs  $W$  in the triangle  $\mathfrak{T}$ .

**Definition 21.** For a positive integer  $n > 0$ , the  *$n$ -out-honeycomb-web*  $H_n^{\text{out}}$  (resp.  *$n$ -in-honeycomb-web*  $H_n^{\text{in}}$ ) in the triangle  $\mathfrak{T}$  is the local web  $H_n$  dual to the  *$n$ -triangulation* of  $\mathfrak{T}$ , where the orientation of  $H_n$  is such that all the arrows go out of (resp. into) the triangle  $\mathfrak{T}$ .

For example, in Figure 17 we show the 5-out-honeycomb-web  $H_5^{\text{out}}$ .

The following statement is implicit in [Kup96, Lemma 6.8] and also appears in [FS20, §10].

**Proposition 22.** *A honeycomb-web  $H_n$  in the triangle  $\mathfrak{T}$  is rung-less and essential. Conversely, given a connected rung-less essential local web  $W$  in  $\mathfrak{T}$  having at least one tri-valent vertex, there exists a unique honeycomb-web  $H_n = H_n^{\text{out}}$  or  $H_n^{\text{in}}$  such that  $W = H_n$ . Consequently, a (possibly disconnected) rung-less essential local web  $W$  in  $\mathfrak{T}$  consists of a unique (possibly empty) honeycomb  $H_n$  together with a collection of disjoint oriented arcs located on the corners of  $\mathfrak{T}$ ; see the left hand side of Figure 18.*

*Proof.* The first statement is immediate.

*Step 1.* Let  $W$  be as in the second statement. Just like the proof of Proposition 19, applying Proposition 13 to the induced web  $\overline{W}$  in the underlying closed disk  $\mathfrak{D}_0$  guarantees that  $\overline{W}$  has at least three fork- and/or H-faces, at most three of which can straddle the three

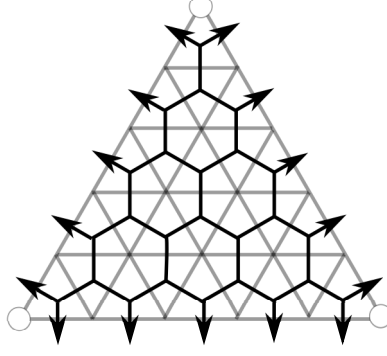
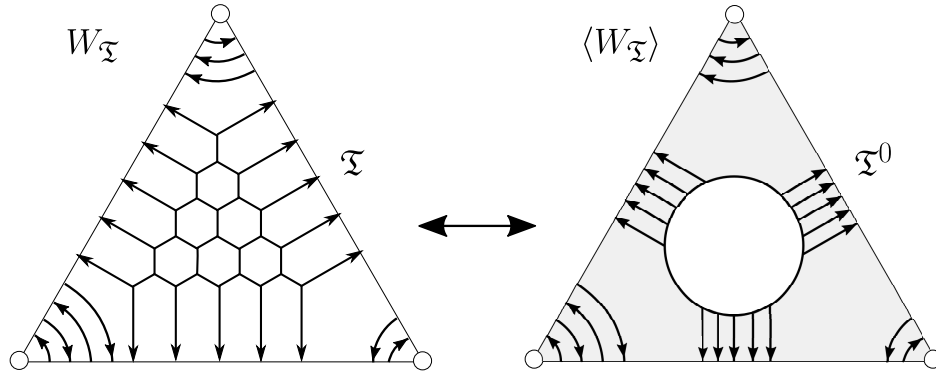


FIGURE 17. Honeycomb-web

FIGURE 18. Rung-less essential local web  $W_{\mathfrak{T}}$  in the triangle, and its corresponding local picture  $\langle W_{\mathfrak{T}} \rangle$  in the holed triangle

punctures of  $\mathfrak{T}$ . Since  $W$  is taut and rung-less,  $W$  has no fork- or H-faces. Thus,  $\overline{W}$  has exactly three fork- and/or H-faces, each of which straddles a puncture. Since these three faces are the only ones with a positive contribution in the formula of Proposition 9, they must be fork-faces. Moreover, since the total contribution of these three fork-faces is  $2\pi$ , every other face has exactly zero contribution. We gather that each interior face of  $W$  is a hexagon-face and each external face of  $W$  is a half-hexagon-face.

*Step 2.* To prove that  $W$  is a honeycomb-web  $H_n$ , we argue by induction on  $n$ , showing that the triangle  $\mathfrak{T}$  can be “tiled” by  $W$  face-by-face, starting from a corner of  $\mathfrak{T}$ .

(2.a) Assume inductively that some number of half-hexagon-faces have been laid down as part of the bottom layer of faces sitting on the bottom edge  $E$ , illustrated in Figure 19.

The strand labeled  $s$  does one of three things: (1) it ends on the right edge  $E'$  of the triangle  $\mathfrak{T}$ , thereby creating a fork straddling the right-most puncture and completing the bottom layer of faces; (2) it ends at a vertex disjoint from the vertices previously laid, hence the strand  $s$  is part of the boundary of the next half-hexagon-face; (3) it ends at one of the vertices previously laid.

In case (1), we continue to the next step of the induction, which deals with laying down the middle layers. In case (2), we repeat the current step. Lastly, we argue that case (3) cannot occur. Indeed, suppose it did. The strand  $s$  is part of the boundary of the next half-hexagon-face  $D_5^{\text{ext}}$ . But, as can be seen from the figure, the external face  $D_5^{\text{ext}}$  has  $\geq 6$  sides, which is a contradiction.

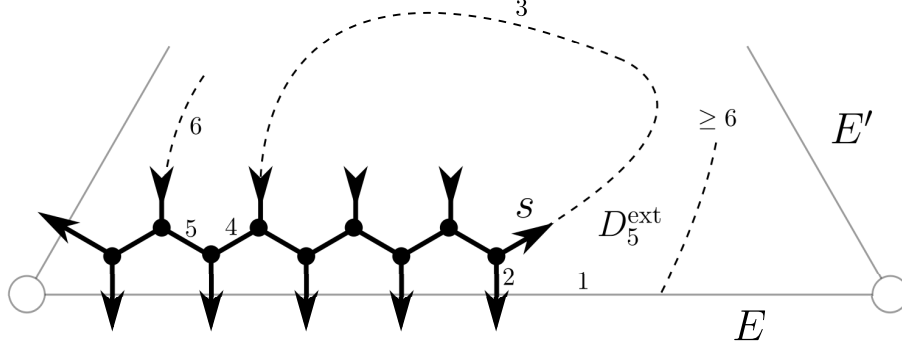


FIGURE 19. Laying down a honeycomb: 1 of 2

(2.b) Assume inductively that the bottom layer and some number of middle layers have been laid down, and moreover that some number of faces have been laid down as part of the current layer, illustrated in Figure 20. Consider the next face  $D$  shown in the figure.

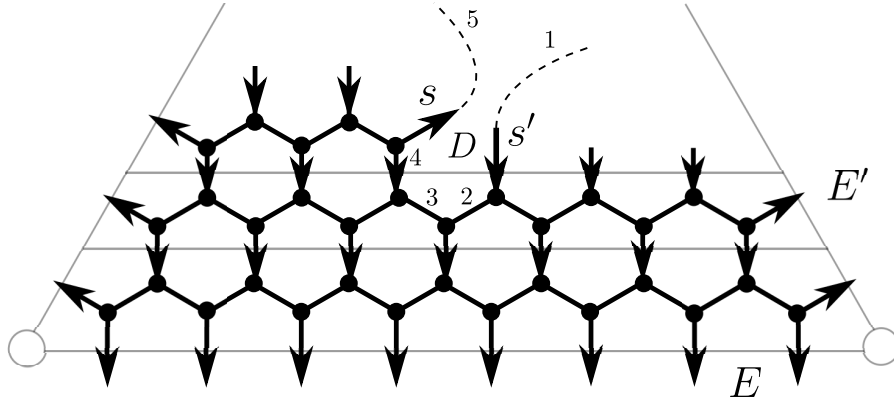


FIGURE 20. Laying down a honeycomb: 2 of 2

The face  $D$  is either external or internal. If it is internal, then  $D$  is a hexagon-face. In this case, the strands  $s$  and  $s'$  end at the fifth and sixth vertices of the hexagon-face, and we repeat the current step. Otherwise,  $D$  is external, so it is a half-hexagon-face,  $D = D_5^{\text{ext}}$ . However, we see from the figure that in this case  $D_5^{\text{ext}}$  has  $\geq 6$  sides, which is a contradiction.

To finish the induction, we repeat this step until the strand  $s'$  does not exist, in which case the strand  $s$  is part of the boundary of a half-hexagon-face lying on the boundary edge  $E'$ .

*Step 3.* The last statement of the proposition follows since each honeycomb-web  $H_n$  attaches to all three boundary edges of the triangle  $\mathfrak{T}$ .  $\square$

Later, in order to assign coordinates to webs, we will need to consider rung-less essential local webs  $W_{\mathfrak{T}}$  in a triangle  $\mathfrak{T}$  up to a certain equivalence relation. Say that a *local parallel-move* applied to  $W_{\mathfrak{T}}$  is a move swapping two arcs on the same corner of  $\mathfrak{T}$ ; see Figure 21.

**Definition 23.** Let  $\mathcal{W}_{\mathfrak{T}}$  denote the collection of rung-less essential local webs in the triangle  $\mathfrak{T}$ . We say that two local webs  $W_{\mathfrak{T}}$  and  $W'_{\mathfrak{T}}$  in  $\mathcal{W}_{\mathfrak{T}}$  are *equivalent up to corner-ambiguity* if they are related by local parallel-moves. The corner-ambiguity equivalence class of a local web  $W_{\mathfrak{T}} \in \mathcal{W}_{\mathfrak{T}}$  is denoted by  $[W_{\mathfrak{T}}]$ , and the set of corner-ambiguity classes is denoted  $[\mathcal{W}_{\mathfrak{T}}]$ .

For technical reasons, in §7 we will need the following concept.

**Definition 24.** Given a triangle  $\mathfrak{T}$ , a *holed triangle*  $\mathfrak{T}^0$  is the triangle minus an open disk  $\mathfrak{T}^0 = \mathfrak{T} - \text{Int}(\mathfrak{D}_0)$ ; see the right hand side of Figure 18 above. Let  $W_{\mathfrak{T}}$  be a rung-less essential local web in  $\mathfrak{T}$ , which by Proposition 22 consists of a honeycomb-web  $H_n$  together with a collection of disjoint oriented corner arcs  $\{\gamma_i\}$ . The *local picture*  $\langle W_{\mathfrak{T}} \rangle$  in  $\mathfrak{T}$  associated to  $W_{\mathfrak{T}}$  is the multi-curve (Definition 17) in the holed triangle  $\mathfrak{T}^0$  consisting of the corner arcs  $\gamma_i$  together with  $3n$  oriented arcs  $\{\gamma'_j\}$  disjoint from each other and from the  $\gamma_i$ , and going either all out of or all into the boundary  $\partial\mathfrak{D}_0$  of the removed disk, such that for each boundary edge  $E$  of the triangle  $\mathfrak{T}$  there are  $n$  arcs  $\gamma'_j$  ending on  $E$ ; see again Figure 18.

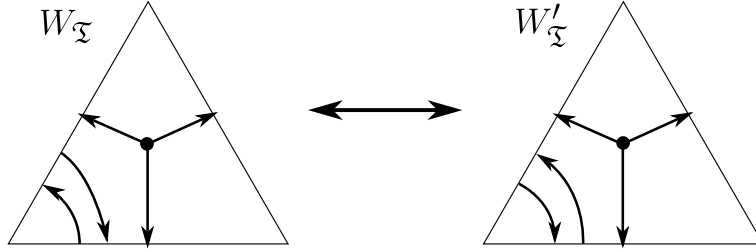


FIGURE 21. Local parallel-move

### 3. GOOD POSITION OF A GLOBAL WEB

Using the technical results about local webs from §2, we continue our study of the topology of global webs  $W$  on the surface  $\mathfrak{S}$ . For the remainder of this article, we assume  $\mathfrak{S}$  is equipped with an ideal triangulation  $\lambda$ ; see §1.1.

#### 3.1. Generic isotopies.

**Definition 25.** A web  $W$  on  $\mathfrak{S}$  is *generic* with respect to  $\lambda$  if none of its vertices intersect the edges  $E$  of  $\lambda$ , and if in addition  $W$  intersects  $\lambda$  transversally.

Two generic webs  $W$  and  $W'$  are *generically isotopic* if they are isotopic through generic webs; see Definition 4.

Whenever there is an ideal triangulation  $\lambda$  present, we always assume that “web” means “generic web”. However, we distinguish between isotopies and generic isotopies.

**3.2. Minimal position.** Recall the notion of two parallel-equivalent webs; see Definition 4.

**Definition 26.** Given a web  $W$  on the surface  $\mathfrak{S}$  and given an edge  $E$  of the ideal triangulation  $\lambda$ , the *local geometric intersection number of the web  $W$  with the edge  $E$*  is

$$I(W, E) = \min_{W'} (\iota(W', E)) \in \mathbb{Z}_{\geq 0} \quad (W' \text{ is parallel-equivalent to } W),$$

where  $\iota(W', E)$  is the number of intersection points of  $W'$  with  $E$ .

The web  $W$  is in *minimal position with respect to  $\lambda$*  if

$$\iota(W, E) = I(W, E) \in \mathbb{Z}_{\geq 0} \quad (\text{for all edges } E \text{ of } \lambda).$$

Let  $W'$  be a web, let  $\mathfrak{T}$  be a triangle in the ideal triangulation  $\lambda$ , and let  $W'_{\mathfrak{T}} = W' \cap \mathfrak{T}$  be the *restriction* of  $W'$  to  $\mathfrak{T}$ . Suppose that the local web  $W'_{\mathfrak{T}}$  is not taut; see Definition 14. Then there is an edge  $E$  of  $\lambda$  and a compact arc  $\alpha$  ending on  $E$  such that  $\iota(W', E) > \iota(W', \alpha)$ ; see Figure 22. We can then isotope the part of  $W'$  that is inside the *bigon*  $B$ , which is bounded

by  $\alpha$  and the segment  $\overline{E}$  of  $E$  delimited by  $\partial\alpha$ , into the adjacent triangle, resulting in a new web  $W$ . This is called a *tightening-move*. Similarly, if the restriction  $W'_\Sigma$  has an H-face, then we may apply an *H-move* to push the H into the adjacent triangle; see again Figure 22.

Note that tightening- and H-moves can be achieved with an isotopy of the web, but not a generic isotopy. Also, by definition, in order to apply an H-move, we assume that the shaded region shown at the bottom of Figure 22 is *empty*, namely it does not intersect the web.

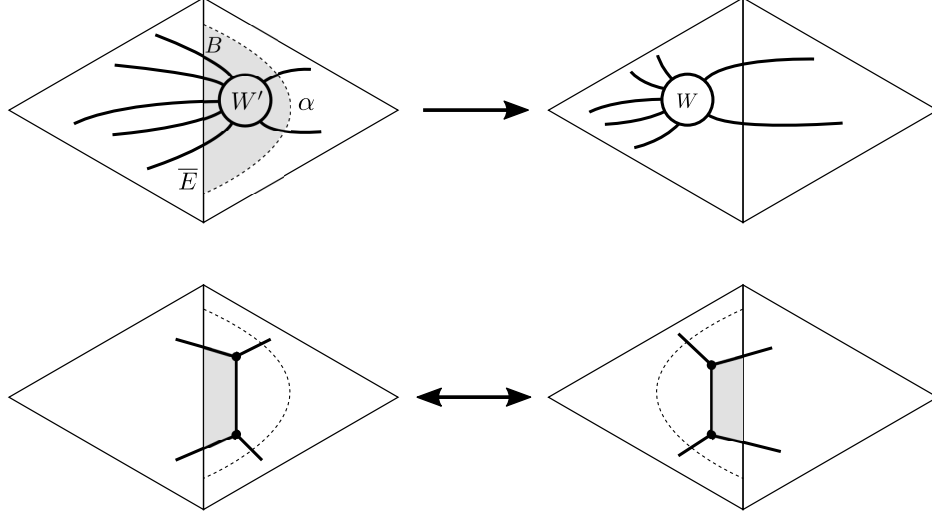


FIGURE 22. Tightening- and H-moves

We borrow the following result from [FS20, §7-8] and give essentially the same proof.

**Proposition 27.** *If  $W'$  is a non-elliptic web on the surface  $\mathfrak{S}$ , then there exists a non-elliptic web  $W$  that is parallel-equivalent to  $W'$  and that is in minimal position with respect to the ideal triangulation  $\lambda$ ; see Definition 6.*

*Moreover, given any two parallel-equivalent non-elliptic webs  $W$  and  $W'$  in minimal position, then  $W$  can be taken to  $W'$  by a sequence of H-moves, global parallel-moves, and generic isotopies; see Definition 4.*

*Proof.* We describe an algorithm that puts the web  $W'$  into minimal position  $W$ . If a tightening-move can be applied, do so. Otherwise, stop. Since tightening-moves strictly decrease the quantity

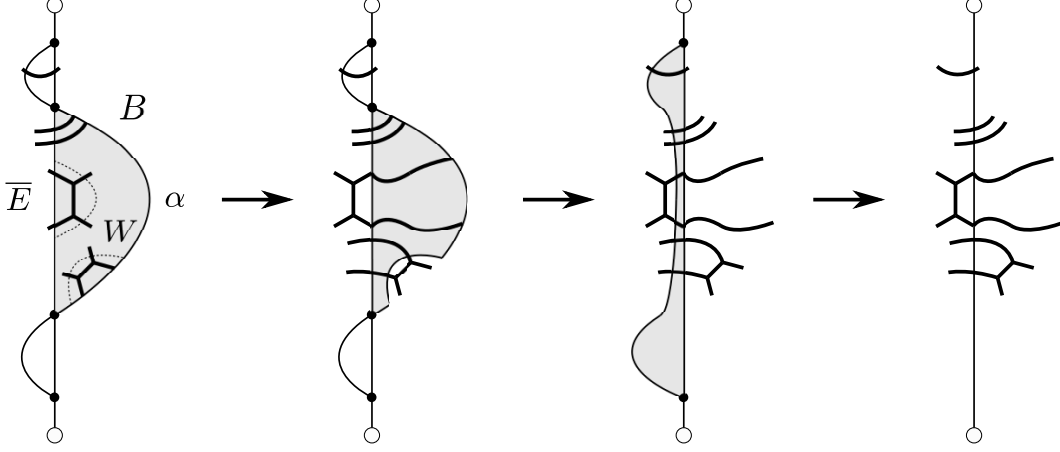
$$\sum_{E \text{ edge of } \lambda} \iota(W', E) \in \mathbb{Z}_{\geq 0},$$

the algorithm stops. We claim that the resulting non-elliptic web  $W$  is in minimal position.

Let  $W$  be as above. Let  $E$  be an edge of  $\lambda$ . By definition of the local geometric intersection number  $I(W, E)$  there exists a non-elliptic web, which by abuse of notation we also call  $W'$ , parallel-equivalent to  $W$  such that  $\iota(W', E) = I(W, E)$ .

By applying global parallel-moves to  $W'$ , we may assume that  $W$  and  $W'$  are isotopic, by an ambient isotopy  $\varphi_t$  of the surface  $\mathfrak{S}$  such that  $\varphi_0$  is the identity and  $\varphi_1(W) = W'$ . We may also assume that the isotopy is fixed near the punctures and satisfies the property that  $E$  and  $\varphi_1^{-1}(E)$  intersect finitely many times. A classical theorem in topology (see, for instance, [Eps66]) guarantees the existence of an embedded bigon  $B$  bounded by a segment  $\overline{E}$  of  $E$  and a segment  $\alpha$  of  $\varphi_1^{-1}(E)$ ; see Figure 23. Note that  $B \cap W$  may be non-empty.



FIGURE 23. Relating  $W$  and  $W'$  by H-moves and generic isotopies

By removing the two intersection points  $\overline{E} \cap \alpha$  from the bigon  $B$ , we obtain a biangle  $\mathfrak{B}$ . The minimality properties of  $W$  and  $W'$  imply that the local web restriction  $W_{\mathfrak{B}}$  is taut. It is also non-elliptic since, essentially by hypothesis,  $W$  is non-elliptic. So  $W_{\mathfrak{B}}$  is essential; Definition 14. By Proposition 19,  $W_{\mathfrak{B}}$  is a ladder-web.

Thus, by performing a finite number of H-moves to (retroactively) adjust  $W$  and  $W'$ , we may assume that  $W_{\mathfrak{B}}$  consists of a finite number of arcs stretching from  $\overline{E}$  to  $\alpha$ ; see Figure 23. By further adjusting  $W$  and  $W'$  by generic isotopies, the bigon  $B$  can be removed completely. Note that this process of adjusting  $W$  and  $W'$  by H-moves and generic isotopies preserves the number of intersection points of  $W$  and  $W'$  with  $\lambda$ , respectively.

By repeating the above step finitely many times in order to remove all of the bigons  $B$ , we may assume that the symmetry  $\varphi_1$  taking  $W$  to  $W'$  restricts to the identity mapping on the edge  $E$ . Hence,  $\iota(W, E) = \iota(W', E) = I(W, E)$ . Since the edge  $E$  was arbitrary, we are done.

The second statement of the proposition is achieved by applying the above argument to each edge  $E_i$  of  $\lambda$ , one at a time. The key observation is that if the symmetry  $\varphi_1$  fixes pointwise the edges  $E_1, E_2, \dots, E_{k-1}$ , then a bigon  $B$  formed between  $E_k$  and  $\varphi_1^{-1}(E_k)$  does not intersect  $E_1 \cup E_2 \cup \dots \cup E_{k-1}$ .

We gather that we may assume the symmetry  $\varphi_1$  sending  $W$  to  $W'$  restricts to the identity mapping on a neighborhood of  $\lambda$ , and also maps  $\mathfrak{T}$  to itself for each triangle  $\mathfrak{T}$  of  $\lambda$ . To finish,  $W$  can be brought to  $W'$  through a generic isotopy fixing pointwise  $\lambda$  (for instance, by Smale's theorem). As a remark, note that throughout this proof we never had to consider the arbitrary behavior of the ambient isotopy  $\varphi_t$  between  $0 < t < 1$ .  $\square$

**3.3. Split ideal triangulations.** From the ideal triangulation  $\lambda$ , we may form the *split ideal triangulation*  $\hat{\lambda}$ , uniquely defined up to ambient isotopy of the surface  $\mathfrak{S}$ , by doubling every edge  $E$  of  $\lambda$ . In other words, we “fatten” each edge  $E$  into a biangle  $\mathfrak{B}$ ; see Figure 24.

The notions of generic web and generic isotopy for webs with respect to the split ideal triangulation  $\hat{\lambda}$  are the same as those for webs with respect to the ideal triangulation  $\lambda$ . We always assume that webs are generic with respect to  $\hat{\lambda}$ .

To avoid cumbersome notation, we identify the triangles  $\mathfrak{T}$  of the ideal triangulation  $\lambda$  to the triangles  $\mathfrak{T}$  of the split ideal triangulation  $\hat{\lambda}$ .

**Remark 28.** For a related usage of split ideal triangulations, in the  $SL_2$ -case, see [BW11].

### 3.4. Good position.

**Definition 29.** A web  $W$  on  $\mathfrak{S}$  is in *good position* with respect to the split ideal triangulation  $\hat{\lambda}$  if the restriction  $W_{\mathfrak{B}} = W \cap \mathfrak{B}$  (resp.  $W_{\mathfrak{T}} = W \cap \mathfrak{T}$ ) of  $W$  to each biangle  $\mathfrak{B}$  (resp. triangle  $\mathfrak{T}$ ) of  $\hat{\lambda}$  is an essential (resp. rung-less essential) local web; see Figure 25.

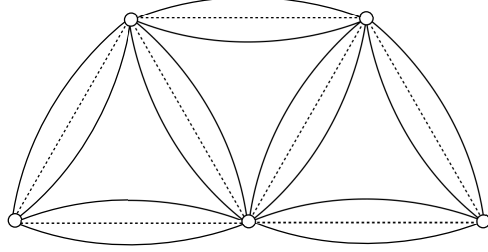


FIGURE 24. Split ideal triangulation

For a web  $W$  in good position, each restriction  $W_{\mathfrak{B}}$  to a biangle  $\mathfrak{B}$  of  $\hat{\lambda}$  is a ladder-web; see Definition 18, Proposition 19, and Figures 13 and 15. Also, each restriction  $W_{\mathfrak{T}}$  to a triangle  $\mathfrak{T}$  of  $\hat{\lambda}$  is a (possibly empty) honeycomb-web  $H_n$  together with a collection of disjoint oriented corner arcs; see Definition 21, Proposition 22, and Figures 17 and 18.

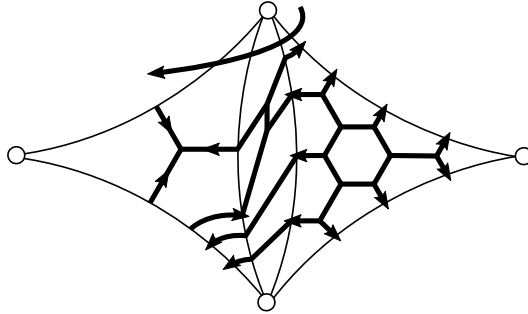


FIGURE 25. (Part of) a web in good position

If  $W$  is a web in good position, then a *modified H-move* carries an H-face in a biangle  $\mathfrak{B}$  to an H-face in an adjacent biangle  $\mathfrak{B}'$ , thereby replacing  $W$  with a new web  $W'$ ; see Figure 26. If, in addition,  $W$  is non-elliptic, then  $W'$  is also in good position. The non-elliptic condition for  $W$  is required to ensure that the new local web restriction  $W'_{\mathfrak{B}'}$  is non-elliptic.

Notice that the effect in the intermediate triangle  $\mathfrak{T}$  of a modified H-move is to swap two “parallel” oppositely-oriented corner arcs; see again Figure 26.

Once more, the following result is implicit in [Kup96, Lemma 6.5 and the proof of Theorem 6.2, pp. 139-140] (in the setting of an ideal  $k$ -polygon  $\mathfrak{D}_k$ ) and also appears in [FS20, §11].

**Proposition 30.** *If  $W'$  is a non-elliptic web on the surface  $\mathfrak{S}$ , then there exists a non-elliptic web  $W$  that is parallel-equivalent to  $W'$  and that is in good position with respect to the split ideal triangulation  $\hat{\lambda}$ .*

*Moreover, given any two parallel-equivalent non-elliptic webs  $W$  and  $W'$  in good position, then  $W$  can be taken to  $W'$  by a sequence of modified H-moves, global parallel-moves, and generic isotopies.*

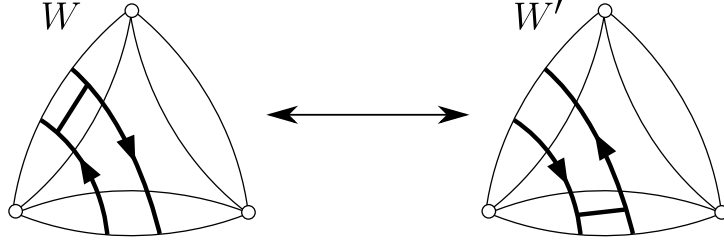


FIGURE 26. Modified H-move

*Proof.* By Proposition 27, we can replace  $W'$  with a non-elliptic web  $W$  that is parallel-equivalent to  $W'$  and that is in minimal position with respect to the ideal triangulation  $\lambda$ . We proceed to construct the split ideal triangulation  $\hat{\lambda}$ .

Let us begin by splitting each edge  $E$  of  $\lambda$  into two edges  $E'$  and  $E''$  that are “very close” to  $E$ . These split edges form a preliminary split ideal triangulation  $\hat{\lambda}$ , whose triangles (resp. biangles) are denoted by  $\hat{\mathfrak{T}}$  (resp.  $\mathfrak{B}_E$ ); see the left hand side of Figure 27.

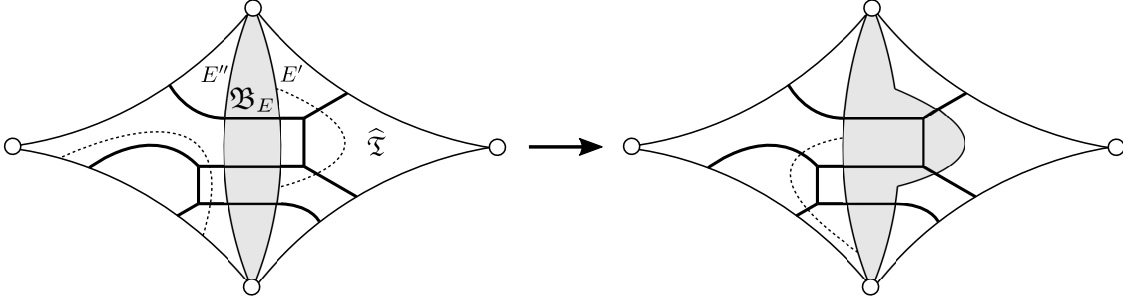


FIGURE 27. Enlarging a biangle

By definition of minimal position, the restriction  $W_{\mathfrak{T}}$  of  $W$  to a triangle  $\mathfrak{T}$  of the ideal triangulation  $\lambda$  is taut. Since, in addition,  $W$  is non-elliptic, we have that  $W_{\mathfrak{T}}$  is essential. If the preliminary split ideal triangulation  $\hat{\lambda}$  is sufficiently close to  $\lambda$ , then the restriction  $W_{\hat{\mathfrak{T}}}$  of  $W$  to the triangle  $\hat{\mathfrak{T}} \subseteq \mathfrak{T}$  associated to  $\mathfrak{T}$  is also an essential local web. If all of the local webs  $W_{\hat{\mathfrak{T}}}$  are rung-less, then  $W$  is in good position with respect to  $\hat{\lambda}$ .

Otherwise, assume  $W_{\hat{\mathfrak{T}}}$  has an H-face on an edge of  $\hat{\lambda}$ , say the edge  $E'$ . Then by isotopy we can enlarge the biangle  $\mathfrak{B}_E$  until it just envelops this H-face. In other words, we can isotope the edge  $E'$  so that it cuts out this H-face from the triangle  $\hat{\mathfrak{T}}$ ; see Figure 27. The result of this step is a new split ideal triangulation  $\hat{\lambda}$ , retaining the property that the local web restrictions  $W_{\hat{\mathfrak{T}}}$  are essential. Repeating this process until all of the local webs  $W_{\hat{\mathfrak{T}}}$  are rung-less, we obtain the desired split ideal triangulation  $\hat{\lambda}$ . Notice it might be the case that there is more than one biangle into which an H-face can be moved; see again Figure 27.

For the second statement of the proposition, note that if a non-elliptic web  $W$  is in good position with respect to  $\hat{\lambda}$ , then  $W$  is minimal with respect to the ideal triangulation  $\lambda$  (which, for the sake of argument, we can take to be contained in  $\hat{\lambda}$ , that is  $\lambda \subseteq \hat{\lambda}$ ). Indeed, this follows by the proof of the first part of Proposition 27. Similarly,  $W'$  is in minimal position. Thus, applying the second part of Proposition 27, we gather that  $W$  can be taken

to  $W'$  by a finite sequence of H-moves, global parallel-moves, and generic isotopies. The result follows from the definition of good position and modified H-moves.  $\square$

#### 4. GLOBAL COORDINATES FOR NON-ELLIPTIC WEBS

Recall that  $\mathcal{W}_{\mathfrak{S}}$  denotes the collection of parallel-equivalence classes of non-elliptic webs on the surface  $\mathfrak{S}$ ; see just below Definition 6. Our goal in this section is to define a function  $\Phi_{\lambda}^{\text{FG}} : \mathcal{W}_{\mathfrak{S}} \rightarrow \mathbb{Z}_{\geq 0}^N$  depending on the ideal triangulation  $\lambda$ , where  $N = -8\chi(\mathfrak{S}) > 0$  is a positive integer depending only on the topology of  $\mathfrak{S}$ . In §5-7, we characterize the image of  $\Phi_{\lambda}^{\text{FG}}$  and prove that it is injective. We think of  $\Phi_{\lambda}^{\text{FG}}$  as putting global coordinates on  $\mathcal{W}_{\mathfrak{S}}$ .

**4.1. Dotted ideal triangulations.** Consider a surface  $\mathfrak{S}' = \mathfrak{S}$  or  $= \mathfrak{T}$  equipped with an ideal triangulation  $\lambda$ , where, only in this sub-section,  $\lambda = \mathfrak{T}$  when  $\mathfrak{S}' = \mathfrak{T}$ . The associated *dotted ideal triangulation* is the pair consisting of  $\lambda$  together with  $N' = N$  or  $= 7$  distinct *dots* attached to the 1- and 2-cells of  $\lambda$ , where there are two *edge-dots* attached to each 1-cell and there is one *triangle-dot* attached to each 2-cell; see Figure 28. Given a triangle  $\mathfrak{T}$  of  $\lambda$  and an edge  $E$  of  $\mathfrak{T}$ , it makes sense to talk about the *left-edge-dot* and *right-edge-dot* as viewed from  $\mathfrak{T}$ ; see Figure 28b. Choosing an ordering for the  $N'$  dots lying on the dotted ideal triangulation  $\lambda$  defines a one-to-one correspondence between functions  $\{\text{dots}\} \rightarrow \mathbb{Z}_{\geq 0}$  and elements of  $\mathbb{Z}_{\geq 0}^{N'}$ . We always assume that such an ordering has been chosen.



FIGURE 28. Dotted ideal triangulations

**4.2. Local coordinate functions.** Consider a dotted ideal triangle  $\mathfrak{T}$ ; see Figure 28b. Recall (Definition 23) that  $\mathcal{W}_{\mathfrak{T}}$  denotes the collection of rung-less essential local webs  $W_{\mathfrak{T}}$  in  $\mathfrak{T}$ , and that  $[\mathcal{W}_{\mathfrak{T}}]$  denotes the set of corner-ambiguity classes  $[W_{\mathfrak{T}}]$  of local webs  $W_{\mathfrak{T}}$  in  $\mathcal{W}_{\mathfrak{T}}$ .

**Definition 31.** An *integer local coordinate function*, or just *local coordinate function*,

$$\Phi_{\mathfrak{T}} : \mathcal{W}_{\mathfrak{T}} \longrightarrow \mathbb{Z}^7$$

is a function assigning to each local web  $W_{\mathfrak{T}}$  in  $\mathcal{W}_{\mathfrak{T}}$  one integer coordinate per dot lying on the dotted triangle  $\mathfrak{T}$ , satisfying the following properties:

- (1) if a local web  $W_{\mathfrak{T}}$  in  $\mathcal{W}_{\mathfrak{T}}$  can be written  $W_{\mathfrak{T}} = W'_{\mathfrak{T}} \sqcup W''_{\mathfrak{T}}$  as the disjoint union of two local webs, each in  $\mathcal{W}_{\mathfrak{T}}$ , then

$$\Phi_{\mathfrak{T}}(W_{\mathfrak{T}}) = \Phi_{\mathfrak{T}}(W'_{\mathfrak{T}}) + \Phi_{\mathfrak{T}}(W''_{\mathfrak{T}}) \in \mathbb{Z}^7;$$

- (2) for an edge  $E$  of  $\mathfrak{T}$ , the ordered pair of coordinates  $(a_E^L, a_E^R)$  of the function  $\Phi_{\mathfrak{T}}$  assigned to the left- and right-edge-dots lying on  $E$ , respectively, depends only on the pair  $(n_E^{\text{in}}, n_E^{\text{out}})$  of numbers of in- and out-strands of the local web  $W_{\mathfrak{T}} \in \mathcal{W}_{\mathfrak{T}}$  on the edge  $E$ ; conversely, different pairs  $(n_E^{\text{in}}, n_E^{\text{out}})$  yield different pairs of coordinates  $(a_E^L, a_E^R)$ ;

- (3) there are two symmetries; the first is that  $\Phi_{\mathfrak{T}}$  respects the rotational symmetry of the triangle, and the second is that if the numbers  $n_E^{\text{in}}$  and  $n_E^{\text{out}}$  of in- and out-stands on an edge  $E$  are exchanged, then the coordinates  $a_E^L$  and  $a_E^R$  are exchanged as well;
- (4) observe that, by Property (1), the function  $\Phi_{\mathfrak{T}}(W_{\mathfrak{T}}) = \Phi_{\mathfrak{T}}(W'_{\mathfrak{T}})$  agrees on local webs  $W_{\mathfrak{T}}$  and  $W'_{\mathfrak{T}}$  in  $\mathcal{W}_{\mathfrak{T}}$  representing the same corner-ambiguity class  $[W_{\mathfrak{T}}] = [W'_{\mathfrak{T}}]$  in  $[\mathcal{W}_{\mathfrak{T}}]$ , consequently inducing a function

$$[\Phi_{\mathfrak{T}}] : [\mathcal{W}_{\mathfrak{T}}] \longrightarrow \mathbb{Z}^7;$$

we require that this induced function  $[\Phi_{\mathfrak{T}}]$  is an injection.

The coordinates assigned by  $\Phi_{\mathfrak{T}}$  to edge-dots (resp. triangle-dots) are called *edge-coordinates* (resp. *triangle-coordinates*).

We illustrate properties (1), (2), (3) in Figures 29 and 30.

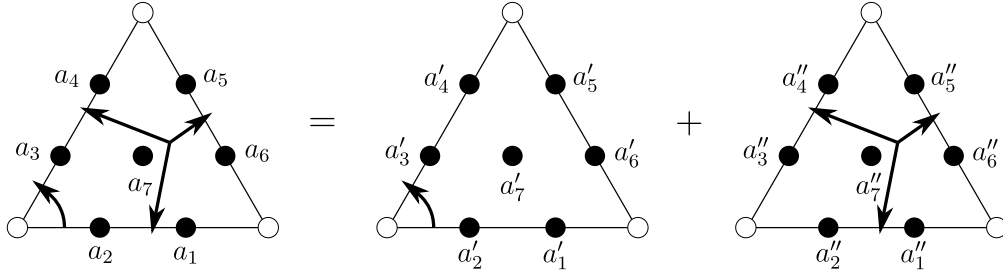


FIGURE 29. Property (1):  $a_i = a'_i + a''_i$

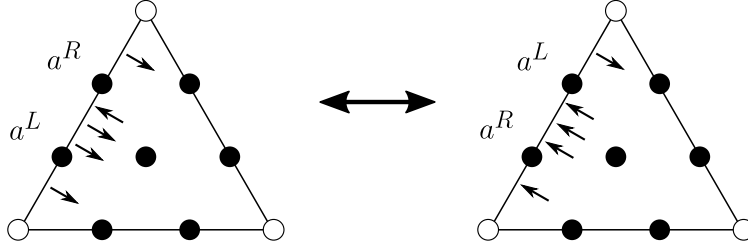


FIGURE 30. Properties (2) and (3)

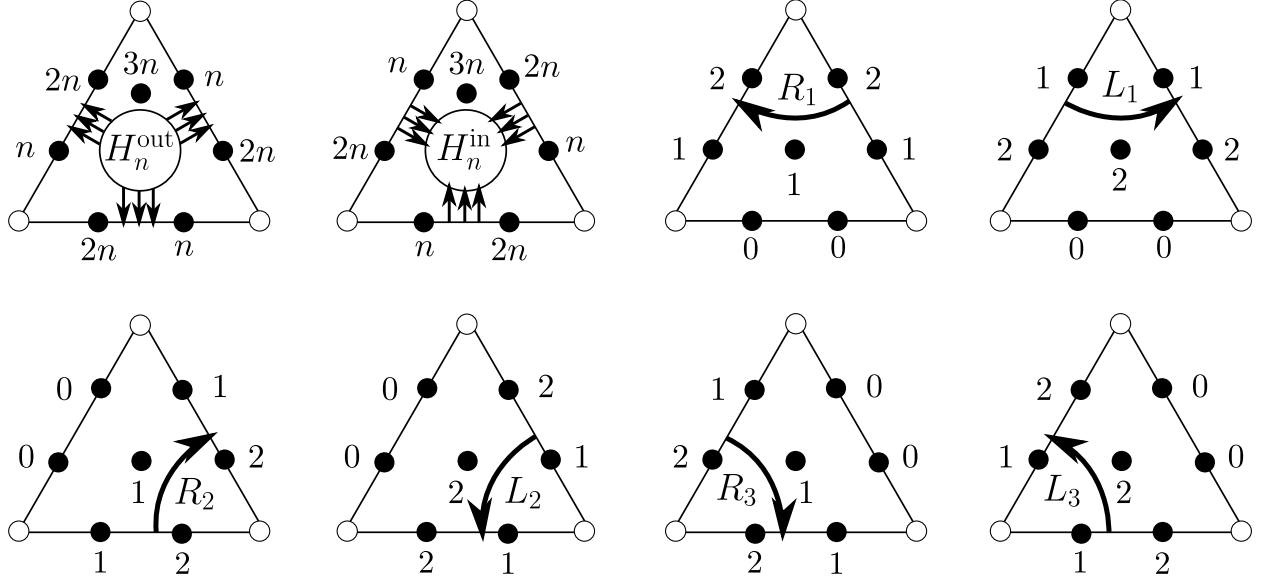
**4.3. Local coordinates from Fock-Goncharov theory.** We define an explicit *Fock-Goncharov local coordinate function*  $\Phi_{\mathfrak{T}}^{\text{FG}} : \mathcal{W}_{\mathfrak{T}} \rightarrow \mathbb{Z}_{\geq 0}^7$  valued in non-negative integers.

By Property (1) in Definition 31, it suffices to define  $\Phi_{\mathfrak{T}}^{\text{FG}}$  on connected local webs in  $\mathcal{W}_{\mathfrak{T}}$ . By Proposition 22, these come in one of exactly eight types  $H_n^{\text{out}}$ ,  $H_n^{\text{in}}$ ,  $R_1$ ,  $L_1$ ,  $R_2$ ,  $L_2$ ,  $R_3$ ,  $L_3$  illustrated in Figure 31. In the figure, note that in the two top left triangles we have, for visibility, drawn the local pictures  $\langle H_n^{\text{out}} \rangle$  and  $\langle H_n^{\text{in}} \rangle$  as a short-hand for the actual  $n$ -out-honeycomb-web  $H_n^{\text{out}}$  and  $n$ -in-honeycomb-web  $H_n^{\text{in}}$ , respectively; see Definition 24. It is immediate that  $\Phi_{\mathfrak{T}}^{\text{FG}}$  satisfies property (3) and the first part of (2). The second part of (2) follows by the invertibility of the matrix  $\begin{pmatrix} 2 & 1 \\ 1 & 2 \end{pmatrix}$ . We will check property (4) in §5.

**Remark 32.**

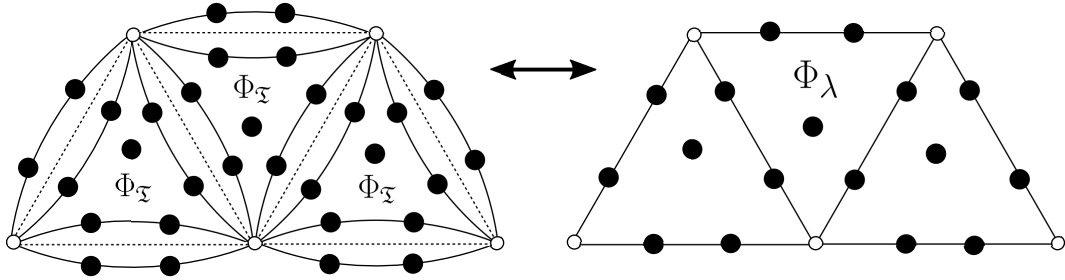
- (1) Xie [Xie13] writes down the same local coordinates (up to a multiplicative factor of 3) for  $R_1$ ,  $L_1$ ,  $R_2$ ,  $L_2$ ,  $R_3$ ,  $L_3$  as well as the 1-honeycomb-webs  $H_1^{\text{out}}$  and  $H_1^{\text{in}}$ .

- (2) The definition of these local coordinates can be checked experimentally by studying the highest terms of the Fock-Goncharov  $\mathrm{SL}_3$ -trace polynomials; see the Introduction.
- (3) The analogous coordinates in the  $\mathrm{SL}_2$ -setting are geometric intersection numbers; see the Introduction. In contrast, these  $\mathrm{SL}_3$ -coordinates depend crucially on the orientation of the surface.

FIGURE 31. Fock-Goncharov local coordinate function  $\Phi_{\mathfrak{T}}^{\mathrm{FG}}$ 

**4.4. Global coordinates from local coordinate functions.** Assume that, for an abstract dotted triangle  $\mathfrak{T}$ , we have chosen an arbitrary local coordinate function  $\Phi_{\mathfrak{T}} : \mathcal{W}_{\mathfrak{T}} \rightarrow \mathbb{Z}^7$ . We show that this induces a *global coordinate function*  $\Phi_{\lambda} : \mathcal{W}_{\mathfrak{S}} \rightarrow \mathbb{Z}^N$  that is well-adapted to the choice of  $\Phi_{\mathfrak{T}}$ . The argument uses only properties (1), the first part of (2), and (3) of  $\Phi_{\mathfrak{T}}$ .

*Step 1.* Consider the split ideal triangulation  $\hat{\lambda}$  (§3.3). We put dots on each triangle  $\mathfrak{T}$  of  $\hat{\lambda}$ . The chosen local coordinate function  $\Phi_{\mathfrak{T}}$  can be associated to each of these dotted triangles  $\mathfrak{T}$ ; see the left hand side of Figure 32.

FIGURE 32. Local coordinates  $\Phi_{\mathfrak{T}}$  attached to the triangles  $\mathfrak{T}$  of  $\hat{\lambda}$  (left), and the corresponding global coordinates  $\Phi_{\lambda}$  attached to  $\lambda$  (right)

*Step 2.* Fix a non-elliptic web  $W$  on  $\mathfrak{S}$  that is in good position (Definition 29) with respect to the split ideal triangulation  $\hat{\lambda}$ . We assign to  $W$  one integer coordinate per dot lying on the dotted ideal triangulation  $\lambda$ , namely an element  $\Phi_{\lambda}(W)$  in  $\mathbb{Z}^N$ .

By good position, the local web restriction  $W_{\mathfrak{T}} = W \cap \mathfrak{T}$  is in  $\mathcal{W}_{\mathfrak{T}}$  for each triangle  $\mathfrak{T}$  of  $\hat{\lambda}$ . So, we may evaluate the local coordinate function  $\Phi_{\mathfrak{T}}$  on  $W_{\mathfrak{T}}$ , obtaining coordinates for each of the seven dots lying on the dotted triangle  $\mathfrak{T}$  of  $\hat{\lambda}$ . For instance, in this way we assign coordinates to all of the dots shown on the left hand side of Figure 32 above. We claim that these coordinates “glue together” along each biangle  $\mathfrak{B}$  of  $\hat{\lambda}$  in such a way that we obtain one coordinate per dot lying on the dotted ideal triangulation  $\lambda$ ; see Figure 32.

Indeed, suppose  $\mathfrak{B}$  is a biangle between two triangles  $\mathfrak{T}'$  and  $\mathfrak{T}''$  of  $\hat{\lambda}$ . Let  $E'$  and  $E''$  be the corresponding boundary edges of  $\mathfrak{B}$ , and let  $a_{E'}^L$  and  $a_{E'}^R$  (resp.  $a_{E''}^L$  and  $a_{E''}^R$ ) be the coordinates assigned by  $\Phi_{\mathfrak{T}'}$  (resp.  $\Phi_{\mathfrak{T}''}$ ) to the left- and right-edge-dots, respectively, lying on  $E'$  (resp.  $E''$ ) as viewed from  $\mathfrak{T}'$  (resp.  $\mathfrak{T}''$ ). Also, denote by  $n_{E'}^{\text{in}}$  and  $n_{E'}^{\text{out}}$  (resp.  $n_{E''}^{\text{in}}$  and  $n_{E''}^{\text{out}}$ ) the numbers of in- and out-strands of the local web restriction  $W_{\mathfrak{T}'}$  (resp.  $W_{\mathfrak{T}''}$ ) lying on the edge  $E'$  (resp.  $E''$ ); see Figure 33.

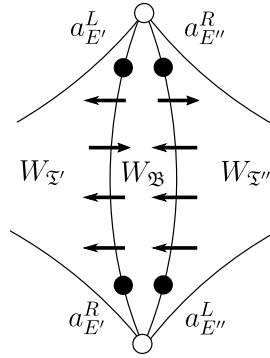


FIGURE 33. Local coordinates attached to a biangle:  $a_{E'}^L = a_{E''}^R$  and  $a_{E'}^R = a_{E''}^L$

Since, by good position, the restriction  $W_{\mathfrak{B}} = W \cap \mathfrak{B}$  is a ladder-web, we have  $n_{E'}^{\text{out}} = n_{E''}^{\text{in}}$  and  $n_{E'}^{\text{in}} = n_{E''}^{\text{out}}$ . It follows immediately from properties (3) and the first part of (2) that the coordinates across from each other agree  $a_{E'}^L = a_{E''}^R$  and  $a_{E'}^R = a_{E''}^L$ . So, we may glue together the two pairs of coordinates into two coordinates lying on the edge  $E$  of  $\lambda$ , as desired.

For an example on the once punctured torus  $\mathfrak{S}$ , using the Fock-Goncharov local coordinate function  $\Phi_{\mathfrak{T}}^{\text{FG}}$ , see Figure 34. Note that the web  $W$  in the example has one hexagon-face. All the other components of  $W^c$  are not contractible. So  $W$  is indeed non-elliptic.

*Step 3.* For a general non-elliptic web  $W'$  on  $\mathfrak{S}$ , by the first part of Proposition 30 there exists a non-elliptic web  $W$  that is parallel-equivalent to  $W'$  and that is in good position with respect to the split ideal triangulation  $\hat{\lambda}$ . Define  $\Phi_{\lambda}(W') = \Phi_{\lambda}(W)$  in  $\mathbb{Z}^N$ .

To show that  $\Phi_{\lambda}(W')$  is well-defined, suppose that  $W_2$  is another web such as  $W$ . By the second part of Proposition 30, the non-elliptic webs  $W$  and  $W_2$  are related by a sequence of modified H-moves and global parallel-moves. The effect of either one of these moves on a web in good position is to swap, possibly many, “parallel” oppositely-oriented corner arcs in the triangles  $\mathfrak{T}$  of  $\hat{\lambda}$ ; recall Figures 26 and 3 above, respectively. By property (1) of  $\Phi_{\mathfrak{T}}$ , we thus have  $\Phi_{\lambda}(W) = \Phi_{\lambda}(W_2)$ , as claimed.

From this point on, our approach diverges from that in [FS20]. In particular, our coordinates are different from theirs.

**Definition 33.** The *Fock-Goncharov global coordinate function*

$$\Phi_{\lambda}^{\text{FG}} : \mathcal{W}_{\mathfrak{S}} \longrightarrow \mathbb{Z}_{\geq 0}^N$$

is the well-defined global coordinate function on  $\mathcal{W}_{\mathfrak{S}}$ , valued in non-negative integers, induced by the Fock-Goncharov local coordinate function  $\Phi_{\mathfrak{T}}^{\text{FG}}$ .

**Proposition 34.** *The Fock-Goncharov global coordinate function  $\Phi_{\lambda}^{\text{FG}}$  is an injection of sets.*

This will be proved in §6-7.

**Remark 35.** Proposition 34 is valid for any global coordinate function  $\Phi_{\lambda} : \mathcal{W}_{\mathfrak{S}} \rightarrow \mathbb{Z}^N$  induced by a local coordinate function  $\Phi_{\mathfrak{T}} : \mathcal{W}_{\mathfrak{T}} \rightarrow \mathbb{Z}^7$ . The proof is the same as the one we will give for the Fock-Goncharov global coordinate function  $\Phi_{\lambda}^{\text{FG}}$ . It turns out that proving the injectivity of  $\Phi_{\lambda}$  uses property (4), but not the second part of property (2). The latter is needed to characterize the image of  $\Phi_{\lambda}$  in terms of the image of the local function  $\Phi_{\mathfrak{T}}$ .

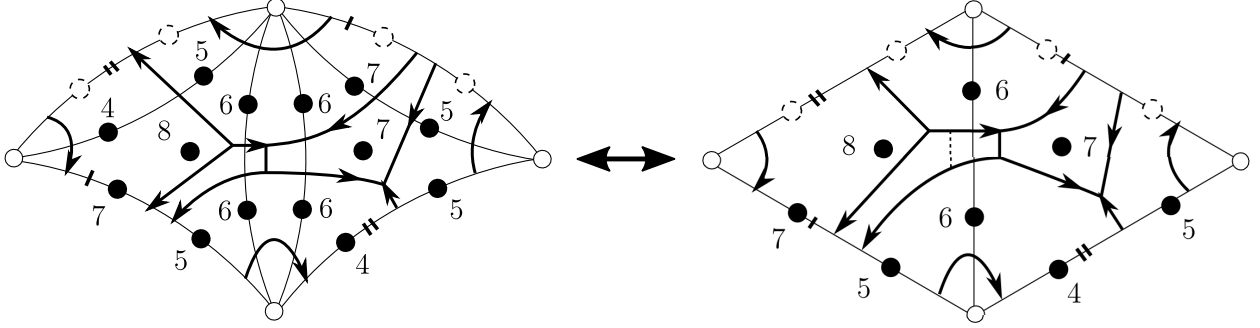


FIGURE 34. Tropical Fock-Goncharov  $\mathcal{A}$ -coordinates for a non-elliptic web

## 5. KNUTSON-TAO CONE

For  $N = -8\chi(\mathfrak{S}) > 0$ , we construct a subset  $\mathcal{C}_{\lambda}^{+} \subseteq \mathbb{Z}_{\geq 0}^N$  that we will show, in §6-7, is the image  $\mathcal{C}_{\lambda}^{+} = \Phi_{\lambda}^{\text{FG}}(\mathcal{W}_{\mathfrak{S}})$  of the mapping  $\Phi_{\lambda}^{\text{FG}} : \mathcal{W}_{\mathfrak{S}} \rightarrow \mathbb{Z}_{\geq 0}^N$  constructed in §4. The subset  $\mathcal{C}_{\lambda}^{+}$  is called the Knutson-Tao cone associated to the ideal triangulation  $\lambda$ , and is defined by finitely many Knutson-Tao rhombus inequalities and modulo 3 congruence conditions.

### 5.1. Integer cones.

**Definition 36.** An *integer cone*, or just *cone*,  $\mathcal{C}$  is a sub-monoid of  $\mathbb{Z}^n$  for some positive integer  $n$ . In other words,  $\mathcal{C} \subseteq \mathbb{Z}^n$  is a subset that contains 0 and is closed under addition. An element  $c \in \mathcal{C}$  is called a *cone point*.

A *partition* of  $\mathcal{C}$  is a decomposition  $\mathcal{C} = \mathcal{C}_1 \sqcup \mathcal{C}_2 \sqcup \cdots \sqcup \mathcal{C}_k$  as a disjoint union of subsets.

A *positive integer cone*, or just *positive cone*,  $\mathcal{C}^{+}$  is a cone that is contained in  $\mathbb{Z}_{\geq 0}^n$ .

We define notions of independence for cones.

**Definition 37.** Let  $\mathcal{C} \subseteq \mathbb{Z}^n \subseteq \mathbb{Q}^n$  be a cone, and let  $\Omega \subseteq \mathbb{Q}$  be a subset such that  $0 \in \Omega$ . Let  $c_1, c_2, \dots, c_k$  be a collection of cone points in  $\mathcal{C}$ . We say that the cone points  $\{c_i\}$

- (1) *span* the cone  $\mathcal{C}$  if every cone point  $c \in \mathcal{C}$  can be written as a  $\mathbb{Z}_{\geq 0}$ -linear combination of the cone points  $\{c_i\}$ ;
- (2) are *weakly independent* over  $\Omega$  if

$$\omega_1 c_1 + \cdots + \omega_k c_k = 0 \in \mathbb{Q}^n \implies \omega_1 = \cdots = \omega_k = 0 \quad (\omega_1, \dots, \omega_k \in \Omega);$$

- (3) form a *weak basis* of  $\mathcal{C}$  if they span  $\mathcal{C}$  and are weakly independent over  $\Omega = \mathbb{Z}_{\geq 0} \subseteq \mathbb{Q}$ ;



(4) are *strongly independent* over  $\Omega$  if

$$\omega_1 c_1 + \cdots + \omega_k c_k = \omega'_1 c_1 + \cdots + \omega'_k c_k \in \mathbb{Q}^n \implies \omega_1 = \omega'_1, \dots, \omega_k = \omega'_k \quad (\omega_i, \omega'_j \in \Omega).$$

As a warm-up:

- strongly independent over  $\Omega \implies$  weakly independent over  $\Omega$ ;
- strongly independent over  $\mathbb{Z}_{\geq 0} \iff$  weakly independent over  $\mathbb{Z} \iff$  linearly independent over  $\mathbb{Q}$  (the usual definition from Linear Algebra).

The following technical fact is immediate from the definitions.

**Lemma 38.** *Let  $\mathcal{C}, \mathcal{C}' \subseteq \mathbb{Z}^n$  be two cones. Consider a  $\mathbb{Z}_{\geq 0}$ -linear bijection  $\psi: \mathcal{C}' \rightarrow \mathcal{C}$  that extends to a  $\mathbb{Q}$ -linear isomorphism  $\tilde{\psi}: \mathbb{Q}^n \rightarrow \mathbb{Q}^n$ . Let  $\{c_i\}$  be cone points of  $\mathcal{C}$  and let  $\{c'_i\}$  be cone points of  $\mathcal{C}'$ , such that  $\psi(c'_i) = c_i$ . Then,*

- (1) *if the cone points  $\{c'_i\}$  span  $\mathcal{C}'$ , then the cone points  $\{c_i\}$  span  $\mathcal{C}$ ;*
- (2) *if the  $\{c'_i\}$  are weakly independent over  $\mathbb{Z}_{\geq 0}$ , then so are the  $\{c_i\}$ ;*
- (3) *therefore, if the  $\{c'_i\}$  form a weak basis of  $\mathcal{C}'$ , then the  $\{c_i\}$  form a weak basis of  $\mathcal{C}$ ;*
- (4) *if the  $\{c'_i\}$  are strongly independent over  $\mathbb{Z}_{\geq 0}$ , then so are the  $\{c_i\}$ ;*
- (5) *the function  $\psi$  sends partitions of  $\mathcal{C}'$  to partitions of  $\mathcal{C}$ .* □

**5.2. Local Knutson-Tao cone.** Let  $\mathfrak{T}$  be a dotted ideal triangle (§4.1); recall Figure 28b above. In this section, we are going to order the dots on  $\mathfrak{T}$  so that if the dots are labeled as in the left hand side of Figure 35, then a point  $c \in \mathbb{Z}^7$  will be written

$$(*) \quad c = (a_{11}, a_{12}, a_{21}, a_{22}, a_{31}, a_{32}, a) \in \mathbb{Z}^7.$$

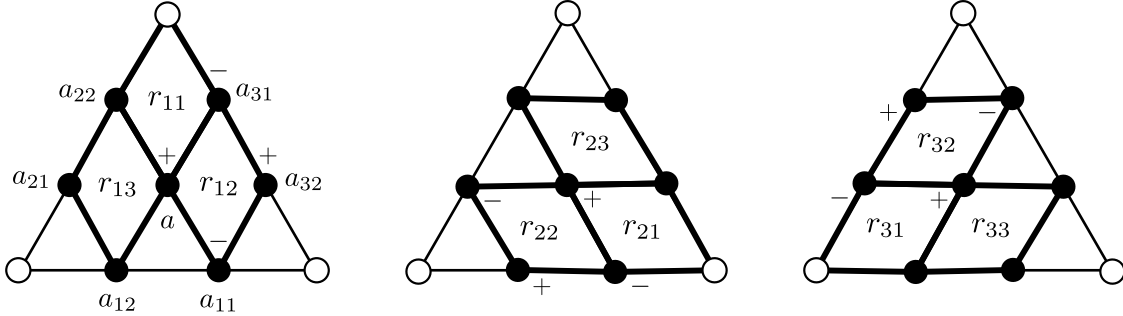


FIGURE 35. Rhombus numbers

Let  $\mathbb{Z}/3 \subseteq \mathbb{Q}$  denote the set of integer thirds within the rational numbers, namely  $\mathbb{Z}/3$  is the image of the map  $\mathbb{Z} \rightarrow \mathbb{Q}$  sending  $n \mapsto n/3$ . Note that  $\mathbb{Z} \subseteq \mathbb{Z}/3$ .

To each point  $c \in \mathbb{Z}^7$ , as in Equation (\*), associate a 9-tuple of *rhombus numbers*

$$r(c) = (r_{11}, r_{12}, r_{13}, r_{21}, r_{22}, r_{23}, r_{31}, r_{32}, r_{33}) \in (\mathbb{Z}/3)^9$$

by the linear equations (see Figure 35 above)

$$\begin{aligned} r_{12} &= (a + a_{32} - a_{11} - a_{31})/3, & r_{11} &= (a_{22} + a_{31} - a - 0)/3, \\ r_{13} &= (a_{21} + a - a_{12} - a_{22})/3; \\ r_{22} &= (a + a_{12} - a_{21} - a_{11})/3, & r_{21} &= (a_{32} + a_{11} - a - 0)/3, \\ r_{23} &= (a_{31} + a - a_{22} - a_{32})/3; \\ r_{32} &= (a + a_{22} - a_{31} - a_{21})/3, & r_{31} &= (a_{12} + a_{21} - a - 0)/3, \\ r_{33} &= (a_{11} + a - a_{32} - a_{12})/3. \end{aligned}$$

**Definition 39.** The *local Knutson-Tao positive cone*, or just *local Knutson-Tao cone* or *local cone*,  $\mathcal{C}_{\mathfrak{T}}^+$  associated to the dotted ideal triangle  $\mathfrak{T}$  is defined by

$$\mathcal{C}_{\mathfrak{T}}^+ = \{c \in \mathbb{Z}^7; \quad r(c) = (r_{11}, r_{12}, r_{13}, r_{21}, r_{22}, r_{23}, r_{31}, r_{32}, r_{33}) \in \mathbb{Z}_{\geq 0}^9 \subseteq (\mathbb{Z}/3)^9\}.$$

By linearity, this indeed defines a cone contained in  $\mathbb{Z}^7$ . We will prove below in this sub-section that  $\mathcal{C}_{\mathfrak{T}}^+ \subseteq \mathbb{Z}_{\geq 0}^7$  is, in fact, a positive cone.

**Remark 40.** The inequalities  $3r_{ij} \geq 0$  are known as the Knutson-Tao rhombus inequalities; see [KT99, Appendix 2] and [GS15, §3.1]. Note that  $3r_{ij}$  is always in  $\mathbb{Z}$  by definition. We impose the additional modulo 3 congruence condition that the  $r_{ij}$  are integers. This is analogous to the parity condition imposed in [Foc97, §3.1] in the case of  $\mathrm{SL}_2$ .

To see that  $\mathcal{C}_{\mathfrak{T}}^+$  is non-trivial, one checks that the image  $\Phi_{\mathfrak{T}}^{\mathrm{FG}}(\mathcal{W}_{\mathfrak{T}})$  of the Fock-Goncharov local coordinate function  $\Phi_{\mathfrak{T}}^{\mathrm{FG}} : \mathcal{W}_{\mathfrak{T}} \rightarrow \mathbb{Z}_{\geq 0}^7$  (§4.3) lies in the local cone  $\Phi_{\mathfrak{T}}^{\mathrm{FG}}(\mathcal{W}_{\mathfrak{T}}) \subseteq \mathcal{C}_{\mathfrak{T}}^+$ . By property (1) in Definition 31, it suffices to check this on the connected local webs in  $\mathcal{W}_{\mathfrak{T}}$ ; recall Figure 31 above. Specifically, using the convention in Equation (\*), we have

$$\begin{aligned} c(R_1) &= \Phi_{\mathfrak{T}}^{\mathrm{FG}}(R_1) = (0, 0, 1, 2, 2, 1, 1), & c(L_1) &= \Phi_{\mathfrak{T}}^{\mathrm{FG}}(L_1) = (0, 0, 2, 1, 1, 2, 2), \\ c(R_2) &= \Phi_{\mathfrak{T}}^{\mathrm{FG}}(R_2) = (2, 1, 0, 0, 1, 2, 1), & c(L_2) &= \Phi_{\mathfrak{T}}^{\mathrm{FG}}(L_2) = (1, 2, 0, 0, 2, 1, 2), \\ c(R_3) &= \Phi_{\mathfrak{T}}^{\mathrm{FG}}(R_3) = (1, 2, 2, 1, 0, 0, 1), & c(L_3) &= \Phi_{\mathfrak{T}}^{\mathrm{FG}}(L_3) = (2, 1, 1, 2, 0, 0, 2), \\ c(H_n^{\mathrm{in}}) &= \Phi_{\mathfrak{T}}^{\mathrm{FG}}(H_n^{\mathrm{in}}) = (2n, n, 2n, n, 2n, n, 3n), \\ c(H_n^{\mathrm{out}}) &= \Phi_{\mathfrak{T}}^{\mathrm{FG}}(H_n^{\mathrm{out}}) = (n, 2n, n, 2n, n, 2n, 3n). \end{aligned}$$

The associated 9-tuples of rhombus numbers are

$$\begin{aligned} r(c(R_1)) &= (1, 0, 0, 0, 0, 0, 0, 0, 0), & r(c(L_1)) &= (0, 1, 1, 0, 0, 0, 0, 0, 0), \\ r(c(R_2)) &= (0, 0, 0, 1, 0, 0, 0, 0, 0), & r(c(L_2)) &= (0, 0, 0, 0, 1, 1, 0, 0, 0), \\ r(c(R_3)) &= (0, 0, 0, 0, 0, 0, 1, 0, 0), & r(c(L_3)) &= (0, 0, 0, 0, 0, 0, 0, 1, 1), \\ r(c(H_n^{\mathrm{in}})) &= (0, 0, n, 0, 0, n, 0, 0, n), \\ r(c(H_n^{\mathrm{out}})) &= (0, n, 0, 0, n, 0, 0, n, 0). \end{aligned}$$

By rank considerations, the eight cone points  $c(R_1)$ ,  $c(L_1)$ ,  $c(R_2)$ ,  $c(L_2)$ ,  $c(R_3)$ ,  $c(L_3)$ ,  $c(H_n^{\mathrm{in}})$ ,  $c(H_n^{\mathrm{out}})$  have a linear dependence relation over  $\mathbb{Z}$ . For instance,

$$c(H_n^{\mathrm{out}}) + c(H_n^{\mathrm{in}}) = n(c(L_1) + c(L_2) + c(L_3)) \in \mathcal{C}_{\mathfrak{T}}^+.$$

See Figure 36. Nevertheless, we can say the following:

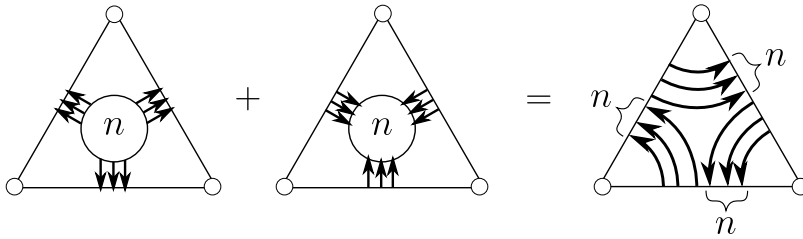


FIGURE 36. Linear dependence relation over  $\mathbb{Z}$

**Proposition 41.** *The collection of eight cone points*

$$c(R_1), c(L_1), c(R_2), c(L_2), c(R_3), c(L_3), c(H_1^{\text{in}}), c(H_1^{\text{out}}) \in \Phi_{\mathfrak{T}}^{\text{FG}}(\mathcal{W}_{\mathfrak{T}}) \subseteq \mathcal{C}_{\mathfrak{T}}^+$$

*forms a weak basis of the Knutson-Tao local cone  $\mathcal{C}_{\mathfrak{T}}^+$ .*

*Among these eight cone points, the seven points*

$$c(R_1), c(L_1), c(R_2), c(L_2), c(R_3), c(L_3), c(H_1^{\text{in}})$$

*are strongly independent over  $\mathbb{Z}_{\geq 0}$ , and the seven points*

$$c(R_1), c(L_1), c(R_2), c(L_2), c(R_3), c(L_3), c(H_1^{\text{out}})$$

*are strongly independent over  $\mathbb{Z}_{\geq 0}$ . Moreover, each cone point  $c$  in  $\mathcal{C}_{\mathfrak{T}}^+$  can be uniquely expressed in exactly one of the following three forms:*

$$\begin{aligned} c &= n_1 c(R_1) + n_2 c(L_1) + \cdots + n_6 c(L_3), \\ c &= n_1 c(R_1) + n_2 c(L_1) + \cdots + n_6 c(L_3) + n c(H_1^{\text{in}}), \\ c &= n_1 c(R_1) + n_2 c(L_1) + \cdots + n_6 c(L_3) + n c(H_1^{\text{out}}), \quad (n_i \in \mathbb{Z}_{\geq 0}, \quad n \in \mathbb{Z}_{> 0}). \end{aligned}$$

**Corollary 42.** *The local Knutson-Tao cone satisfies the property that  $\mathcal{C}_{\mathfrak{T}}^+ = \Phi_{\mathfrak{T}}^{\text{FG}}(\mathcal{W}_{\mathfrak{T}}) \subseteq \mathbb{Z}_{\geq 0}^7$ . In particular,  $\mathcal{C}_{\mathfrak{T}}^+$  is a positive cone.  $\square$*

**Corollary 43.** *The Fock-Goncharov local coordinate function  $\Phi_{\mathfrak{T}}^{\text{FG}} : \mathcal{W}_{\mathfrak{T}} \rightarrow \mathcal{C}_{\mathfrak{T}}^+$  satisfies property (4) in Definition 31, namely, the induced function  $[\Phi_{\mathfrak{T}}^{\text{FG}}] : [\mathcal{W}_{\mathfrak{T}}] \hookrightarrow \mathcal{C}_{\mathfrak{T}}^+$ , defined on the collection of corner-ambiguity classes  $[W_{\mathfrak{T}}]$  of local webs  $W_{\mathfrak{T}}$  in  $\mathcal{W}_{\mathfrak{T}}$ , is an injection.*

*Proof.* Assume  $\Phi_{\mathfrak{T}}^{\text{FG}}(W_{\mathfrak{T}}) = \Phi_{\mathfrak{T}}^{\text{FG}}(W'_{\mathfrak{T}}) \in \mathcal{C}_{\mathfrak{T}}^+$ . This cone point falls into one of the three families in Proposition 41. For the sake of argument, suppose

$$\Phi_{\mathfrak{T}}^{\text{FG}}(W_{\mathfrak{T}}) = \Phi_{\mathfrak{T}}^{\text{FG}}(W'_{\mathfrak{T}}) = n_1 c(R_1) + n_2 c(L_1) + \cdots + n_6 c(L_3) + n c(H_1^{\text{in}}) \quad (n_i \in \mathbb{Z}_{\geq 0}, \quad n \in \mathbb{Z}_{> 0}).$$

Note that  $n c(H_1^{\text{in}}) = c(H_n^{\text{in}})$  in  $\mathcal{C}_{\mathfrak{T}}^+$ ; see Figure 31. By the uniqueness property in Proposition 41 together with property (1) in Definition 31, we gather that  $W_{\mathfrak{T}}$  and  $W'_{\mathfrak{T}}$  have  $1 + \sum_{i=1}^6 n_i$  connected components, one of which is a  $n$ -in-honeycomb  $H_n^{\text{in}}$ , and  $n_1$  (resp.  $n_2, n_3, n_4, n_5, n_6$ ) of which are corner arcs  $R_1$  (resp.  $L_1, R_2, L_2, R_3, L_3$ ). The only ambiguity is how these corner arcs are permuted on their respective corners, that is  $[W_{\mathfrak{T}}] = [W'_{\mathfrak{T}}]$  in  $[\mathcal{W}_{\mathfrak{T}}]$ .  $\square$

*Proof of Proposition 41.* Define two subsets  $\overline{(\mathcal{C}_{\mathfrak{T}}^+)^{\text{in}}}$  and  $(\mathcal{C}_{\mathfrak{T}}^+)^{\text{out}}$  of  $\mathcal{C}_{\mathfrak{T}}^+$  by

$$(\#) \quad \overline{(\mathcal{C}_{\mathfrak{T}}^+)^{\text{in}}} = \text{Span}_{\mathbb{Z}_{\geq 0}}(c(R_1), c(L_1), c(R_2), c(L_2), c(R_3), c(L_3)) + \mathbb{Z}_{\geq 0} \cdot c(H_1^{\text{in}}),$$

$$(\#\#) \quad (\mathcal{C}_{\mathfrak{T}}^+)^{\text{out}} = \text{Span}_{\mathbb{Z}_{\geq 0}}(c(R_1), c(L_1), c(R_2), c(L_2), c(R_3), c(L_3)) + \mathbb{Z}_{> 0} \cdot c(H_1^{\text{out}}).$$

(Here,  $A + B = \{a + b; \quad a \in A \text{ and } b \in B\}$ .) Put

$$\begin{aligned} c_1 &= c(R_1), & c_2 &= c(L_1), & c_3 &= c(R_2), & c_4 &= c(L_2), \\ c_5 &= c(R_3), & c_6 &= c(L_3), & c_7 &= c(H_1^{\text{in}}), & c_8 &= c(H_1^{\text{out}}). \end{aligned}$$

By Lemma 38, with  $\mathcal{C} = \mathcal{C}_{\mathfrak{T}}^+$ , in order to prove Proposition 41 it suffices to establish:

**Claim 44.** *There exists*

- (1) *a cone  $\mathcal{C}' \subseteq \mathbb{Z}^7$ ;*
- (2) *a collection of cone points  $c'_1, \dots, c'_8$  in  $\mathcal{C}'$ ;*
- (3) *a partition  $\mathcal{C}' = \overline{(\mathcal{C}')^{>0}} \sqcup (\mathcal{C}')^{<0}$ ;*
- (4) *a  $\mathbb{Z}_{\geq 0}$ -linear bijection  $\psi : \mathcal{C}' \rightarrow \mathcal{C}_{\mathfrak{T}}^+$ ;*

(5) an extension  $\tilde{\psi}$  of  $\psi$  to a  $\mathbb{Q}$ -linear isomorphism  $\tilde{\psi}: \mathbb{Q}^7 \rightarrow \mathbb{Q}^7$ ;

such that

- (1) we have  $\psi(c'_i) = c_i$ ;
- (2) we have  $\psi(\overline{(\mathcal{C}')^{>0}}) = \overline{(\mathcal{C}'^+)^{\text{in}}}$  and  $\psi((\mathcal{C}')^{<0}) = (\mathcal{C}'^+)^{\text{out}}$ ;
- (3) the eight cone points  $c'_1, \dots, c'_6, c'_7, c'_8$  form a weak basis of the cone  $\mathcal{C}'$ ;
- (4) the seven cone points  $c'_1, \dots, c'_6, c'_7$  are strongly independent over  $\mathbb{Z}_{\geq 0}$ ;
- (5) the seven cone points  $c'_1, \dots, c'_6, c'_8$  are strongly independent over  $\mathbb{Z}_{\geq 0}$ .

We prove the claim. Define  $\mathcal{C}' \subseteq \mathbb{Z}_{\geq 0}^6 \times \mathbb{Z} \subseteq \mathbb{Z}^7$  by

$$(**) \quad \mathcal{C}' = \{(r_{11}, r_{12}, r_{21}, r_{22}, r_{31}, r_{32}, x) \in \mathbb{Z}_{\geq 0}^6 \times \mathbb{Z}; \quad -x \leq \min(r_{12}, r_{22}, r_{32})\}.$$

It follows from the definition that  $\mathcal{C}'$  is a cone. Put

$$\begin{aligned} c'_1 &= (1, 0, 0, 0, 0, 0, 0), & c'_2 &= (0, 1, 0, 0, 0, 0, 0), \\ c'_3 &= (0, 0, 1, 0, 0, 0, 0), & c'_4 &= (0, 0, 0, 1, 0, 0, 0), \\ c'_5 &= (0, 0, 0, 0, 1, 0, 0), & c'_6 &= (0, 0, 0, 0, 0, 1, 0), \\ c'_7 &= (0, 0, 0, 0, 0, 0, 1), & c'_8 &= (0, 1, 0, 1, 0, 1, -1). \end{aligned}$$

One checks that  $c'_1, \dots, c'_8$  are in  $\mathcal{C}'$ . Define

$$\overline{(\mathcal{C}')^{>0}} = \mathcal{C}' \cap (\mathbb{Z}_{\geq 0}^6 \times \mathbb{Z}_{\geq 0}), \quad (\mathcal{C}')^{<0} = \mathcal{C}' \cap (\mathbb{Z}_{\geq 0}^6 \times \mathbb{Z}_{<0}).$$

Then  $\mathcal{C}' = \overline{(\mathcal{C}')^{>0}} \sqcup (\mathcal{C}')^{<0}$  is a partition.

First, we show  $c'_1, \dots, c'_6, c'_7, c'_8$  spans  $\mathcal{C}'$ . We see that

$$(\dagger) \quad \overline{(\mathcal{C}')^{>0}} = \text{Span}_{\mathbb{Z}_{\geq 0}}(c'_1, \dots, c'_6) + \mathbb{Z}_{\geq 0} \cdot c'_7 \quad (= \mathbb{Z}_{\geq 0}^6 \times \mathbb{Z}_{\geq 0}).$$

If  $c' \in (\mathcal{C}')^{<0}$ , then its last coordinate is  $x \leq -1$ . Since  $-x > 0$  and  $-x \leq \min(r_{12}, r_{22}, r_{32})$ ,

$$c' = (r_{11}, -x + r'_{12}, r_{21}, -x + r'_{22}, r_{31}, -x + r'_{32}, -x \cdot -1)$$

for some  $r_{11}, r'_{12}, r_{21}, r'_{22}, r_{31}, r'_{32} \in \mathbb{Z}_{\geq 0}$  and  $-x \in \mathbb{Z}_{>0}$ . That is,

$$c' = r_{11}c'_1 + r'_{12}c'_2 + r_{21}c'_3 + r'_{22}c'_4 + r_{31}c'_5 + r'_{32}c'_6 + (-x)c'_8 \in \text{Span}_{\mathbb{Z}_{\geq 0}}(c'_1, \dots, c'_6) + \mathbb{Z}_{>0} \cdot c'_8.$$

Thus,

$$(\dagger\dagger) \quad (\mathcal{C}')^{<0} = \text{Span}_{\mathbb{Z}_{\geq 0}}(c'_1, \dots, c'_6) + \mathbb{Z}_{>0} \cdot c'_8,$$

where the  $\supseteq$  containment follows since  $\text{Span}_{\mathbb{Z}_{\geq 0}}(c'_1, \dots, c'_6) + \mathbb{Z}_{>0} \cdot c'_8 \subseteq \mathbb{Z}_{\geq 0}^6 \times \mathbb{Z}_{<0}$ .

Next, we show  $c'_1, \dots, c'_6, c'_7, c'_8$  are weakly independent over  $\mathbb{Z}_{\geq 0}$ . Indeed, if  $n_1c'_1 + \dots + n_8c'_8 = 0$ , then  $n_1 = n_3 = n_5 = 0$  and  $n_2 + n_8, n_4 + n_8, n_6 + n_8, n_7 - n_8 = 0$ . Since all  $n_i \in \mathbb{Z}_{\geq 0}$ , it follows that  $n_2 = n_4 = n_6 = n_8 = 0$ , and so  $n_7 = n_8 = 0$ , as desired.

We gather that  $c'_1, \dots, c'_6, c'_7, c'_8$  form a weak basis of  $\mathcal{C}'$ .

Next, we show  $c'_1, \dots, c'_6, c'_7$  are strongly independent over  $\mathbb{Z}_{\geq 0}$ . This is equivalent to being linearly independent over  $\mathbb{Q}$ , which follows from the definitions. Similarly, it follows from the definitions that  $c'_1, \dots, c'_6, c'_8$  are strongly independent over  $\mathbb{Z}_{\geq 0}$ .

We now define a  $\mathbb{Z}_{\geq 0}$ -linear bijection  $\varphi: \mathcal{C}'_{\mathbb{Z}} \rightarrow \mathcal{C}'$ . Its inverse will be the desired  $\mathbb{Z}_{\geq 0}$ -linear bijection  $\psi = \varphi^{-1}: \mathcal{C}' \rightarrow \mathcal{C}'_{\mathbb{Z}}$ . Let  $c$  be a cone point in  $\mathcal{C}'_{\mathbb{Z}}$ , written as in Equation \*. Put

$$\begin{aligned} x &= (a_{11} - a_{12} + a_{21} - a_{22} + a_{31} - a_{32})/3 \\ &= r_{13} - r_{12} = r_{23} - r_{22} = r_{33} - r_{32} \\ &\geq -r_{12} \text{ and } -r_{22} \text{ and } -r_{32} \end{aligned}$$

where the rhombus numbers  $r_{ij}$  are in  $\mathbb{Z}_{\geq 0}$  since  $c \in \mathcal{C}_{\mathfrak{T}}^+$ ; see Figure 37. Thus,

$$x \geq \max(-r_{12}, -r_{22}, -r_{32}) = -\min(r_{12}, r_{22}, r_{32}).$$

Therefore, recalling  $\mathcal{C}' \subseteq \mathbb{Z}_{\geq 0}^6 \times \mathbb{Z}$  (Equation (\*\*)), we may define the function  $\varphi: \mathcal{C}_{\mathfrak{T}}^+ \rightarrow \mathcal{C}'$  by

$$\varphi(c) = (r_{11}, r_{12}, r_{21}, r_{22}, r_{31}, r_{32}, x).$$

It follows from the definition that  $\varphi: \mathcal{C}_{\mathfrak{T}}^+ \rightarrow \mathcal{C}'$  is  $\mathbb{Z}_{\geq 0}$ -linear. One checks that  $\varphi(c_i) = c'_i$ . Since the  $c'_i$  span  $\mathcal{C}'$ , it follows that  $\varphi$  is surjective. Thus, by Equations  $(\#), (\#\#), (\dagger), (\dagger\dagger)$ ,

$$\varphi\left(\overline{(\mathcal{C}_{\mathfrak{T}}^+)^{\mathrm{in}}}\right) = \overline{(\mathcal{C}')^{>0}} \quad \text{and} \quad \varphi\left(\overline{(\mathcal{C}_{\mathfrak{T}}^+)^{\mathrm{out}}}\right) = (\mathcal{C}')^{<0}.$$

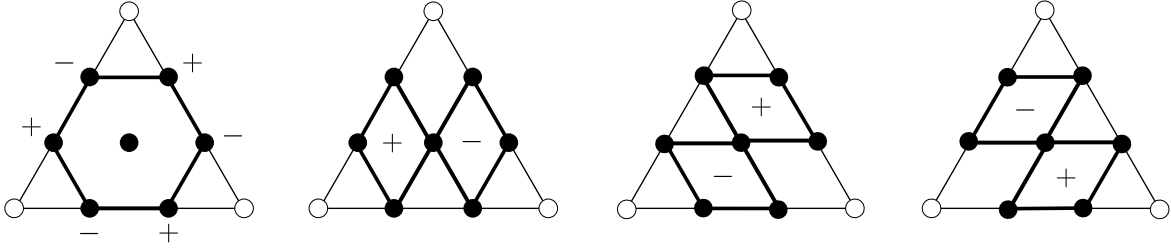


FIGURE 37. Four ways to view the tropical Fock-Goncharov  $\mathcal{X}$ -coordinate  $x$

The formula for  $\varphi$  extends to define a  $\mathbb{Q}$ -linear isomorphism  $\tilde{\varphi}: \mathbb{Q}^7 \rightarrow \mathbb{Q}^7$ , and its inverse is the desired  $\mathbb{Q}$ -linear isomorphism  $\tilde{\psi} = \tilde{\varphi}^{-1}: \mathbb{Q}^7 \rightarrow \mathbb{Q}^7$ . Indeed, the bijectivity of  $\tilde{\varphi}$  follows by computing the values on the standard column basis of  $\mathbb{Q}^7$ , giving the invertible matrix

$$\tilde{\varphi}(\vec{e}_1, \vec{e}_2, \vec{e}_3, \vec{e}_4, \vec{e}_5, \vec{e}_6, \vec{e}_7) = \frac{1}{3} \begin{pmatrix} 0 & 0 & 0 & 1 & 1 & 0 & -1 \\ -1 & 0 & 0 & 0 & -1 & 1 & 1 \\ 1 & 0 & 0 & 0 & 0 & 1 & -1 \\ -1 & 1 & -1 & 0 & 0 & 0 & 1 \\ 0 & 1 & 1 & 0 & 0 & 0 & -1 \\ 0 & 0 & -1 & 1 & -1 & 0 & 1 \\ 1 & -1 & 1 & -1 & 1 & -1 & 0 \end{pmatrix}.$$

So  $\tilde{\psi} = \tilde{\varphi}^{-1}$  is defined. Since  $\tilde{\varphi}$  is an injection, so is its restriction  $\varphi: \mathcal{C}_{\mathfrak{T}}^+ \rightarrow \mathcal{C}'$ . Also, since, as we argued above,  $\varphi$  is a surjection, we gather  $\varphi$  is a bijection. Thus,  $\psi = \varphi^{-1}: \mathcal{C}' \rightarrow \mathcal{C}_{\mathfrak{T}}^+$  is defined. This completes the proof of the claim, thereby establishing the proposition.  $\square$

**5.3. Global Knutson-Tao cone.** Given the dotted ideal triangulation  $\lambda$  on the surface  $\mathfrak{S}$ , an element  $c$  of  $\mathbb{Z}^N$  corresponds to a function  $\{\text{dots on } \lambda\} \rightarrow \mathbb{Z}$ ; see §4.1. If  $\mathfrak{T}$  is a dotted triangle of  $\lambda$ , then an element  $c$  of  $\mathbb{Z}^N$  induces a function  $\{\text{dots on } \mathfrak{T}\} \rightarrow \mathbb{Z}$ , which likewise corresponds to an element  $c_{\mathfrak{T}}$  of  $\mathbb{Z}^7$ .

**Definition 45.** The *global Knutson-Tao positive cone*, or just *Knutson-Tao cone* or *global cone*,  $\mathcal{C}_{\lambda}^+ \subseteq \mathbb{Z}_{\geq 0}^N$  is defined by

$$\mathcal{C}_{\lambda}^+ = \{c \in \mathbb{Z}^N; \quad c_{\mathfrak{T}} \text{ is in } \mathcal{C}_{\mathfrak{T}}^+ \subseteq \mathbb{Z}_{\geq 0}^7 \text{ for all triangles } \mathfrak{T} \text{ of } \lambda\}.$$

It follows from the definition that  $\mathcal{C}_{\lambda}^+$  is indeed a positive cone.

In §4, we defined the global coordinate function  $\Phi_{\lambda}^{\mathrm{FG}}: \mathcal{W}_{\mathfrak{S}} \rightarrow \mathbb{Z}_{\geq 0}^N$ ; see Definition 33. Since the image  $\Phi_{\mathfrak{T}}^{\mathrm{FG}}(\mathcal{W}_{\mathfrak{T}}) \subseteq \mathcal{C}_{\mathfrak{T}}^+$  (which is, in fact, an equality by Corollary 42), it follows by the construction of  $\Phi_{\lambda}^{\mathrm{FG}}$  that the image  $\Phi_{\lambda}^{\mathrm{FG}}(\mathcal{W}_{\mathfrak{S}}) \subseteq \mathcal{C}_{\lambda}^+$ ; recall, for instance, Figure 34 above.

**Proposition 46.** *We have, moreover,*

$$\Phi_\lambda^{\text{FG}}(\mathcal{W}_\mathfrak{S}) = \mathcal{C}_\lambda^+.$$

This will be proved in §6-7.

## 6. MAIN THEOREM: GLOBAL COORDINATES

We summarize what we have done so far. Consider a punctured surface  $\mathfrak{S}$  with empty boundary; see §1. Let  $\mathcal{W}_\mathfrak{S}$  denote the collection of parallel-equivalence classes of global non-elliptic webs on  $\mathfrak{S}$ . Assume that  $\mathfrak{S}$  is equipped with an ideal triangulation  $\lambda$ . For  $N = -8\chi(\mathfrak{S})$ , in §4 we defined the Fock-Goncharov global coordinate function  $\Phi_\lambda^{\text{FG}} : \mathcal{W}_\mathfrak{S} \rightarrow \mathbb{Z}_{\geq 0}^N$ , depending on the choice of the ideal triangulation  $\lambda$ . Proposition 34, which still needs to be proved, says that the mapping  $\Phi_\lambda^{\text{FG}}$  is injective. In §5, we defined the global Knutson-Tao positive cone  $\mathcal{C}_\lambda^+ \subseteq \mathbb{Z}_{\geq 0}^N$ , which also depends on the ideal triangulation  $\lambda$ . By construction, the image  $\Phi_\lambda^{\text{FG}}(\mathcal{W}_\mathfrak{S}) \subseteq \mathcal{C}_\lambda^+$ . According to Proposition 46, which also still needs to be proved,  $\Phi_\lambda^{\text{FG}}$  maps  $\mathcal{W}_\mathfrak{S}$  onto  $\mathcal{C}_\lambda^+$ . Therefore, assuming Propositions 34 and 46 to be true, we have proved the following main result.

**Theorem 47.** *The Fock-Goncharov global coordinate function*

$$\Phi_\lambda^{\text{FG}} : \mathcal{W}_\mathfrak{S} \xrightarrow{\sim} \mathcal{C}_\lambda^+$$

*is a bijection of sets.* □

**Remark 48.** The appropriate extension of this result should hold in the more general setting of surfaces-with-boundary, with similar proofs; compare [FS20]. We have chosen to focus on the case of empty boundary for the sake of clarity.

**6.1. Inverse mapping.** Our strategy for proving Propositions 34 and 46 (equivalently, Theorem 47) is to construct an explicit inverse mapping

$$\Psi_\lambda^{\text{FG}} : \mathcal{C}_\lambda^+ \longrightarrow \mathcal{W}_\mathfrak{S}$$

namely a function that is both a left and a right inverse for the function  $\Phi_\lambda^{\text{FG}}$ . The definition of the mapping  $\Psi_\lambda^{\text{FG}}$  is relatively straightforward, and it will be automatic that it is an inverse for  $\Phi_\lambda^{\text{FG}}$ . The more challenging part will be to show that  $\Psi_\lambda^{\text{FG}}$  is well-defined.

**6.2. Inverse mapping: ladder gluing construction.** Recall that for a triangle  $\mathfrak{T}$  we denote by  $\mathcal{W}_\mathfrak{T}$  the collection of rung-less essential local webs  $W_\mathfrak{T}$  in  $\mathfrak{T}$ ; see Definition 23. We will once again make use of the split ideal triangulation  $\hat{\lambda}$ ; see §3.3.

**Definition 49.** A collection  $\{W_\mathfrak{T}\}_{\mathfrak{T} \in \hat{\lambda}}$  of local webs  $W_\mathfrak{T} \in \mathcal{W}_\mathfrak{T}$ , varying over the triangles  $\mathfrak{T}$  of  $\hat{\lambda}$ , is *compatible* if for each biangle  $\mathfrak{B}$ , with boundary edges  $E'$  and  $E''$ , sitting between two triangles  $\mathfrak{T}'$  and  $\mathfrak{T}''$ , respectively, the number of out-strands (resp. in-strands) of  $W_{\mathfrak{T}'}$  on  $E'$  is equal to the number of in-strands (resp. out-strands) of  $W_{\mathfrak{T}''}$  on  $E''$ .

For example, see the third row of Figure 38.

To a compatible collection  $\{W_\mathfrak{T}\}_{\mathfrak{T} \in \hat{\lambda}}$  of local webs, we will associate a global web  $W$  on  $\mathfrak{S}$  that need not be non-elliptic and that is in good position with respect to  $\hat{\lambda}$ ; recall Definition 29. The global web  $W$  is well-defined up to ambient isotopy of  $\mathfrak{S}$  respecting  $\hat{\lambda}$ .

*Construction of  $W$ .* Consider a biangle  $\mathfrak{B}$  sitting between two triangles  $\mathfrak{T}'$  and  $\mathfrak{T}''$ . The local webs  $W_{\mathfrak{T}'}$  and  $W_{\mathfrak{T}''}$  determine strand sets  $S'$  and  $S''$  on the boundary edges  $E'$  and  $E''$ ,

respectively. By the compatibility property, the strand-set pair  $S = (S', S'')$  is symmetric; see Definition 18. Let  $W_{\mathfrak{B}} = W_{\mathfrak{B}}(S)$  be the induced ladder-web in  $\mathfrak{B}$ ; see again Definition 18.

Define  $W$  to be the global web obtained by gluing together the local webs  $\{W_{\mathfrak{T}}\}_{\mathfrak{T} \in \hat{\lambda}}$  and  $\{W_{\mathfrak{B}}\}_{\mathfrak{B} \in \hat{\lambda}}$  in the obvious way; see the fourth row and the left side of the fifth row of Figure 38.

**Definition 50.** We say that the global web  $W$  has been obtained from the compatible collection  $\{W_{\mathfrak{T}}\}_{\mathfrak{T} \in \hat{\lambda}}$  of local webs by applying the *ladder gluing construction*.

The following statement is immediate.

**Lemma 51.** *A global web  $W$  obtained via the ladder gluing construction is in good position with respect to  $\hat{\lambda}$ . Conversely, if  $W$  is a global web in good position, then  $W$  can be recovered as the result of applying the ladder gluing construction to  $\{W_{\mathfrak{T}} = W \cap \mathfrak{T}\}_{\mathfrak{T} \in \hat{\lambda}}$ .*  $\square$

If the global web  $W$  is obtained via the ladder gluing construction, then  $W$  could be (1) non-elliptic, for example see the left side of the fifth row of Figure 38, or (2) elliptic, for example see the fourth row of Figure 38.

**6.3. Inverse mapping: resolving an elliptic web.** Recall the notion of a local parallel-move; see Figure 21. Note that if  $\{W'_{\mathfrak{T}}\}_{\mathfrak{T} \in \hat{\lambda}}$  is a compatible collection of local webs, and if  $W_{\mathfrak{T}}$  is related to  $W'_{\mathfrak{T}}$  by a sequence of local parallel-moves, then  $\{W_{\mathfrak{T}}\}_{\mathfrak{T} \in \hat{\lambda}}$  is also compatible.

**Lemma 52.** *Given a compatible collection  $\{W'_{\mathfrak{T}}\}_{\mathfrak{T} \in \hat{\lambda}}$  of local webs, there exist local webs  $\{W_{\mathfrak{T}}\}_{\mathfrak{T} \in \hat{\lambda}}$  such that  $W_{\mathfrak{T}}$  is related to  $W'_{\mathfrak{T}}$  by a sequence of local parallel-moves, and the global web  $W$  obtained by applying the ladder gluing construction to  $\{W_{\mathfrak{T}}\}_{\mathfrak{T} \in \hat{\lambda}}$  is non-elliptic.*

*Proof.* Suppose that the global web  $W'$  obtained by applying the ladder gluing construction to the local webs  $\{W'_{\mathfrak{T}}\}_{\mathfrak{T} \in \hat{\lambda}}$  is elliptic.

*Step 1.* We show that the elliptic global web  $W'$  has no disk- or bigon-faces. If there were a disk- or bigon-face, then it could not lie completely in a triangle  $\mathfrak{T}$  or biangle  $\mathfrak{B}$  of  $\hat{\lambda}$ , for this would violate that the local web restriction  $W'_{\mathfrak{T}}$  or  $W'_{\mathfrak{B}}$  is essential (in particular, non-elliptic) by Lemma 51. Consequently, there is a cap- or fork-face lying in some  $\mathfrak{T}$  or  $\mathfrak{B}$ , contradicting that the local web restriction  $W'_{\mathfrak{T}}$  or  $W'_{\mathfrak{B}}$  is essential (in particular, taut).

*Step 2.* We consider the possible positions of square-faces relative to the split ideal triangulation  $\hat{\lambda}$ . We claim that a square-face can only appear as demonstrated at the top of Figure 39, namely having two H-faces in two (possibly identical) biangles  $\mathfrak{B}$  and, in between, having opposite sides traveling “parallel” through the intermediate triangles  $\mathfrak{T}$  and biangles  $\mathfrak{B}$ . Indeed, otherwise there would be a square-, cap-, or fork-face, similar to Step 1.

*Step 3.* We remove the square-faces. Since the square-faces are positioned in this way, given a fixed square-face there is a well-defined “state” into which the square-face can be “resolved”, illustrated in Figure 39. The resulting global web  $W_1$  is in good position with respect to  $\hat{\lambda}$ . Also,  $W_1$  is less complex than  $W'$ , where the *complexity* of a global web in good position is measured by the total number of vertices lying in the union  $\cup_{\mathfrak{B} \in \hat{\lambda}} \mathfrak{B}$  of all of the biangles  $\mathfrak{B}$ . Note that resolving a square-face decreases the complexity by 4.

The effect of resolving a square-face is to perform, in each triangle  $\mathfrak{T}$ , some number (possibly zero) of local parallel-moves. Thus, the original local webs  $\{W'_{\mathfrak{T}}\}_{\mathfrak{T} \in \hat{\lambda}}$  are replaced with new local webs  $\{(W_1)_{\mathfrak{T}}\}_{\mathfrak{T} \in \hat{\lambda}}$  such that  $(W_1)_{\mathfrak{T}}$  is equivalent to  $W'_{\mathfrak{T}}$  up to corner-ambiguity.

*Step 4.* By a complexity argument, we can repeat the previous step until we obtain a sequence  $W' = W_0, W_1, W_2, \dots, W_n = W$  of global webs in good position such that  $\{(W_{i+1})_{\mathfrak{T}}\}_{\mathfrak{T} \in \hat{\lambda}}$  is related to  $\{(W_i)_{\mathfrak{T}}\}_{\mathfrak{T} \in \hat{\lambda}}$  by a sequence of parallel-moves, and such that  $W$  has

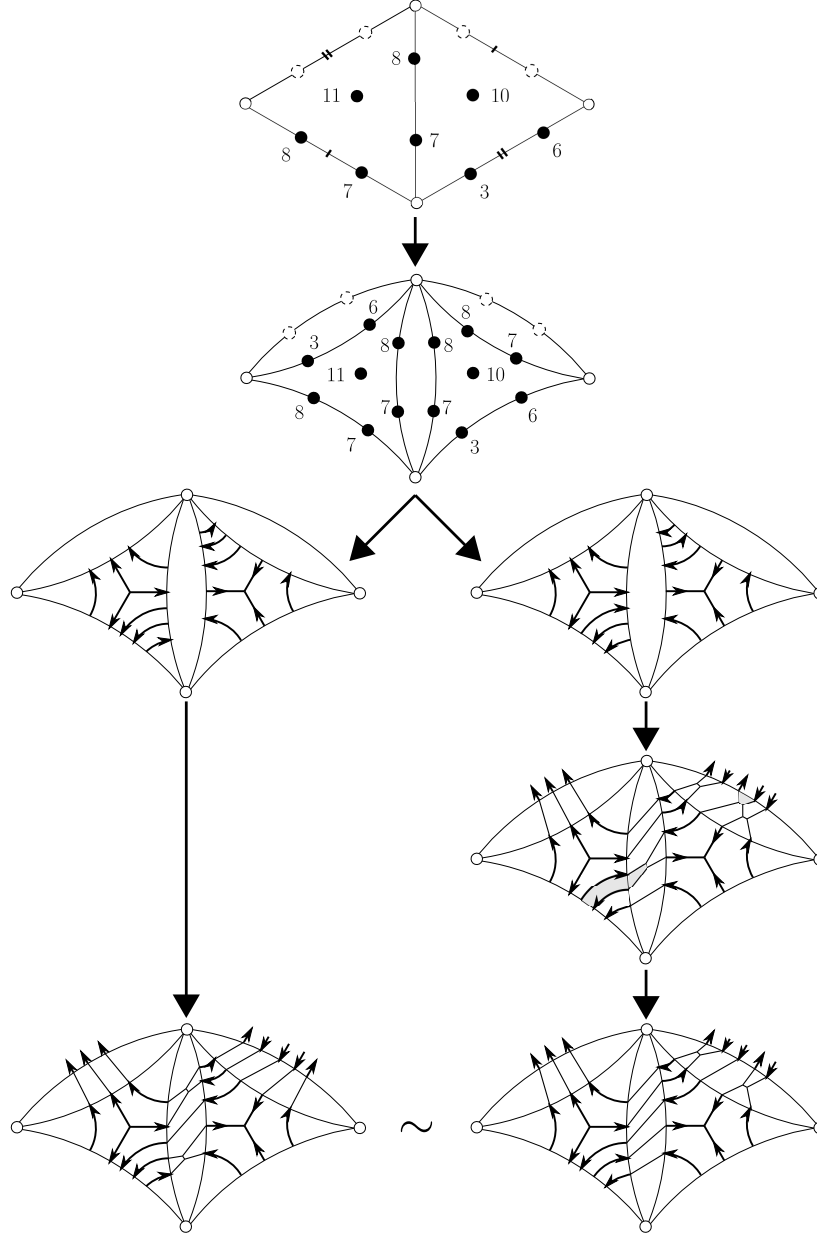


FIGURE 38. Ladder gluing construction. Shown are two different ways of assigning the local webs, differing by permutations of corner arcs. On the left, the result of the gluing is a non-elliptic web. On the right, the result is an elliptic web, which has to be resolved by removing a square before becoming a non-elliptic web. The two non-elliptic webs obtained in this way are equivalent

no square-faces. By Lemma 51,  $W$  is recovered by applying the ladder gluing construction to  $\{W_{\mathfrak{T}}\}_{\mathfrak{T} \in \widehat{\lambda}}$ . Also, by Step 1,  $W$  has no disk- or bigon-faces. Thus,  $W$  is non-elliptic.  $\square$

We refer to the algorithm used in the proof of Lemma 52 as the *square removing algorithm*. For example, see the fourth row and the right side of the fifth row of Figure 38.

Note that the algorithm removes the square-faces at random, thus the local webs  $\{W_{\mathfrak{T}}\}_{\mathfrak{T} \in \widehat{\lambda}}$  satisfying the conclusion of Lemma 52 are not necessarily unique. For example, see Figure 40.



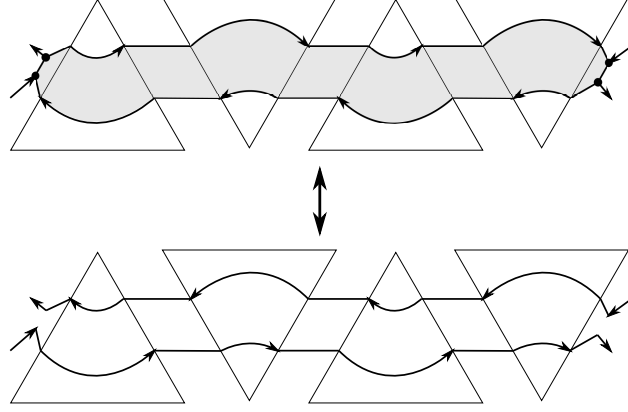


FIGURE 39. Resolving a square-face

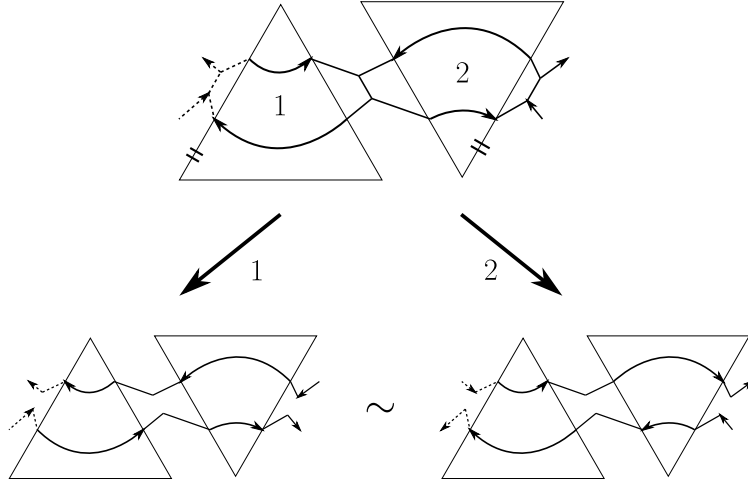


FIGURE 40. Elliptic web resulting from the ladder gluing construction (top), and two different applications of the square removing algorithm, yielding different, but parallel-equivalent, non-elliptic webs (bottom)

**6.4. Inverse mapping: definition.** Let  $c$  be a cone point in the global cone  $\mathcal{C}_\lambda^+$ ; see Definition 45. Our goal is to associate to  $c$  a parallel-equivalence class  $\Psi_\lambda^{\text{FG}}(c) \in \mathcal{W}_\mathfrak{S}$  of global non-elliptic webs on  $\mathfrak{S}$ . Equivalently, we want to associate to  $c$  a non-elliptic web  $\tilde{\Psi}_\lambda^{\text{FG}}(c)$  on  $\mathfrak{S}$  well-defined up to parallel-equivalence; see Definition 4. Recall that we identify the triangles  $\mathfrak{T}$  of the ideal triangulation  $\lambda$  with the triangles  $\mathfrak{T}$  of the split ideal triangulation  $\hat{\lambda}$ .

*Construction of  $\tilde{\Psi}_\lambda^{\text{FG}}(c)$ .* The global cone point  $c$  determines a local cone point  $c_{\mathfrak{T}}$  in the local cone  $\mathcal{C}_{\mathfrak{T}}^+$  for each triangle  $\mathfrak{T}$  of  $\lambda$ ; see just before Definition 45. By the triangle identifications between  $\lambda$  and  $\hat{\lambda}$ , the local cone point  $c_{\mathfrak{T}} \in \mathcal{C}_{\mathfrak{T}}^+$  is assigned to each triangle  $\mathfrak{T}$  of  $\hat{\lambda}$ ; see the first and second rows of Figure 38.

Note that, by construction, corresponding edge-coordinates located across a biangle  $\mathfrak{B}$  take the same value. More precisely, if  $\mathfrak{B}$  sits between two triangles  $\mathfrak{T}'$  and  $\mathfrak{T}''$  and if the boundary edges of  $\mathfrak{B}$  are  $E'$  and  $E''$ , respectively, then the coordinate  $a_{E'}^L$  (resp.  $a_{E'}^R$ ) lying on the left-edge-dot (resp. right-edge-dot) as viewed from  $\mathfrak{T}'$  agrees with the coordinate  $a_{E''}^R$  (resp.  $a_{E''}^L$ ) lying on the right-edge-dot (resp. left-edge-dot) as viewed from  $\mathfrak{T}''$ ; see Figure 38.

By Corollaries 42 and 43, for each local cone point  $c_{\mathfrak{T}} \in \mathcal{C}_{\mathfrak{T}}^+$  assigned to a triangle  $\mathfrak{T}$  of  $\widehat{\lambda}$ , there exists a unique corner-ambiguity class  $[W_{\mathfrak{T}}]$  of local webs  $W_{\mathfrak{T}}$  in  $\mathcal{W}_{\mathfrak{T}}$  such that  $\Phi_{\mathfrak{T}}^{\text{FG}}(W_{\mathfrak{T}}) = c_{\mathfrak{T}}$  for any representative  $W_{\mathfrak{T}}$  of  $[W_{\mathfrak{T}}]$ .

Crucially, we now make a choice of such a representative  $W_{\mathfrak{T}}$  for each  $\mathfrak{T}$ . Two different choices  $W_{\mathfrak{T}}$  and  $W'_{\mathfrak{T}}$  of local webs representing  $[W_{\mathfrak{T}}] = [W'_{\mathfrak{T}}]$  are, by definition, related by local parallel-moves; see the third row of Figure 38.

Since, by above, corresponding edge-coordinates across biangles agree, the collection  $\{W_{\mathfrak{T}}\}_{\mathfrak{T} \in \widehat{\lambda}}$  of local webs is compatible (Definition 49). Indeed, this follows by properties (2) and (3) in Definition 31 (the argument uses the fact that if  $W_{\mathfrak{T}} \in \mathcal{W}_{\mathfrak{T}}$ , then the opposite web  $W_{\mathfrak{T}}^{\text{op}}$  obtained by reversing all of the orientations of  $W_{\mathfrak{T}}$  is also in  $\mathcal{W}_{\mathfrak{T}}$ ).

By Lemma 52, this critical choice of a compatible collection  $\{W_{\mathfrak{T}}\}_{\mathfrak{T} \in \widehat{\lambda}}$  of local webs can be made (in a non-unique way) such that the global web  $W$  on  $\mathfrak{S}$  obtained by applying the ladder gluing construction to  $\{W_{\mathfrak{T}}\}_{\mathfrak{T} \in \widehat{\lambda}}$  is non-elliptic. Finally, we define  $\widetilde{\Psi}_{\lambda}^{\text{FG}}(c) = W$ . In order for the global web  $\widetilde{\Psi}_{\lambda}^{\text{FG}}(c)$  to be well-defined up to parallel-equivalence, we require:

**Main Lemma 53.** *Assume that each of  $\{W_{\mathfrak{T}}\}_{\mathfrak{T} \in \widehat{\lambda}}$  and  $\{W'_{\mathfrak{T}}\}_{\mathfrak{T} \in \widehat{\lambda}}$  is a compatible collection of local webs in  $\mathcal{W}_{\mathfrak{T}}$ , satisfying*

- (1) *for each triangle  $\mathfrak{T}$ , the local webs  $W_{\mathfrak{T}}$  and  $W'_{\mathfrak{T}}$  are equivalent up to corner-ambiguity;*
- (2) *both global webs  $W$  and  $W'$ , obtained from the compatible collections  $\{W_{\mathfrak{T}}\}_{\mathfrak{T} \in \widehat{\lambda}}$  and  $\{W'_{\mathfrak{T}}\}_{\mathfrak{T} \in \widehat{\lambda}}$ , respectively, by applying the ladder gluing construction, are non-elliptic.*

*Then, the non-elliptic webs  $W$  and  $W'$  represent the same parallel-equivalence class in  $\mathcal{W}_{\mathfrak{S}}$ .*

**Definition 54.** The *inverse mapping*

$$\Psi_{\lambda}^{\text{FG}} : \mathcal{C}_{\lambda}^+ \longrightarrow \mathcal{W}_{\mathfrak{S}}$$

is defined by sending a cone point  $c$  in the global Knutson-Tao cone  $\mathcal{C}_{\lambda}^+$  to the parallel-equivalence class in  $\mathcal{W}_{\mathfrak{S}}$  of the global non-elliptic web  $\widetilde{\Psi}_{\lambda}^{\text{FG}}(c)$  on  $\mathfrak{S}$ .

*Proof of Propositions 34 and 46.* Assuming Main Lemma 53 to be true, it follows immediately from the constructions that the well-defined mapping  $\Psi_{\lambda}^{\text{FG}} : \mathcal{C}_{\lambda}^+ \rightarrow \mathcal{W}_{\mathfrak{S}}$  is the set-functional inverse of the Fock-Goncharov global coordinate function  $\Phi_{\lambda}^{\text{FG}} : \mathcal{W}_{\mathfrak{S}} \rightarrow \mathcal{C}_{\lambda}^+$ .  $\square$

In summary, we have reduced the proof of Theorem 47 to proving the main lemma.

## 7. PROOF OF THE MAIN LEMMA

In this section, we prove Main Lemma 53. In particular, we provide an explicit algorithm taking one web to the other by a sequence of modified H-moves and global parallel-moves.

**7.1. Preparation: global pictures on the surface.** We introduce a technical device. For a web  $W$  on  $\mathfrak{S}$  in good position with respect to the split ideal triangulation  $\widehat{\lambda}$ , the restrictions  $W_{\mathfrak{B}} = W \cap \mathfrak{B}$  and  $W_{\mathfrak{T}} = W \cap \mathfrak{T}$  in the biangles  $\mathfrak{B}$  and triangles  $\mathfrak{T}$  of  $\widehat{\lambda}$  are essential and rung-less essential local webs, respectively. By Definitions 20 and 24, we may consider the corresponding local pictures  $\langle W_{\mathfrak{B}} \rangle$  and  $\langle W_{\mathfrak{T}} \rangle$ , which are in particular immersed multi-curves in the biangle  $\mathfrak{B}$  and the holed triangle  $\mathfrak{T}^0$ , respectively; see Definition 17 and Figures 15 and 18.

**Definition 55.** The *holed surface*  $\mathfrak{S}^0$  is the surface  $\mathfrak{S}$  minus one open disk per triangle  $\mathfrak{T}$  of  $\widehat{\lambda}$ . The *global picture*  $\langle W \rangle$  corresponding to a web  $W$  in good position with respect to  $\widehat{\lambda}$

is the multi-curve on the holed surface  $\mathfrak{S}^0$  obtained by gluing together in the obvious way the collection of local pictures  $\{\langle W_{\mathfrak{B}} \rangle\}_{\mathfrak{B} \in \hat{\lambda}}$  and  $\{\langle W_{\mathfrak{T}} \rangle\}_{\mathfrak{T} \in \hat{\lambda}}$  associated to the biangles  $\mathfrak{B}$  and triangles  $\mathfrak{T}$  of  $\hat{\lambda}$ , well-defined up to ambient isotopy of  $\mathfrak{S}^0$  respecting  $\hat{\lambda}$ .

For an example, see Figure 41.

Figure 42 depicts how a modified H-move between webs  $W$  and  $W'$  in good position looks when viewed from the perspective of the global pictures  $\langle W \rangle$  and  $\langle W' \rangle$ ; see Figure 26.

By definition, the global picture  $\langle W \rangle$  has no *U-turns* on any edge of  $\hat{\lambda}$ , meaning there are no bigons formed between a component  $\gamma$  of  $\langle W \rangle$  and  $\hat{\lambda}$ . We call this the *no-switchbacks property*.

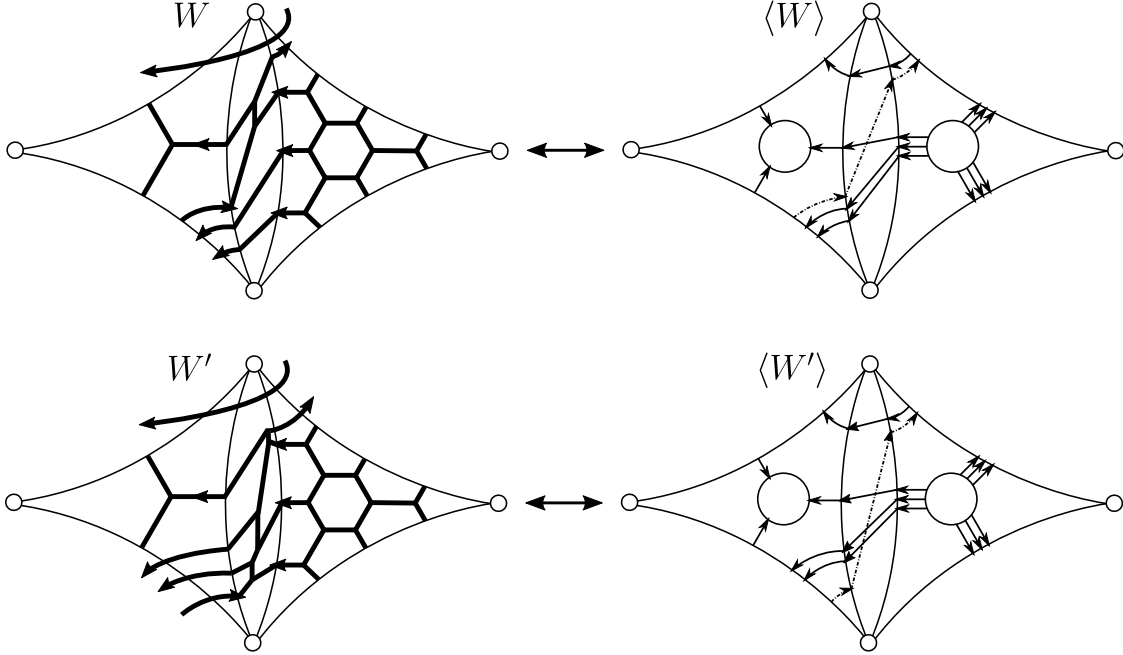


FIGURE 41. (Parts of) two webs  $W$  and  $W'$  in good position on the surface, and their corresponding global pictures  $\langle W \rangle$  and  $\langle W' \rangle$  on the holed surface. Note that, over triangles,  $W$  and  $W'$  differ by a permutation of corner arcs

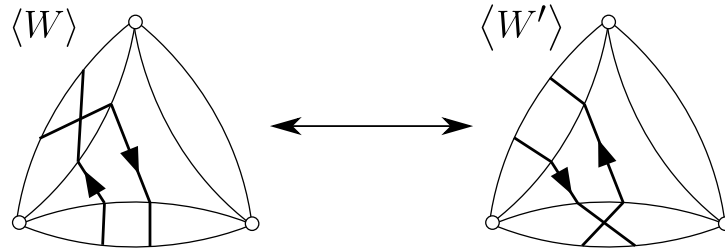


FIGURE 42. Modified H-move from the perspective of global pictures

**Definition 56.** A *based multi-curve*  $(\Gamma, \{x_0^j\})$  on the holed surface  $\mathfrak{S}^0$  is a multi-curve  $\Gamma = \{\gamma_i\}$  equipped with a base point  $x_0^j \in \gamma_j$  for each loop component  $\gamma_j$  of  $\Gamma$ , such that the base points  $x_0^j$  do not lie on any edges of the split ideal triangulation  $\hat{\lambda}$ ; see Definition 17.

**7.2. Preparation: sequences.** A *connected subset*  $I \subseteq \mathbb{Z}$  of the integers is a subset such that if  $n, m \in I$  are integers, then all the integers between  $n$  and  $m$  are in  $I$ .

A *sequence*  $(a_i)_{i \in I}$  valued in a set  $\mathcal{A}$  is a function  $I \rightarrow \mathcal{A}$ ,  $i \mapsto a_i$ , where  $I \subseteq \mathbb{Z}$  is a connected subset of the integers.

Given a sequence  $(a_i)_{i \in I}$ , a *subsequence*  $(a_{i_k})_{k \in K}$  is the sequence  $K \rightarrow \mathcal{A}$  induced by a connected subset  $K \subseteq \mathbb{Z}$  together with an order preserving function  $K \rightarrow I$ ,  $k \mapsto i_k$ .

Given a sequence  $(a_i)_{i \in I}$ , a *connected subsequence*  $(a_{i_k})_{k \in K}$  is a subsequence such that the image  $I'$  of  $K$  in  $I$  under the function  $K \rightarrow I$  is a connected subset of  $\mathbb{Z}$ .

Given two sequences  $(a_i)_{i \in I}$  and  $(b_j)_{j \in J}$  taking values in the same set, a *common subsequence*  $\{(a_{i_k})_{k \in K}, (b_{j_k})_{k \in K}\}$  is a pair of subsequences having the same indexing set  $K$ , such that  $a_{i_k} = b_{j_k}$  for all  $k \in K$ . For convenience, we always assume  $0 \in K$ .

A *connected common subsequence*  $\{(a_{i_k})_{k \in K}, (b_{j_k})_{k \in K}\}$  is a common subsequence such that both subsequences  $(a_{i_k})_{k \in K}$  and  $(b_{j_k})_{k \in K}$  are connected.

A *maximal connected common subsequence*  $\{(a_{i_k})_{k \in K}, (b_{j_k})_{k \in K}\}$  is a connected common subsequence, such that there does not exist the following:  $I \subsetneq I'$ ,  $J \subsetneq J'$ ,  $K \subsetneq K'$ , a pair of sequences  $(a'_{i'})_{i' \in I'}$  and  $(b'_{j'})_{j' \in J'}$ , and a connected common subsequence  $\{(a'_{i'_k})_{k \in K'}, (b'_{j'_k})_{k \in K'}\}$ , satisfying  $a'_i = a_i$  for  $i \in I$ ,  $b'_j = b_j$  for  $j \in J$ , and  $i'_k = i_k$  and  $j'_k = j_k$  for  $k \in K$ .

**7.3. Preparation: edge-sequences and the Fellow-Traveler Lemma.** Let  $W$  be a web on  $\mathfrak{S}$  in good position with respect to  $\hat{\lambda}$  such that its global picture  $(\langle W \rangle, \{x_0^j\})$  is based.

Let  $\gamma$  be a loop or arc in  $\langle W \rangle$ . Associated to the component  $\gamma$  is an *edge-sequence*  $(E_i)_{i \in I}$  where  $E_i$  is an edge of the split ideal triangulation  $\hat{\lambda}$ . More precisely, the sequence  $(E_i)_{i \in I}$  describes the  $i$ -th edge crossed by  $\gamma$  listed in order according to  $\gamma$ 's orientation. In the case where  $\gamma$  is an arc, we put  $I = \{0, 1, \dots, n\} \subseteq \mathbb{Z}$ , and the edge-sequence is well-defined. In the case where  $\gamma$  is a loop with base point  $x_0$ , we put  $I = \mathbb{Z}$ , and the edge-sequence is well-defined by sending 0 to the first edge  $E_0$  encountered by  $\gamma$  after passing  $x_0$ .

We also associate an *inverse edge-sequence*  $(E_i^{-1})_{i \in I^{-1}}$  to the inverse curve  $\gamma^{-1}$ , defined as follows. In the case of an arc put  $I^{-1} = \{-n, \dots, 1, 0\}$ , and in the case of a loop put  $I^{-1} = \mathbb{Z}$ . Then the inverse edge-sequence is defined by  $E_i^{-1} = E_{-i}$  for all  $i \in I^{-1}$ .

Another name for a loop or arc  $\gamma$  in the global picture  $\langle W \rangle$  is a *traveler*. Another name for an inverse curve  $\gamma^{-1}$  is a *past-traveler*. The edge-sequence  $(E_i)_{i \in I}$  associated to a traveler  $\gamma$  is called its *route*, and the edge-sequence  $(E_i^{-1})_{i \in I^{-1}}$  associated to a past-traveler  $\gamma^{-1}$  is called its *past-route*; see Figure 43. Two travelers  $\gamma$  in  $\langle W \rangle$  and  $\gamma'$  in  $\langle W' \rangle$  are called *fellow-travelers* if they have the same routes  $(E_i)_{i \in I} = (E'_i)_{i \in I'}$ ,  $I = I'$ . In particular, if  $\gamma$  is a loop (resp. arc), then  $\gamma'$  is also a loop (resp. arc).

The following statement is the key to proving the main lemma.

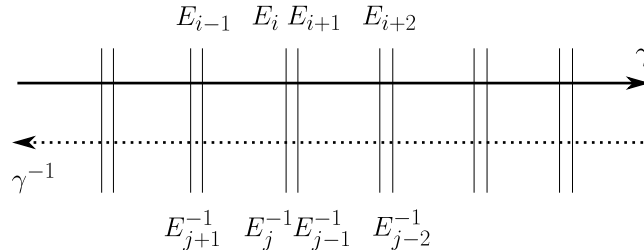


FIGURE 43. Route and past-route

**Lemma 57** (Fellow-Traveler Lemma). *Fix local webs  $\{W_{\mathfrak{T}}\}_{\mathfrak{T} \in \hat{\lambda}}$  and  $\{W'_{\mathfrak{T}}\}_{\mathfrak{T} \in \hat{\lambda}}$  in  $\mathcal{W}_{\hat{\lambda}}$  satisfying the hypotheses of Main Lemma 53, and let  $W$  and  $W'$  be the induced global webs obtained by the ladder gluing construction. Then, there exists a natural one-to-one correspondence*

$$\gamma \longleftrightarrow \gamma' = \varphi(\gamma)$$

*between the collection of travelers  $\gamma$  in the global picture  $\langle W \rangle$  and the collection of travelers  $\gamma' = \varphi(\gamma)$  in  $\langle W' \rangle$ , and there exists a choice of base points  $x_0$  and  $x'_0$  for the loops  $\gamma$  and  $\gamma'$  in  $\langle W \rangle$  and  $\langle W' \rangle$ , respectively, such that  $\gamma$  and  $\gamma' = \varphi(\gamma)$  are fellow-travelers for all travelers  $\gamma$ .*

For an example of the Fellow-Traveler Lemma on the once punctured torus, see Figure 44.

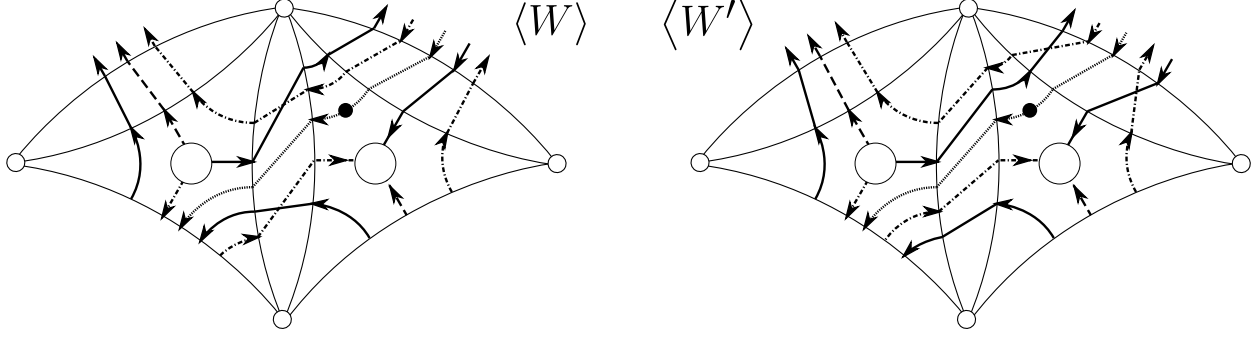


FIGURE 44. Fellow-Traveler Lemma

*Proof of Lemma 57.* Let  $E$  be an edge of  $\hat{\lambda}$ . This is associated to a unique triangle  $\mathfrak{T}$  of  $\hat{\lambda}$  containing  $E$  in its boundary. Let  $S^{(E)\text{out}} = (s_i^{(E)\text{out}})_{i=1, \dots, n_E^{\text{out}}}$  (resp.  $S'^{(E)\text{out}} = (s'_i{}^{(E)\text{out}})_{i=1, \dots, n_E'^{\text{out}}}$ ) denote the sequence of out-strands of the global picture  $\langle W \rangle$  (resp.  $\langle W' \rangle$ ) lying on the edge  $E$ , ordered, say, from left to right as viewed from  $\mathfrak{T}$ . Note that, by hypothesis,  $n_E^{\text{out}} = n_E'^{\text{out}}$ . Let  $\gamma_i^{(E)}$  denote the unique traveler in  $\langle W \rangle$  containing the strand  $s_i^{(E)\text{out}}$ . Similarly, define travelers  $\gamma'_i{}^{(E)}$  with respect to  $\langle W' \rangle$ . The mapping  $\varphi$  is defined by

$$\varphi\left(\gamma_i^{(E)}\right) = \gamma'_i{}^{(E)} \quad (i = 1, 2, \dots, n_E^{\text{out}} = n_E'^{\text{out}}).$$

Note that every traveler  $\gamma$  in  $\langle W \rangle$  (resp.  $\gamma'$  in  $\langle W' \rangle$ ) is of the form  $\gamma_i^{(E)}$  (resp.  $\gamma'_i{}^{(E)}$ ).

To establish that  $\varphi$  is well-defined, we show that  $\gamma_{i_1}^{(E_1)} = \gamma_{i_2}^{(E_2)}$  implies  $\gamma'_{i_1}{}^{(E_1)} = \gamma'_{i_2}{}^{(E_2)}$ . This property follows immediately from:

**Claim 58.** *For some  $k \in \{1, 2, \dots, n_E^{\text{out}} = n_E'^{\text{out}}\}$ , let  $s_k^{(E)\text{out}} \in S^{(E)\text{out}}$  and  $s'_k{}^{(E)\text{out}} \in S'^{(E)\text{out}}$  be out-strands of  $\langle W \rangle$  and  $\langle W' \rangle$ , respectively, lying on an edge  $E$  of a triangle  $\mathfrak{T}$  of  $\hat{\lambda}$ . Note that each of these strands, according to its orientation, enters via the edge  $E$  into a biangle  $\mathfrak{B}$ , exits via an edge  $E_2$  into a triangle  $\mathfrak{T}_2$ , and then either*

- (1) *turns left in  $\mathfrak{T}_2$ , ending as a strand  $s$  or  $s'$ , respectively, lying on an edge  $E_3$ ;*
- (2) *turns right in  $\mathfrak{T}_2$ , ending as a strand  $s$  or  $s'$ , respectively, lying on an edge  $E_3$ ;*
- (3) *terminates in a honeycomb  $H_n$ .*

*The claim is that if the forward motion of the strand  $s_k^{(E)\text{out}}$  is described by item (i) above for  $i \in \{1, 2, 3\}$ , then the forward motion of the strand  $s'_k{}^{(E)\text{out}}$  is also described by item (i). Consequently, in cases (1) or (3), there exists some  $k_3 \in \{1, 2, \dots, n_{E_3}^{\text{out}} = n_{E_3}'^{\text{out}}\}$  such that*

$$s = s_{k_3}^{(E_3)\text{out}} \in S^{(E_3)\text{out}} \quad \text{and} \quad s' = s'_{k_3}{}^{(E_3)\text{out}} \in S'^{(E_3)\text{out}}.$$

The claim is true since, by hypothesis, on each corner of each triangle,  $\langle W \rangle$  and  $\langle W' \rangle$  have the same number of clockwise-oriented (resp. counterclockwise-oriented) corner arcs, together with the fact that only oppositely-oriented arcs cross in the biangles; see Figure 45.

Having established that  $\varphi$  is well-defined, it follows by the definition that  $\varphi$  is a bijection. Another consequence of Claim 58 is that if  $\gamma$  is an arc, then  $\gamma' = \varphi(\gamma)$  is an arc such that  $\gamma$  and  $\gamma'$  are fellow-travelers. Also, if  $\gamma = \gamma_i^{(E)}$  is a loop, then  $\gamma' = \varphi(\gamma) = \gamma_i'^{(E)}$  is a loop. Choosing base points  $x_0$  and  $x'_0$  on the out-strands  $s_i^{(E)\text{out}}$  and  $s_i'^{(E)\text{out}}$ , respectively, just before the strands cross the edge  $E$  makes the loops  $\gamma$  and  $\gamma'$  into fellow-travelers.  $\square$

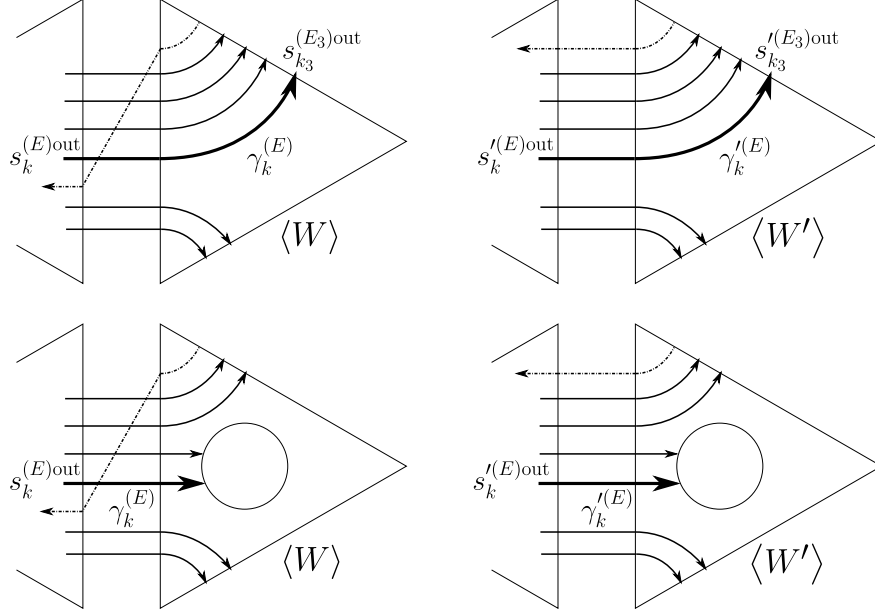


FIGURE 45. Cases (1) (left) and (3) (right) in Claim 58

**7.4. Preparation: shared-routes.** As in the previous sub-section, let  $W$  be a web on  $\mathfrak{S}$  in good position with respect to  $\hat{\lambda}$  such that its global picture  $(\langle W \rangle, \{x_0^j\})$  is based.

Let  $\gamma$  be a traveler in  $\langle W \rangle$  having route  $(E_i)_{i \in I}$ . For some  $i \in I$  indexing an edge  $E_i$ , by definition of the route there is a corresponding point  $y_i$  of  $\gamma$  lying on  $E_i$ . Consider the associated *segment*  $\overline{\gamma}_i$  of  $\gamma$  lying between the points  $y_i$  and  $y_{i+1}$ . Similarly, define segments  $\overline{(\gamma^{-1})}_i$  associated to the past-traveler  $\gamma^{-1}$  with respect to its past-route  $(E_i^{-1})_{i \in I^{-1}}$ .

**Definition 59.** Let  $\gamma_1, \gamma_2$  be travelers in  $\langle W \rangle$  and  $\gamma_1^{-1}, \gamma_2^{-1}$  the corresponding past-travelers, with routes  $(E_i^1)_{i \in I}$  and  $(E_j^2)_{j \in J}$  and past-routes  $((E_i^1)^{-1})_{i \in I^{-1}}$  and  $((E_j^2)^{-1})_{j \in J^{-1}}$ .

An *oppositely-oriented shared-route*, or just *shared-route*,  $SR$  for the ordered pair  $(\gamma_1, \gamma_2)$  of travelers is a maximal connected common subsequence  $SR = \{(E_{i_k}^1)_{k \in K}, ((E_{j_k}^2)^{-1})_{k \in K}\}$  for the route  $(E_i^1)_{i \in I}$  of  $\gamma_1$  and the past-route  $((E_j^2)^{-1})_{j \in J^{-1}}$  of  $\gamma_2^{-1}$ .

A shared-route is *open* (resp. *closed*) if its domain  $K$  is not equal to (resp. equal to)  $\mathbb{Z}$ .

A shared-route is *crossing* if there exists an index  $k \in K$  such that the associated segments  $\overline{(\gamma_1)_{i_k}}$  and  $\overline{(\gamma_2^{-1})_{j_k}^{-1}}$  intersect, say at a point  $p_k$ . We call  $p_k$  an *intersection point* of the crossing shared-route. Note that an intersection point must lie inside a biangle  $\mathfrak{B}$  of  $\hat{\lambda}$ . A shared-route is *non-crossing* if it has no intersection points.

For some examples, see Figures 46 and 47. Our pictures for crossing shared-routes and open non-crossing shared-routes, such as in Figures 46 and 47a, are only schematics, since the actual shared-route might cross the same edge multiple times. That is, there might exist  $k \neq k'$  such that  $E_{i_k}^1 = (E^2)_{j_k}^{-1} = E_{i_{k'}}^1 = (E^2)_{j_{k'}}^{-1}$ . Alternatively, one could think of these pictures at the level of the universal cover. On the other hand, our pictures for closed non-crossing shared-routes, such as in Figure 47b, are actually as they are seen on the surface.

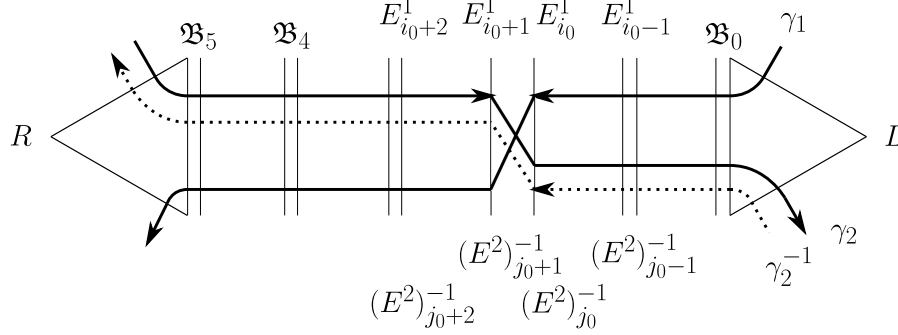


FIGURE 46. Crossing shared-route

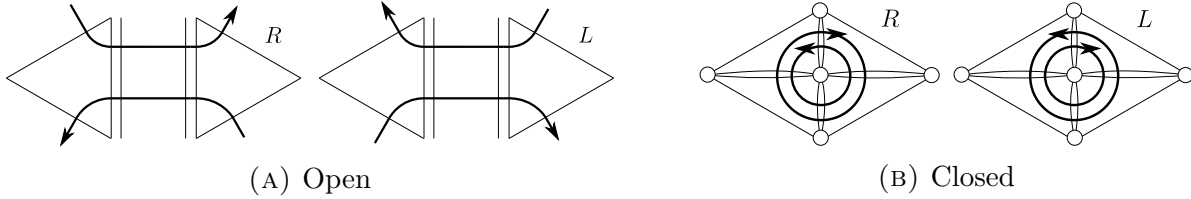


FIGURE 47. Non-crossing shared-routes

**Lemma 60.** *Assume in addition that  $W$  is non-elliptic. Then any shared-route  $SR$  has at most one intersection point  $p$ . In particular, a crossing shared-route is necessarily open.*

*Proof.* The second statement follows from the first since otherwise the oriented holed surface  $\mathfrak{S}^0$  would contain a Möbius strip.

Suppose, for an ordered pair  $(\gamma_1, \gamma_2)$  of travelers, there were a crossing shared-route  $\{(E_{i_k}^1)_{k \in K}, ((E^2)_{j_k}^{-1})_{k \in K}\}$  that has more than one intersection point. There are only finitely-many intersection points, denoted  $p_{k_1}, p_{k_2}, \dots, p_{k_m}$  with  $k_i < k_{i+1}$ . The intersection points  $p_{k_1}$  and  $p_{k_2}$  form the “tips” of an *immersed bigon*  $B$ , which we formalize as the connected common subsequence  $B = \{(E_{i_k}^1)_{k_1 \leq k \leq k_2+1}, ((E^2)_{j_k}^{-1})_{k_1 \leq k \leq k_2+1}\}$ ; see the bottom of Figure 48. Alternatively, we think of  $B$  as “bounded” by the segments of  $\gamma_1$  and  $\gamma_2$  between  $p_{k_1}$  and  $p_{k_2}$ .

Let  $p$  be the projection map from the universal cover  $\widetilde{\mathfrak{S}}^0$  to the holed surface  $\mathfrak{S}^0$ . Equip  $\widetilde{\mathfrak{S}}^0$  with the lifted split ideal triangulation  $\widetilde{\lambda} = p^{-1}(\widehat{\lambda})$ . For a traveler  $\gamma$ , consider one of its lifts  $\widetilde{\gamma}$  in  $\widetilde{\mathfrak{S}}^0$ . By the no-switchbacks property (§7.1), and the fact that the dual graph of  $\widetilde{\lambda}$  in  $\widetilde{\mathfrak{S}}^0$  is a tree, the lifted curve  $\widetilde{\gamma}$  does not cross the same edge  $\widetilde{E}$  in the universal cover  $\widetilde{\mathfrak{S}}^0$  more than once. Therefore, the immersed bigon  $B$  lifts to an actual embedded topological bigon  $\widetilde{B}$  in  $\widetilde{\mathfrak{S}}^0$ , bounded by segments of lifts  $\widetilde{\gamma}_1$  and  $\widetilde{\gamma}_2$  of the curves  $\gamma_1$  and  $\gamma_2$ ; see Figure 48.

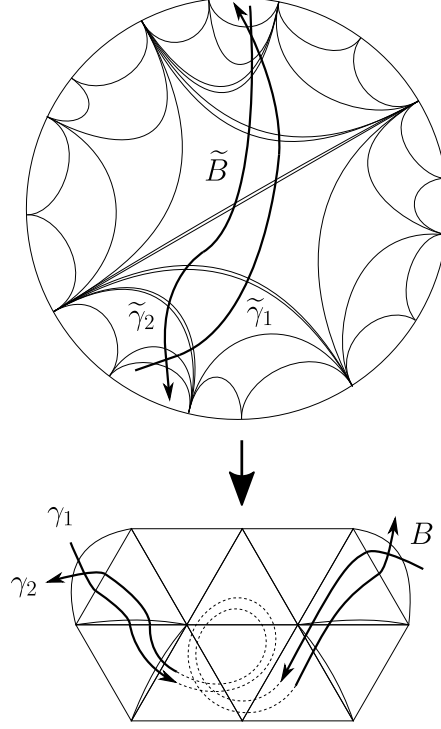


FIGURE 48. Immersed bigons do not exist: 1 of 2

Now, the preimage  $\tilde{W} = p^{-1}(W)$  of the web  $W$  is a web in  $\tilde{\mathfrak{S}}^0$ . Moreover,  $\tilde{W}$  is in good position with respect to  $\tilde{\lambda}$ . Since  $W$  is non-elliptic, so is  $\tilde{W}$ . Indeed, a face  $\tilde{D}$  of  $\tilde{W}$  projects to a face  $D$  of  $W$ . If  $\tilde{D}$  had at most 4 sides, then so would  $D$ , violating non-ellipticity. Let  $\langle \tilde{W} \rangle$  be the global picture associated to  $\tilde{W}$ . Note that the lifted curves  $\tilde{\gamma}_1$  and  $\tilde{\gamma}_2$  are in  $\langle \tilde{W} \rangle$ . Observe that it is possible for  $\text{int}(\tilde{B}) \cap \langle \tilde{W} \rangle \neq \emptyset$  to be non-empty; see Figure 49. However, by the no-switchbacks property, there are no closed curves of  $\langle \tilde{W} \rangle$  in this interior.

The rest of the proof is similar to the proof of Proposition 19; see Figure 16. Here, the web orientation plays a crucial role. Specifically, since only (locally) oppositely-oriented (with respect to biangles) curves in the global picture  $\langle \tilde{W} \rangle$  can intersect, it follows by the no-switchbacks property that if a curve  $\tilde{\gamma}$  enters the embedded bigon  $\tilde{B}$  via a boundary edge  $E$ , then  $\tilde{\gamma}$  must leave through  $E$  as well. Consequently, there exists an inner-most embedded bigon  $\tilde{B}' \subseteq \tilde{B}$  whose interior does not intersect  $\langle \tilde{W} \rangle$ ; see Figure 49. But then  $\tilde{B}'$  corresponds to a square-face  $\tilde{D}$  in the lifted non-elliptic web  $\tilde{W}$ , which is a contradiction.  $\square$

**Definition 61.** Consider a crossing shared-route  $SR$  for an ordered pair  $(\gamma_1, \gamma_2)$  of travelers in  $\langle W \rangle$ , which is open by Lemma 60.

We say that the *source-end*  $\mathcal{E}$  of the shared-route  $SR$  is the unique end  $\mathcal{E}$  of  $SR$  such that the traveler  $\gamma_1$  enters the shared-route  $SR$  through the end  $\mathcal{E}$ .

We say that the unique intersection point  $p$  in the crossing shared-route  $SR$  lies in the  $i$ -th shared-route-biangle  $\mathfrak{B}_i$ , denoted  $p \in_{SR} \mathfrak{B}_i$ ,  $i \geq 0$ , if  $\gamma_1$  crosses  $\gamma_2^{-1}$  (at the point  $p$ ) inside the  $i$ -th biangle through which  $\gamma_1$  travels after entering  $SR$  through the source-end  $\mathcal{E}$ .



For example, in Figure 46, the source-end  $\mathcal{E}$  of  $SR$  is the end labeled  $L$ .

Also, in Figure 46,  $p$  is in the shared-route-biangle  $p \in_{SR} \mathfrak{B}_2$ . Note that there is a unique index  $i$  such that  $p \in_{SR} \mathfrak{B}_i$ . This definition, albeit somewhat clumsy, will be very important later on. It is specially designed to circumvent the situation where  $\mathfrak{B}_i$  and  $\mathfrak{B}_j$  represent the same biangle  $\mathfrak{B}$  on the surface for different indices  $i \neq j$ . For example, in Figure 46, even if, say,  $\mathfrak{B}_5$  represented the same biangle  $\mathfrak{B}$  as  $\mathfrak{B}_2$ , we would say  $p \in_{SR} \mathfrak{B}_2$  and  $p \notin_{SR} \mathfrak{B}_5$ . Alternatively, one could think of this distinction at the level of the universal cover.

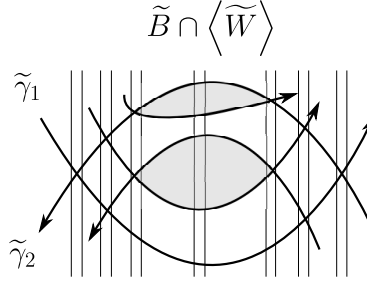


FIGURE 49. Immersed bigons do not exist: 2 of 2

**7.5. Preparation: oriented shared-routes.** As previously, let  $W$  be a web on  $\mathfrak{S}$  in good position with respect to  $\hat{\lambda}$  such that its global picture  $(\langle W \rangle, \{x_0^j\})$  is based.

We say that a non-crossing shared-route  $SR$  for an ordered pair  $(\gamma_1, \gamma_2)$  of travelers in  $\langle W \rangle$  is *left-oriented* (resp. *right-oriented*) if for either of the travelers  $\gamma_1$  or  $\gamma_2$ , call it  $\gamma$ , the other traveler appears on the left (resp. right) of  $\gamma$  with respect to  $\gamma$ 's orientation; see Figure 47.

**Definition 62.** The web  $W$  is *closed-left-oriented* (resp. *closed-right-oriented*) if all of  $\langle W \rangle$ 's closed non-crossing shared-routes are left-oriented (resp. right-oriented); see Figure 47b.

Observe that  $W$  can always be replaced with a closed-left-oriented or closed-right-oriented web by performing a sequence of global parallel-moves; see Figure 3.

We also want to define a notion of orientation for crossing shared-routes. Unlike for non-crossing shared-routes, this will depend crucially on the ordering of the pair  $(\gamma_1, \gamma_2)$ .

With this goal in mind, we say that a crossing shared-route  $SR$  for an ordered pair  $(\gamma_1, \gamma_2)$  of travelers in  $\langle W \rangle$  is *left-oriented* (resp. *right-oriented*) if its source-end  $\mathcal{E}$  is left-oriented (resp. right-oriented) in the same sense as for non-crossing shared-routes; see Definition 61.

For example, the crossing shared-route shown in Figure 46 is left-oriented.

**7.6. Proof of the main lemma: intersection points.** We now begin the formal proof of Main Lemma 53. Fix local webs  $\{W_{\mathfrak{T}}\}_{\mathfrak{T} \in \hat{\lambda}}$  and  $\{W'_{\mathfrak{T}}\}_{\mathfrak{T} \in \hat{\lambda}}$  in  $\mathcal{W}_{\mathfrak{T}}$  satisfying the hypotheses of the main lemma, and let  $W$  and  $W'$  be the induced global webs obtained by the ladder gluing construction. By applying global parallel-moves, we may assume that both  $W$  and  $W'$  are closed-left-oriented, say. Assume that the global pictures  $(\langle W \rangle, \{x_0^j\})$  and  $(\langle W' \rangle, \{x_0'^j\})$  are based, and that the base points  $x_0^j$  and  $x_0'^j$  satisfy the conclusion of the Fellow-Traveler Lemma 57. Throughout, for each traveler  $\gamma$  in  $\langle W \rangle$  we denote by  $\gamma'$  the corresponding traveler in  $\langle W' \rangle$  as provided by the Fellow-Traveler Lemma.

Let  $\mathcal{P}$  (resp.  $\mathcal{P}'$ ) denote the set of intersection points  $p$  of all travelers in  $\langle W \rangle$  (resp.  $\langle W' \rangle$ ).

Recall, by Lemma 60, that crossing shared-routes  $SR$  have a unique intersection point  $p$ .

**Definition 63.** Let  $p \in \mathcal{P}$ . We define the *left-oriented crossing shared-route generated by  $p$* , denoted  $SR(p)$ , to be the left-oriented crossing shared-route in  $\langle W \rangle$  whose unique intersection point is  $p$ . (Technically speaking, the shared-route  $SR(p) = \{(E^1_{i_k})_{k \in K}, ((E^2)_{j_k}^{-1})_{k \in K}\}$  is only uniquely determined after choosing the two edges  $E^1_{i_0} = (E^2)_{j_0}^{-1}$  assigned by  $0 \in K$ .)

**Corollary 64.** *There is a natural bijection  $\varphi : \mathcal{P} \xrightarrow{\sim} \mathcal{P}'$ . We write  $p' = \varphi(p)$ .*

*Proof.* Consider the left-oriented crossing shared-route  $SR(p)$  in  $\langle W \rangle$  generated by the intersection point  $p$ . By the Fellow-Traveler Lemma, there is a corresponding shared-route  $SR'$  in  $\langle W' \rangle$ , which is necessarily open; see Figure 46. Moreover, the ends  $\mathcal{E}'$  of  $SR'$  have orientations matching those of the ends  $\mathcal{E}$  of  $SR(p)$ . It follows that  $SR'$  is crossing. Its unique intersection point  $p'$  is the desired image of  $p$ ; see Figure 50. (Notice that since  $SR(p)$  is left-oriented, so is  $SR' = SR'(p')$ .)  $\square$

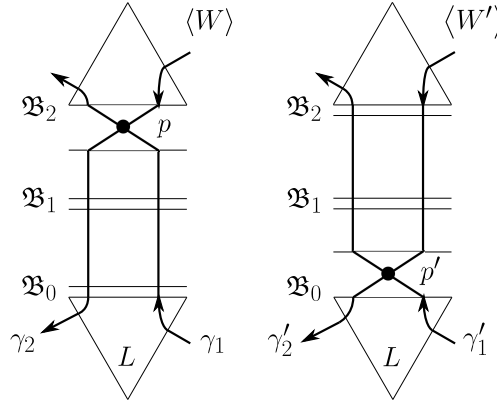


FIGURE 50. Natural one-to-one correspondence between intersection points

Recall that a crossing shared-route  $SR$  for the ordered pair  $(\gamma_1, \gamma_2)$  comes with an ordering of the shared-route-biangles  $\mathfrak{B}_i$  appearing along  $\gamma_1$ 's route, starting from the source-end  $\mathcal{E}$ ; see Definition 61. If  $p$  and  $p'$  are intersection points as in Corollary 64 and its proof, then the crossing shared-routes  $SR(p)$  and  $SR'(p')$  have the same associated sequence of shared-route-biangles  $\mathfrak{B}_i$ . However, if  $p \in_{SR(p)} \mathfrak{B}_i$  and  $p' \in_{SR'(p')} \mathfrak{B}_j$  (see again Definition 61), it need not be true that  $i = j$ ; see Figure 50.

**Definition 65.** We say that two corresponding intersection points  $p$  and  $p'$ , as in Corollary 64, *lie in the same shared-route-biangle* if there is an index  $i$  such that  $p \in_{SR(p)} \mathfrak{B}_i \ni_{SR'(p')} p'$ , where the sequence of shared-route-biangles  $\{\mathfrak{B}_i\}$  is defined with respect to the left-oriented crossing shared-routes  $SR(p)$  and  $SR'(p')$  generated by  $p$  and  $p'$ , respectively.

For example, in Figure 50, even if it were true that  $\mathfrak{B}_0$  and  $\mathfrak{B}_2$  represented the same biangle  $\mathfrak{B}$  on the surface, we would not say that  $p$  and  $p'$  lie in the same shared-route-biangle.

**Lemma 66.** *There is a sequence of modified H-moves applicable to the web  $W$  and a sequence of modified H-moves applicable to  $W'$ , after which the bijection  $\mathcal{P} \leftrightarrow \mathcal{P}'$  from Corollary 64 satisfies the property that each intersection point  $p$  in the global picture  $\langle W \rangle$  and its corresponding intersection point  $p'$  in  $\langle W' \rangle$  lie in the same shared-route-biangle  $\mathfrak{B}_i$ .*

Before giving the proof, we first reduce the proof of the main lemma to that of Lemma 66.

**7.7. Proof of the main lemma: finishing the argument.** Assuming corresponding intersection points lie in the same shared-route-biangle, we claim that we are done,  $W = W'$ .

By the proof of the Fellow-Traveler Lemma, not only is there a natural bijection of travelers  $\gamma \leftrightarrow \gamma'$ , moreover for each edge  $E$  of  $\hat{\lambda}$  there is a natural bijection of oriented strands  $s \leftrightarrow s'$  of  $\langle W \rangle$  and  $\langle W' \rangle$ , respectively, on  $E$ . This satisfies that  $s$  lies in  $\gamma$  if and only if  $s'$  lies in  $\gamma'$ , and  $s$  is an out-strand (resp. in-strand) if and only if  $s'$  is an out-strand (resp. in-strand).

Fix an edge  $E$  adjacent to a triangle  $\mathfrak{T}$ . Let  $S = (s_i)$  be the full sequence of oriented strands on the edge  $E$  measured from left to right, say, with respect to  $\mathfrak{T}$ . In particular, both in- and out-strands occur in  $S$ . Similarly, define  $S' = (s'_i)$ .

**Lemma 67.** *Assuming corresponding intersection points lie in the same shared-route-biangle, we have that  $S = S'$ , for every edge  $E$  of  $\hat{\lambda}$ ; see Definition 65.*

*Proof of Main Lemma 53.* By Lemma 66, we may assume that corresponding intersection points lie in the same shared-route-biangle. Initially, the webs  $W$  and  $W'$  differ over triangles  $\mathfrak{T}$  by permutations of corner arcs. However, we gather from Lemma 67 that they in fact have the same orderings of corner arcs in each triangle  $\mathfrak{T}$ . Also, since the ladder-webs in the biangles  $\mathfrak{B}$  are uniquely determined by their boundary-edge sequences, it follows that  $W$  and  $W'$  have the same ladder-web in each biangle  $\mathfrak{B}$ ; see Proposition 19.  $\square$

*Proof of Lemma 67.* It suffices to prove the following statement.

**Claim 68.** *If  $s^{\text{out}}$  is an out-strand of  $S$ , and if  $s^{\text{in}}$  is an in-strand of  $S$ , then*

$$s^{\text{out}} \text{ lies to the left of } s^{\text{in}} \iff s'^{\text{out}} \text{ lies to the left of } s'^{\text{in}}.$$

See Figure 51. To prove the forward direction of the claim, suppose otherwise, that is suppose  $s'^{\text{out}}$  lies to the right of  $s'^{\text{in}}$ . Let  $SR$  (resp.  $SR'$ ) be a shared-route containing  $s^{\text{out}}$  and  $s^{\text{in}}$  (resp.  $s'^{\text{out}}$  and  $s'^{\text{in}}$ ). By the Fellow-Traveler Lemma,  $SR$  is crossing (resp. open/closed non-crossing) if and only if  $SR'$  is crossing (resp. open/closed non-crossing). In addition, again by the Fellow-Traveler Lemma, in the case that  $SR$  is open, then the orientations of the ends  $\mathcal{E}$  of  $SR$  agree with those of the ends  $\mathcal{E}'$  of  $SR'$ .

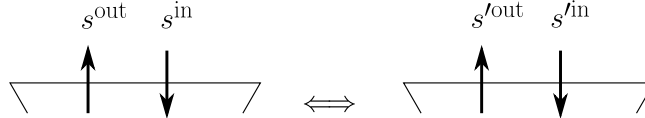


FIGURE 51. Identical oriented strand-sequences on each edge

Suppose  $SR$  is crossing. Then we may assume that  $SR$  and  $SR'$  have been chosen as the left-oriented crossing shared-routes generated by their unique intersection points  $p$  and  $p'$ , respectively; see Definition 63. In particular, they are open by Lemma 60. By hypothesis,  $p$  and  $p'$  lie in the same shared-route-biangle, call it  $\mathfrak{B}_i$ , that is  $p \in_{SR(p)} \mathfrak{B}_i \ni_{SR'(p')} p'$ . This immediately leads to a contradiction, specifically, that each traveler in  $\langle W' \rangle$  making up the shared-route  $SR'(p')$  is oriented in two directions at once; see Figure 52.

Similarly, if  $SR$  and  $SR'$  are non-crossing, then the contradiction is that one of the shared-routes is left-oriented, and the other is right-oriented; see §7.5. Indeed, in the open case (Figure 47a), this violates that their ends have matching orientations, and in the closed case (Figure 47b), this violates that we are assuming that both  $W$  and  $W'$  are closed-left-oriented; see the beginning of §7.6.

The backward direction of the claim is proved by symmetry.  $\square$

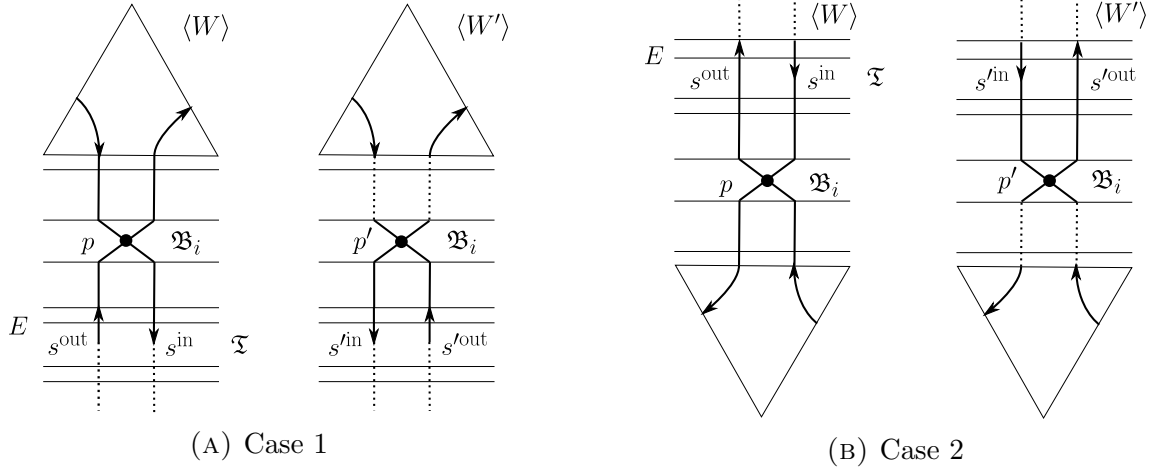


FIGURE 52. Proof of Claim 68, by contradiction

**7.8. Proof of the main lemma: proof of Lemma 66.** We have reduced the proof of the main lemma to proving Lemma 66. We begin by laying some groundwork.

Let  $\mathfrak{B}$  be a biangle, and let  $\mathcal{P}_{\mathfrak{B}} = \mathcal{P} \cap \mathfrak{B}$  be the set of intersection points of  $\langle W \rangle$  in  $\mathfrak{B}$ . Let  $E$  be a boundary edge of the biangle  $\mathfrak{B}$ , and let  $\mathfrak{B}_1$  and  $\mathfrak{B}_2$  be the two biangles opposite  $\mathfrak{B}$  across the triangle  $\mathfrak{T}$  adjacent to the edge  $E$ ; see Figure 53.

Let  $p \in \mathcal{P}_{\mathfrak{B}}$  be an intersection point in  $\mathfrak{B}$  of two travelers  $\gamma_1$  and  $\gamma_2$  in  $\langle W \rangle$ . We denote by  $\bar{\gamma}_1(p, E)$  the half-segment of  $\gamma_1$  connecting  $p$  to  $E$ . Define similarly  $\bar{\gamma}_2(p, E)$ . The *pyramid*  $\Delta(p, E)$  bounded by  $p$  and  $E$  is the triangular subset of the biangle  $\mathfrak{B}$  bordered by the boundary edge  $E$  and the two half-segments  $\bar{\gamma}_1(p, E)$  and  $\bar{\gamma}_2(p, E)$ ; see Figure 53.

Let  $P \subseteq \mathcal{P}_{\mathfrak{B}}$  be a subset of intersection points. We call  $P$  *saturated with respect to  $E$*  if

$$\mathcal{P}_{\mathfrak{B}} \cap \left( \bigcup_{p \in P} \Delta(p, E) \right) = P \subseteq \mathcal{P}_{\mathfrak{B}}.$$

In other words, there are no intersection points in the pyramids  $\Delta(p, E)$  that are not in  $P$ .

An intersection point  $p \in \mathcal{P}_{\mathfrak{B}}$  is *movable with respect to  $E$*  if, after crossing  $E$ , the half-segments  $\bar{\gamma}_1(p, E)$  and  $\bar{\gamma}_2(p, E)$  extend “parallel” to each other across the adjacent triangle  $\mathfrak{T}$ , thus landing in the same opposite biangle, either  $\mathfrak{B}_1$  or  $\mathfrak{B}_2$ ; see Figure 53, where on the left, six points are movable, in the middle, four points are movable, and on the right, none are movable. We say a subset  $P \subseteq \mathcal{P}_{\mathfrak{B}}$  is *movable with respect to  $E$*  if each  $p \in P$  is movable.

**Claim 69.** *Let  $P \subseteq \mathcal{P}_{\mathfrak{B}}$  be a subset of intersection points that is saturated and movable with respect to  $E$ . Then, there exists a sequence  $W = W_0, W_1, \dots, W_n$  of webs and a sequence  $P_{-1} = \emptyset \subsetneq P_0 \subsetneq P_1 \subsetneq \dots \subsetneq P_{n-1} = P \subseteq \mathcal{P}_{\mathfrak{B}}$  of intersection points of  $\langle W \rangle$  in the biangle  $\mathfrak{B}$ , such that  $W_{i+1}$  is obtained from  $W_i$  by a finite number of modified  $H$ -moves in such a way that the points  $P_i - P_{i-1}$  are carried into the two biangles  $\mathfrak{B}_1 \cup \mathfrak{B}_2$  and no other intersection points are moved. After this process is complete,  $P$  has been moved into  $\mathfrak{B}_1 \cup \mathfrak{B}_2$  and all of the other intersection points  $\mathcal{P} - P$  remain un-moved in their original biangles.*

The proof of the claim will use the upcoming fact. First, we give a definition.

We say that  $p \in \mathcal{P}_{\mathfrak{B}}$  is *immediately movable with respect to  $E$*  if it is movable and there are no other intersection points in the pyramid  $\Delta(p, E)$ , that is  $\Delta(p, E) \cap \mathcal{P}_{\mathfrak{B}} = \{p\}$ . Equivalently,

$\text{Int}(\Delta(p, E)) \cap \langle W \rangle = \emptyset$ , hence a modified H-move can be applied to carry  $p$  across the edge  $E$ , across the adjacent triangle  $\mathfrak{T}$ , and into one of the opposite biangles  $\mathfrak{B}_1$  or  $\mathfrak{B}_2$ ; see Figure 53, where on the left and in the middle, two and three points are immediately movable.

The following statement is immediate from the ladder-web structure in the biangle  $\mathfrak{B}$ .

**Fact 70** (Nested pyramids). *If  $q \in \mathcal{P}_{\mathfrak{B}} \cap \Delta(p, E)$  is an intersection point in the pyramid  $\Delta(p, E)$ , then  $\Delta(q, E) \subseteq \Delta(p, E)$ . Consequently, if  $p$  is movable, then so is  $q$ . Therefore, if  $p$  is movable, then there exists an inner-most  $q$  in  $\Delta(p, E)$  that is immediately movable.*  $\square$

*Proof of Claim 69.* By induction, assume  $W_i$  and  $P_{i-1}$  are given. At this stage, the intersection points  $P_{i-1}$  have been moved into  $\mathfrak{B}_1 \cup \mathfrak{B}_2$ , and the intersection points  $P - P_{i-1} \neq \emptyset$  are still in  $\mathfrak{B}$ . Note that, since  $P$  is saturated in  $\langle W \rangle$ ,  $P - P_{i-1}$  is saturated in  $\langle W_i \rangle$ , that is

$$P - P_{i-1} = \mathcal{P}_{\mathfrak{B}}^{(i)} \cap \left( \bigcup_{p \in P - P_{i-1}} \Delta^{(i)}(p, E) \right) \subseteq \langle W_i \rangle.$$

Since by hypothesis each  $p \in P - P_{i-1}$  is movable, by Fact 70 the subset

$$Q_i = \{q \in \mathcal{P}_{\mathfrak{B}}^{(i)} \cap (\bigcup_{p \in P - P_{i-1}} \Delta^{(i)}(p, E)); \quad q \text{ is immediately movable}\} \neq \emptyset,$$

is non-empty. In particular,  $Q_i \subseteq P - P_{i-1}$ . We can thus apply modified H-moves to  $W_i$  to move the intersection points  $Q_i$  from the biangle  $\mathfrak{B}$  into the two biangles  $\mathfrak{B}_1 \cup \mathfrak{B}_2$ , yielding the new web  $W_{i+1}$ . Putting  $P_i = P_{i-1} \cup Q_i$  finishes the induction step; see Figure 53.  $\square$

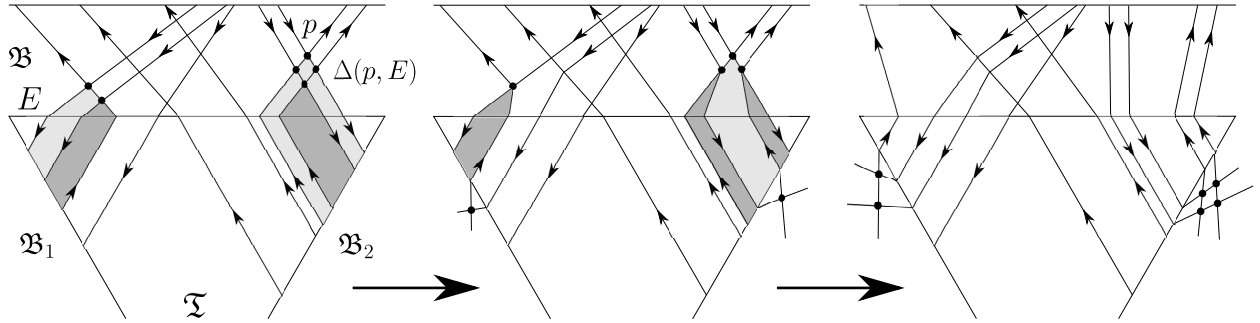


FIGURE 53. Pushing a saturated movable set  $P$  out of the biangle into adjacent biangles

The following statement is immediate from Fact 70.

**Fact 71** (Saturation of a subset of intersection points). *For any subset  $Q \subseteq \mathcal{P}_{\mathfrak{B}}$ , the set*

$$P = \mathcal{P}_{\mathfrak{B}} \cap \left( \bigcup_{q \in Q} \Delta(q, E) \right) \subseteq \mathcal{P}_{\mathfrak{B}},$$

*is saturated with respect to  $E$ .*  $\square$

We continue moving toward the proof of Lemma 66. We are now dealing with two webs  $W$  and  $W'$ . Let  $E, \mathfrak{T}, \mathfrak{B}, \mathfrak{B}_1, \mathfrak{B}_2$  be as before. We begin by setting some notation.

Given a subset  $P \subseteq \mathcal{P}_{\mathfrak{B}}$ , put

$$P'(P, E) = \mathcal{P}'_{\mathfrak{B}} \cap \left( \bigcup_{\{p \in P; \quad p \text{ and } p' \text{ lie in the same shared-route-biangle}\}} \Delta(p', E) \right) \subseteq \mathcal{P}'_{\mathfrak{B}}.$$

In other words,  $P'(P, E)$  consists of the points in  $\mathcal{P}'_{\mathfrak{B}}$  lying in the pyramids  $\Delta(p', E)$  generated by those intersection points  $p'$  in  $\mathcal{P}'_{\mathfrak{B}}$  whose corresponding intersection point  $p$  lies in the same shared-route-biangle as  $p'$  and satisfies  $p \in P$ . Symmetrically, given a subset  $P' \subseteq \mathcal{P}'_{\mathfrak{B}}$ , put

$$P(P', E) = \mathcal{P}_{\mathfrak{B}} \cap \left( \bigcup_{\{p' \in P'; \quad p' \text{ and } p \text{ lie in the same shared-route-biangle}\}} \Delta(p, E) \right) \subseteq \mathcal{P}_{\mathfrak{B}}.$$

Note that (1) the above shared-route-biangles necessarily represent the biangle  $\mathfrak{B}$ , and (2) generally, either of the sets  $P'(P, E)$  or  $P(P', E)$  may be empty.

**Fact 72.** *The union of movable sets is movable. Let  $P \subseteq \mathcal{P}_{\mathfrak{B}}$  (resp.  $P' \subseteq \mathcal{P}'_{\mathfrak{B}}$ ) be movable with respect to  $E$ . Then  $P'(P, E) \subseteq \mathcal{P}'_{\mathfrak{B}}$  (resp.  $P(P', E) \subseteq \mathcal{P}_{\mathfrak{B}}$ ) is movable with respect to  $E$ .*

*Proof.* The first statement is obvious. For the second, if  $p \in P$  is movable and if  $p'$  lies in the same shared-route-biangle as  $p$ , then, by the Fellow-Traveler Lemma,  $p'$  is movable. By Fact 70,  $\mathcal{P}'_{\mathfrak{B}} \cap \Delta(p', E) \subseteq \mathcal{P}'_{\mathfrak{B}}$  is movable. Thus, by the first statement,  $P'(P, E)$  is movable.  $\square$

*Proof of Lemma 66. Step 1.* Let  $N$  equal the cardinality  $N = |\mathcal{P}| = |\mathcal{P}'|$ . Define

$$N(W, W') = |\{p \in \mathcal{P}; \quad p \text{ and } p' \text{ lie in the same shared-route-biangle}\}| \in \mathbb{Z}_{\geq 0}.$$

If  $N(W, W') = N$ , then we are done. Assume  $N(W, W') < N$ .

*Step 2.* Let  $E, \mathfrak{T}, \mathfrak{B}, \mathfrak{B}_1, \mathfrak{B}_2$  be as above.

**Claim 73.** *Let  $p_0 \in \mathcal{P}_{\mathfrak{B}}$  be movable with respect to  $E$ . Then, there exist subsets  $p_0 \in P(p_0) \subseteq \mathcal{P}_{\mathfrak{B}}$  and  $P'(p_0) \subseteq \mathcal{P}'_{\mathfrak{B}}$ , and webs  $W_1$  and  $W'_1$  obtained by applying finitely many modified  $H$ -moves to  $W$  and  $W'$ , respectively, such that, in  $\langle W_1 \rangle$  and  $\langle W'_1 \rangle$  the subsets  $P(p_0)$  and  $P'(p_0)$  have been moved into  $\mathfrak{B}_1 \cup \mathfrak{B}_2$ , and  $\mathcal{P} - P(p_0)$  and  $\mathcal{P}' - P'(p_0)$  are un-moved. Moreover,*

$$(*) \quad N \geq N(W_1, W'_1) \geq N(W, W') \in \mathbb{Z}_{\geq 0}.$$

We prove the claim. Our main task is to define two subsets  $P(p_0) \subseteq \mathcal{P}_{\mathfrak{B}}$  and  $P'(p_0) \subseteq \mathcal{P}'_{\mathfrak{B}}$  that are saturated and movable with respect to  $E$ , satisfying the property that

$$(**) \quad \begin{aligned} p \in P(p_0), \quad p \text{ and } p' \text{ lie in the same shared-route-biangle} \\ \iff \\ p' \in P'(p_0), \quad p' \text{ and } p \text{ lie in the same shared-route-biangle.} \end{aligned}$$

We do this simultaneously by a kind of “ping-pong” procedure.

Put  $P_1 = \mathcal{P}_{\mathfrak{B}} \cap \Delta(p_0, E)$  and  $P'_1 = P'(P_1, E) \subseteq \mathcal{P}'_{\mathfrak{B}}$ . Having defined  $P_i \subseteq \mathcal{P}_{\mathfrak{B}}$  and  $P'_i \subseteq \mathcal{P}'_{\mathfrak{B}}$ , put  $P_{i+1} = P_i \cup P(P'_i, E)$  and  $P'_{i+1} = P'_i \cup P'(P_{i+1}, E)$ . This defines two nested infinite sequences  $P_1 \subseteq P_2 \subseteq \dots \subseteq \mathcal{P}_{\mathfrak{B}}$  and  $P'_1 \subseteq P'_2 \subseteq \dots \subseteq \mathcal{P}'_{\mathfrak{B}}$ . Since  $\mathcal{P}_{\mathfrak{B}}$  and  $\mathcal{P}'_{\mathfrak{B}}$  are finite, these sequences stabilize:  $P_i = P_{i+1}$  and  $P'_i = P'_{i+1}$  for all  $i \geq i_0$ . Set  $P(p_0) = P_{i_0}$  and  $P'(p_0) = P'_{i_0}$ .

Note that, by construction, there exists  $Q \subseteq \mathcal{P}_{\mathfrak{B}}$  and  $Q' \subseteq \mathcal{P}'_{\mathfrak{B}}$  such that

$$P(p_0) = \mathcal{P}_{\mathfrak{B}} \cap \left( \bigcup_{q \in Q} \Delta(q, E) \right) \quad \text{and} \quad P'(p_0) = \mathcal{P}'_{\mathfrak{B}} \cap \left( \bigcup_{q' \in Q'} \Delta(q', E) \right).$$

By Fact 71,  $P(p_0)$  and  $P'(p_0)$  are saturated with respect to  $E$ .

Observe also that since  $p_0 \in \mathcal{P}_{\mathfrak{B}}$  is movable by hypothesis,  $P_1 = \mathcal{P}_{\mathfrak{B}} \cap \Delta(p_0, E)$  is movable by Fact 70, hence  $P(p_0) \subseteq \mathcal{P}_{\mathfrak{B}}$  and  $P'(p_0) \subseteq \mathcal{P}'_{\mathfrak{B}}$  are movable by Fact 72.

To check Equation (\*\*), by symmetry it suffices to check one direction. Assume  $p \in P(p_0)$  and that  $p$  and  $p'$  lie in the same shared-route-biangle. Let  $i$  be such that  $p \in P_i$ . Then

$$p' \in \mathcal{P}'_{\mathfrak{B}} \cap \Delta(p', E) \subseteq P'(P_i, E) \subseteq P'_i \subseteq P'(p_0).$$

To prove Equation (\*), we use Claim 69 to move the saturated and movable sets  $P(p_0)$  and  $P'(p_0)$ , and only these sets, into the opposite biantles  $\mathfrak{B}_1 \cup \mathfrak{B}_2$  via finitely many modified H-moves applied to  $W$  and  $W'$ , yielding the desired webs  $W_1$  and  $W'_1$ . If  $p \in P(p_0)$  moves into the biangle  $\mathfrak{B}_1$  (resp.  $\mathfrak{B}_2$ ), and if  $p'$  lies in the same shared-route-biangle as  $p$ , so that  $p' \in P'(p_0)$  by Equation (\*\*), then by the Fellow-Traveler Lemma  $p'$  also moves into the biangle  $\mathfrak{B}_1$  (resp.  $\mathfrak{B}_2$ ), and similarly if the roles of  $p$  and  $p'$  are reversed.

*Step 3.* To finish the proof, assume that  $p$  and  $p'$  do not lie in the same shared-route-biangle. Then it makes sense to talk about which of  $p$  or  $p'$  is *farthest away* from the source-end  $\mathcal{E}$  or  $\mathcal{E}'$  of the left-oriented crossing  $SR(p)$  or  $SR'(p')$  which it generates, respectively. More precisely, if  $p \in_{SR(p)} \mathfrak{B}_i$  and  $p' \in_{SR'(p')} \mathfrak{B}_j$ ,  $i, j \geq 0$ , then  $i \neq j$  and  $p$  being farthest away is equivalent to  $i > j$ .

Assume  $p$  is farthest away, so that  $i > j$ . By applying Claim 73, we can push  $p$  one step closer to the source-end  $\mathcal{E}$ , that is we can push  $p$  into  $\mathfrak{B}_{i-1}$ . For this step,  $p'$  either (1) stays in  $\mathfrak{B}_j$ , (2) is pushed into  $\mathfrak{B}_{j-1}$ , or (3) is pushed into  $\mathfrak{B}_{j+1}$ ; see Figure 54. Notice that, crucially, by the no-switchbacks property, case (3) can only happen if  $j < i - 1$ . Also, again by Claim 73, as a result of this step the number  $N(W, W')$  only increases or stays the same.

After multiple applications of this step, since the indices  $i, j$  are bounded below, eventually  $p$  and  $p'$  fall into the same shared-route-biangle, at which point  $N(W, W')$  strictly increases. Repeating this procedure for each pair  $p$  and  $p'$  completes the proof of Lemma 66.  $\square$

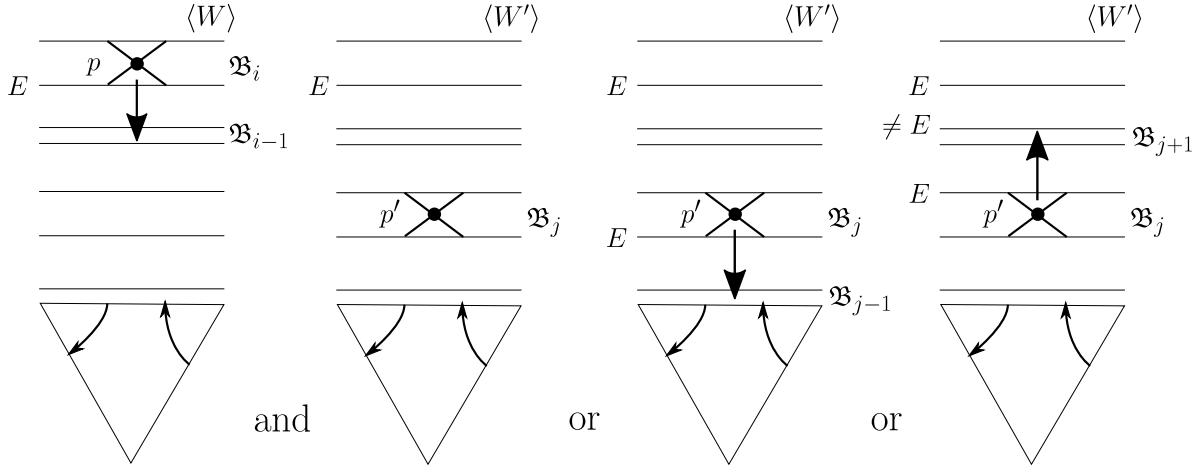


FIGURE 54. Moving intersection points into the same shared-route-biangle

## REFERENCES

- [AK17] D. G. L. Allegretti and H. K. Kim. A duality map for quantum cluster varieties from surfaces. *Adv. Math.*, 306:1164–1208, 2017.
- [Bul97] D. Bullock. Rings of  $SL_2(\mathbb{C})$ -characters and the Kauffman bracket skein module. *Comment. Math. Helv.*, 72:521–542, 1997.
- [BW11] F. Bonahon and H. Wong. Quantum traces for representations of surface groups in  $SL_2(\mathbb{C})$ . *Geom. Topol.*, 15:1569–1615, 2011.

- [Dou] D. C. Douglas. Quantum traces for  $SL_n(\mathbb{C})$ : the case  $n = 3$ . In preparation.
- [Dou20] D. C. Douglas. *Classical and quantum traces coming from  $SL_n(\mathbb{C})$  and  $U_q(\mathfrak{sl}_n)$* . PhD thesis, University of Southern California, 2020.
- [DSa] D. C. Douglas and Z. Sun. Tropical Fock-Goncharov coordinates for  $SL_3$ -webs on surfaces II: naturality. In preparation.
- [DSb] D. C. Douglas and Z. Sun. What is the meaning of 42? In preparation.
- [Eps66] D. B. A. Epstein. Curves on 2-manifolds and isotopies. *Acta Mathematica*, 115:83–107, 1966.
- [FG06] V. V. Fock and A. B. Goncharov. Moduli spaces of local systems and higher Teichmüller theory. *Publ. Math. Inst. Hautes Études Sci.*, 103:1–211, 2006.
- [FG07] V. V. Fock and A. B. Goncharov. Moduli spaces of convex projective structures on surfaces. *Adv. Math.*, 208:249–273, 2007.
- [FKK13] B. Fontaine, J. Kamnitzer, and G. Kuperberg. Buildings, spiders, and geometric Satake. *Compos. Math.*, 149:1871–1912, 2013.
- [Foc97] V. V. Fock. Dual Teichmüller spaces. <https://arxiv.org/abs/dg-ga/9702018>, 1997.
- [FP16] S. Fomin and P. Pylyavskyy. Tensor diagrams and cluster algebras. *Adv. Math.*, 300:717–787, 2016.
- [FS20] C. Frohman and A. Sikora.  $SU(3)$ -skein algebras and webs on surfaces. <https://arxiv.org/abs/2002.08151>, 2020.
- [GHKK18] M. Gross, P. Hacking, S. Keel, and M. Kontsevich. Canonical bases for cluster algebras. *J. Amer. Math. Soc.*, 31:497–608, 2018.
- [GS15] A. B. Goncharov and L. Shen. Geometry of canonical bases and mirror symmetry. *Invent. Math.*, 202:487–633, 2015.
- [GS18] A. B. Goncharov and L. Shen. Donaldson-Thomas transformations of moduli spaces of  $G$ -local systems. *Adv. Math.*, 327:225–348, 2018.
- [Hit92] N. J. Hitchin. Lie groups and Teichmüller space. *Topology*, 31:449–473, 1992.
- [HP93] J. Hoste and J. H. Przytycki. The  $(2, \infty)$ -skein module of lens spaces; a generalization of the Jones polynomial. *J. Knot Theory Ramifications*, 2:321–333, 1993.
- [HS19] Y. Huang and Z. Sun. McShane identities for higher Teichmüller theory and the Goncharov-Shen potential, to appear in *Mem. Amer. Math. Soc.* <https://arxiv.org/abs/1901.02032>, 2019.
- [KT99] A. Knutson and T. Tao. The honeycomb model of  $GL_n(\mathbb{C})$  tensor products I: proof of the saturation conjecture. *J. Amer. Math. Soc.*, 12:1055–1090, 1999.
- [Kup96] G. Kuperberg. Spiders for rank 2 Lie algebras. *Comm. Math. Phys.*, 180:109–151, 1996.
- [Lab06] F. Labourie. Anosov flows, surface groups and curves in projective space. *Invent. Math.*, 165:51–114, 2006.
- [MFK94] D. Mumford, J. Fogarty, and F. Kirwan. *Geometric invariant theory. Third edition*. Springer-Verlag, Berlin, 1994.
- [Pro76] C. Procesi. The invariant theory of  $n \times n$  matrices. *Adv. Math.*, 19:306–381, 1976.
- [Prz91] J. H. Przytycki. Skein modules of 3-manifolds. *Bull. Polish Acad. Sci. Math.*, 39:91–100, 1991.
- [Sik01] A. S. Sikora.  $SL_n$ -character varieties as spaces of graphs. *Trans. Amer. Math. Soc.*, 353:2773–2804, 2001.
- [SW07] A. S. Sikora and B. W. Westbury. Confluence theory for graphs. *Algebr. Geom. Topol.*, 7:439–478, 2007.
- [Xie13] D. Xie. Higher laminations, webs and  $\mathcal{N} = 2$  line operators. <https://arxiv.org/abs/1304.2390>, 2013.

DEPARTMENT OF MATHEMATICS, YALE UNIVERSITY, NEW HAVEN CT 06511, U.S.A.

Email address: [daniel.douglas@yale.edu](mailto:daniel.douglas@yale.edu)

IHES, 35 ROUTE DE CHARTRES, 91440 BURES-SUR-YVETTE, FRANCE

Email address: [sun.zhe@ihes.fr](mailto:sun.zhe@ihes.fr)